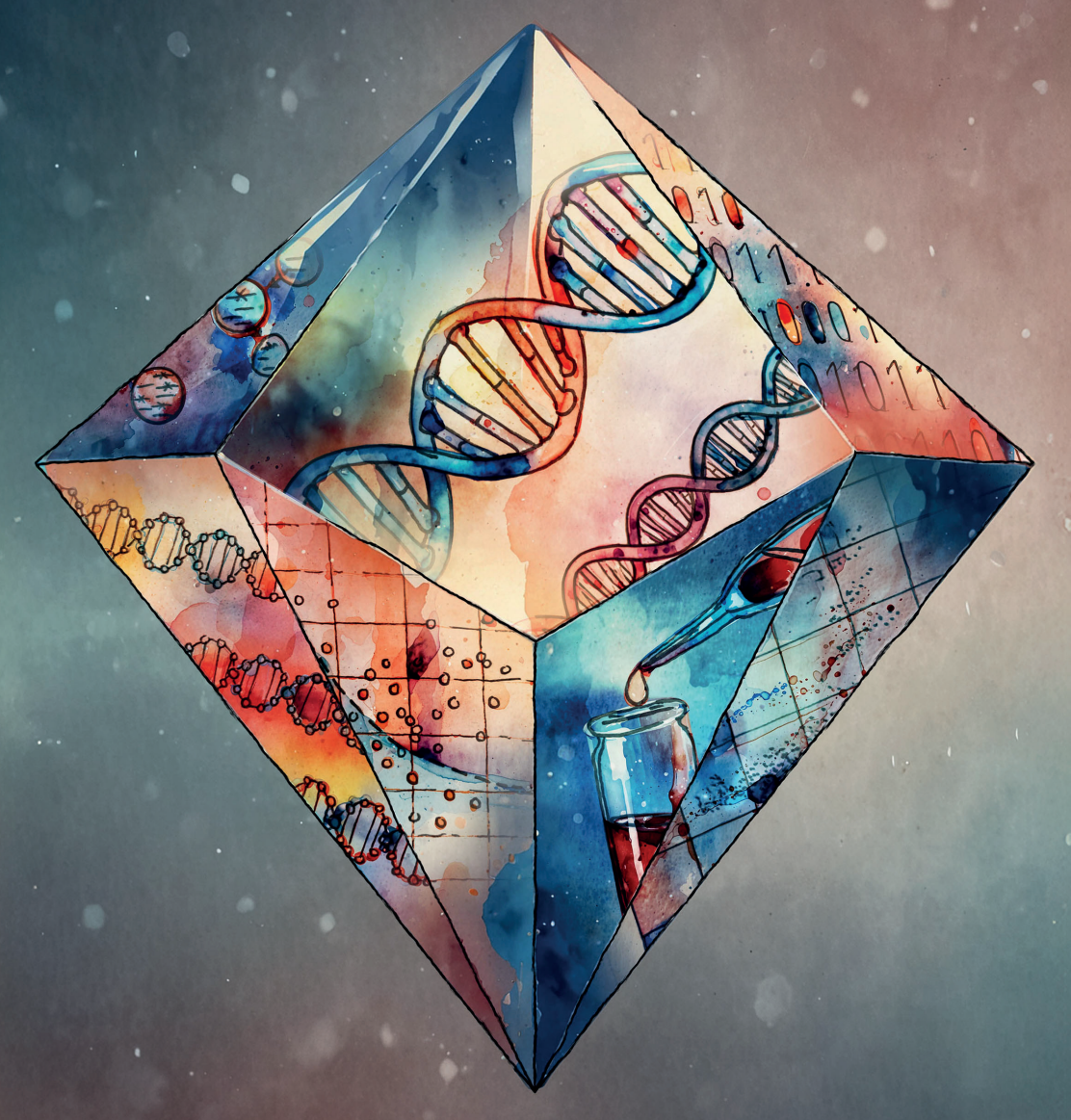
Making more of the data we have



Daan C.L. Vessies

RADBOUD UNIVERSITY PRESS

Radboud Dissertation Series

Daan Christiaan Laurens Vessies

Daan Christiaan Laurens Vessies

Radboud Dissertation Series

ISSN: 2950-2772 (Online); 2950-2780 (Print)

Published by RADBOUD UNIVERSITY PRESS Postbus 9100, 6500 HA Nijmegen, The Netherlands www.radbouduniversitypress.nl

Design: Proefschrift AIO | Guus Gijben Cover and artwork: Auke de Vries Printing: DPN Rikken/Pumbo

ISBN: 9789465150444

DOI: 10.54195/9789465150444

Free download at: https://doi.org/10.54195/9789465150444

© 2025 Daan Christiaan Laurens Vessies

RADBOUD UNIVERSITY PRESS

This is an Open Access book published under the terms of Creative Commons Attribution-Noncommercial-NoDerivatives International license (CC BY-NC-ND 4.0). This license allows reusers to copy and distribute the material in any medium or format in unadapted form only, for noncommercial purposes only, and only so long as attribution is given to the creator, see http://creativecommons.org/licenses/by-nc-nd/4.0/.

Making more of the data we have

Proefschrift ter verkrijging van de graad van doctor aan de Radboud Universiteit Nijmegen op gezag van de rector magnificus prof. dr. J.M. Sanders, volgens besluit van het college voor promoties in het openbaar te verdedigen op

> donderdag 12 juni 2025 om 10:30 uur precies

> > door

Daan Christiaan Laurens Vessies geboren op 2 november 1988 te Alkemade

Promotor:

Prof. dr. M.M. van den Heuvel

Copromotor:

Dr. D. van den Broek (Antoni van Leeuwenhoek)

Manuscriptcommissie:

Prof. dr. M.J.L. Ligtenberg

Prof. dr. ir. V. Scharnhorst (Technische Universiteit Eindhoven)

Dr. J. de Langen (Antoni van Leeuwenhoek)

Table of contents

Chapter 1 – General introduction	7
Chapter 2 – An automated correction algorithm (ALPACA) for ddPCR data using adaptive limit of blank and correction of false positive events improves specificity of mutation detection	29
Chapter 3 – Performance of four platforms for <i>KRAS</i> mutation detection in plasma cell-free DNA: ddPCR, ldylla, COBAS z480 and BEAMing	49
Chapter 4 – Clinical utility of plasma-based comprehensive molecular profiling in advanced non–small-cell lung cancer	75
Chapter 5 – Combining variant detection and fragment length analysis improves detection of minimal residual disease in postsurgery circulating tumour DNA of stage II–IIIA NSCLC patients	95
Chapter 6 – General discussion and future perspectives	127
Chapter 7 – Addenda	151



Chapter 1

General introduction

1. General introduction

1.1 Solid malignancies

Cancers are subdivided into fluid malignancies like cancers of the blood or bone marrow, and solid malignancies. Solid malignancies encompass a diverse group of cancers arising from various tissues and organs, characterized by the uncontrolled growth of abnormal cells that form solid tumours. These tumours, such as those found in the breast, lung, colon, or prostate, contribute significantly to cancer-related morbidity and mortality worldwide and nationally (1).

Of these, non-small cell lung cancer (NSCLC) and colorectal cancer (CRC) are among the most prevalent and deadly cancers. Lung cancer was diagnosed 14,806 times in 2022 in the Netherlands and caused the highest number of cancer-related deaths in the Netherlands that year: 10,896 in total, or almost 22% of all cancer-related deaths. Colorectal cancer has the highest incidence amongst all cancers in the Netherlands, at 17,670 new diagnoses in 2022. With 6,465 deaths, it accounts for another 13% of cancer-related deaths in the Netherlands, making it the second-leading cause of cancer-related deaths after lung cancer (1,2).

Personalised medicine and diagnostics in solid malignancies

In the past decades, treatment for solid malignancies has shifted from one-size-fits-all chemotherapy towards more individualised approaches, tailored towards specific tumour characteristics. This shift, along with earlier cancer detection, has significantly improved long-term survival in many solid malignancies (2,3). Personalized medicine in this context aims to deliver the right treatment for the right patient at the right time (4). To identify which treatments are likely to benefit each patient, detailed information about the tumour is necessary.

Different cancers, even within the same tissue or organ, can vary significantly in behaviour and treatment response. Traditionally the diagnosis, prognosis, and monitoring of solid malignancies have relied on tissue biopsies – an invasive procedure that provides a sample of tumour tissue for pathological examination. These biopsies yield insights into tumour diagnosis, staging, origin, and therapy selection through various microscopic techniques that help classify cancer type (e.g. adenocarcinoma, squamous cell carcinoma, etc) and guide selection of the most effective treatment.

Increasingly, tissue biopsies are also used for molecular profiling; revealing specific genetic mutations or protein markers that identify targetable variants, thus

enabling genomically informed therapies. Such targeted therapies focus on specific alterations in tumour cells absent in healthy cells and can be highly effective. In 2020, it was estimated that up to 27% of all cancer patients in the US were eligible for some form of genomically informed therapy (5). As a result, genetic testing has become part of national and international guidelines for standard-of-care diagnostics, including for NSCLC and CRC (6–10).

On the downside, tissue biopsies come with inherent limitations. They are invasive, carry risks and costs, and not all patients are eligible for them due to health status or tumour accessibility. Diagnostically, biopsies represent only a small section of the tumour, and intra- and inter-tumoral heterogeneity can cause subclonal aberrations to be missed. Furthermore, tissue biopsies provide only a single snapshot in time, whereas frequent monitoring could offer more real-time information on tumour evolution and early detection of resistance (11,12).

While tissue biopsies remain the gold standard for diagnosing solid tumours and guiding treatment decisions, their limitations highlight the need for more flexible, less invasive diagnostic approaches.

1.2 Liquid biopsies

One such approach is the liquid biopsy, a method that detects tumour-derived material circulating in bodily fluids like blood. Unlike tissue biopsies, which require invasive sampling directly from the tumour itself, liquid biopsies involve a routine blood draw to capture fragments of circulating DNA, cells, or other markers that tumours shed into the bloodstream. These shed materials, known as circulating tumour markers, offer valuable clues about a cancer's presence, type, and evolution, making it possible to monitor changes over time with minimal invasiveness (13–15).

Examples of circulating tumour markers include circulating tumour cells, extracellular vesicles, tumour-derived proteins and metabolites, and circulating cell-free DNA (cfDNA) (16). These are most commonly investigated in blood, but can also be examined in other bodily fluids like urine, cerebrospinal fluid, saliva, and others (16,17). Many factors influence the abundance of circulating tumour markers in their respective fluids, most notably the extent and location of disease (18–20). Due to their dynamic nature, liquid biopsies enable monitoring of disease over time.

Among the circulating tumour markers in liquid biopsies, cfDNA has gained particular interest. Within the cfDNA reservoir, a fraction known as circulating

tumour DNA (ctDNA) originates specifically from tumour cells and can offer insights into a cancer's genetic landscape. In the following section, we will explore cfDNA and ctDNA in more depth, examining its characteristics, how it can be used to inform personalised treatment decisions, and its current limitations.

Cell-free DNA

When cells die – whether through apoptosis, necrosis, or other processes – they can release fragmented DNA into the bloodstream as cell-free DNA, cfDNA fragments are short, typically ranging from 150 to 200 base pairs (bp), and circulate in the plasma. Most cfDNA in healthy individuals originates from hematopoietic cells, like white blood cells, but small amounts can also come from other cell types, including those from specific organs or tissue. In patients with cancer, cfDNA originating from the tumour cells is referred to as ctDNA and carries genetic information reflective of the tumour's unique mutations and characteristics.

The proportion of cfDNA that is tumour-derived, referred to as the tumour fraction (TF), varies widely depending on factors like tumour size, location, and stage (20). In early-stage cancers or certain types of tumours, ctDNA may represent only a tiny fraction of the total cfDNA – sometimes as low as parts-per-million. In more advanced cancers, or in tumours with greater vascularisation, this proportion can exceed 10%. For most cancers, the tumour fraction is typically below 1%, demanding highly sensitive techniques to identify low-frequency tumour-derived variants with high specificity and sensitivity (14,18).

1.3 ctDNA detection

The detection of ctDNA relies on identifying tumour-derived variants within the cfDNA. A cancer cell's genome is notoriously unstable, and as a result tumour-derived variants can come in many different shapes, ranging from large chromosomal rearrangements, copy number alterations, to small insertions and deletions to variants at the single nucleotide level. Of these, single nucleotide variants (SNVs) are highly abundant and relatively easy to detect and have therefore gained primary interest in cfDNA-based diagnostic approaches. However, the probability of detecting tumour-related SNVs is hampered by both biological and technical factors that we will discuss in more detail below.

Biological factors

The rate of cell division and cell death in the tumour are key determinants of ctDNA concentration in plasma (19). In healthy tissue these rates are usually balanced in homeostasis, but they may be dysregulated in cancer tissue. Consequently, differences in tumour cellular turnover may cause biases in representation of certain tumour sites (12,20).

Secondly, the location, size, and stage of the tumour are correlated to ctDNA concentrations (18). For example, tumours of the lung and colon often exhibit relatively high levels of ctDNA in plasma, while tumours in the brain do not (18). Similarly, ctDNA levels were found to be overall higher in larger and more aggressive tumours. On the contrary, organs that are encapsulated in barriers like the blood-brain barrier – are speculated to restrict ctDNA movement, making detection more challenging for certain cancer types. However, when such barriers are compromised, as in cases of inflammation or metastasis, ctDNA levels in circulation may rise (20,21).

Tumour vascularisation also plays an important role in ctDNA levels. Tumouradjacent blood vessels provide a direct route for ctDNA to enter circulation. Poorly vascularised tumours with limited blood supply may become hypoxic, inducing further necrosis while at the same time releasing the ctDNA differently compared to well-vascularised tumours. This illustrates a complex dynamic between increased cell turnover but potentially reduced shedding to the bloodstream, that makes it hard to capture such relationships in simple correlations or mathematical approximations (20).

ctDNA dynamics are further influenced by the rate of clearance from the circulation. The half-life of cfDNA is estimated between 30 minutes and 2 hours, meaning that cfDNA levels can fluctuate and make ctDNA a snapshot of recent tumour activity rather than a stable biomarker (22). The rate of clearance depends on factors such as DNase activity and renal and hepatic function, each of which could be altered in cancer patients due to treatment toxicity or disease progression (20,23).

Lastly, ctDNA detection sensitivity is impacted by the total cfDNA background in circulation, which is predominantly derived from haematopoietic cells including white blood cells. In conditions of inflammation, infection, or physical trauma, cfDNA levels from non-tumour cells can increase substantially, diluting the ctDNA signal and decreasing the relative TF.

In summary, these biological processes and systemic factors describe a nuanced dynamic balance between numerous factors that is not fully understood at this moment.

Technological factors

While biological factors dominate the availability of ctDNA in a blood sample, technological factors determine whether these molecules will be detected. Advancements in ctDNA detection have evolved rapidly in response to this challenge. Early ctDNA detection primarily focused on single SNVs per patient, using quantitative polymerase chain reaction (qPCR) methods. However, qPCR lacked the requisite sensitivity for detecting low-abundance mutations in a high background of non-mutated, wildtype cfDNA.

Droplet digital PCR (ddPCR) emerged as a highly sensitive alternative, enabling the detection of rare mutations even at low TF. This was achieved by partitioning the PCR reaction into thousands of droplets, allowing for individual analysis of each droplet, significantly enhancing sensitivity for mutation detection (24,25). Despite these improvements, ddPCR is typically limited to analysing single or small sets of SNVs. It requires prior knowledge of target mutations, which is restrictive when there is a need to screen for a broader spectrum of possible tumour mutations.

To address this limitation, multiplex PCR methods such as BEAMing, COBAS z480, and Idylla were developed (26–28). These methods enable simultaneous detection of a handful of known mutations, particularly those that are frequently activating or targetable in certain cancers. However, the number of mutations screened with such multiplex PCR methods is still limited, and repeated testing is limited by the scarcity of available material. It was therefore desirable to detect many more mutations at once with a single test.

Next-generation sequencing (NGS) platforms, particularly amplicon-based and hybrid-capture-based methods, allow for high-throughput sequencing of numerous genes in a single run, making it possible to analyse a broad range of potential mutations across many loci at once. Yet, NGS presents its own challenges, primarily in terms of error suppression: the natural error rate of sequencing and PCR (~0.1%) is similar to the frequency range of genuine mutations in ctDNA. This overlap can cause false positives and diminish confidence in the detected variants.

To enhance accuracy, NGS techniques now frequently employ unique molecular identifiers (UMIs) (29–32). UMIs are small, unique barcode sequences added to each DNA fragment prior to amplification. Since bona fide mutations are shared across the family of sequenced fragments with the same UMI, while PCR- and sequencing errors are more random, it is possible to reliably identify mutations at low variant allele frequencies (VAF), even those present at fractions below 0.1%. This is offset by a need to sequence each fragment multiple times, requiring greater sequencing depth and cost.

Each of these technological advancements has contributed to improved performance in ctDNA testing, with the trend moving from single-mutation detection to broader panels capable of capturing diverse genetic profiles. Each approach still has limitations and is selected based on the clinical context, specific cancer type, and availability of prior mutation knowledge.

Beyond SNVs

Although SNVs are commonly used for ctDNA detection, other biomarkers such as copy number variations (CNVs), DNA methylation, and fragmentomics are established or emerging as indicators of tumour presence.

CNVs are amplifications or deletions of larger DNA segments, often linked to cancer development and progression. Detection of CNVs happens not by deep evaluation of a limited number of sites in the genome, but frequently by shallow whole genome seguencing (shWGS). By counting the relative number of DNA fragments in binned segments of the genome, a profile arises that shows larger scale gains and losses. However, at low ctDNA fractions, it becomes difficult to distinguish CNV signals from background cfDNA, limiting its utility in early detection or cancers with low cfDNA levels (33,34).

DNA methylation is an epigenetic process that involves addition of a methyl molecule to a cytosine nucleotide, most frequently in a cytosine-phosphatequanine (CpG) context. Methylation is involved in gene expression, and certain cancers display unique methylation profiles. Methylation assays can be highly sensitive and specific for identifying tumour-related changes, especially as aberrant methylation is often an early event in cancer development. However, they require specialised laboratory steps like bisulfite or enzymatic conversion, reducing the yield of measurable cfDNA and complicating analysis (35).

The emerging field of cfDNA fragmentomics assesses the size, distribution, and sequence context of cfDNA fragments. ctDNA often exhibits characteristic fragmentation patterns, influenced by factors like gene expression and methylation (36,37). This approach holds promise for enhancing ctDNA detection sensitivity, even at low TF. However, fragmentomics can be computationally demanding, requiring sophisticated bioinformatic methods to interpret subtle patterns in the data. Additionally, it remains a relatively novel field with methodological variability, where the influence of pre-analytical factors are not well-described, creating challenges for standardized application in clinical settings (38–40).

Each of these markers has the potential to enhance ctDNA detection; however, they also present limitations in consistency, scalability, or practical implementation. For this thesis, we have chosen to mainly focus on SNVs due to their direct interpretability and the extensive technological framework already established for SNV detection

1.4 Applications of ctDNA analysis

At present, liquid tumour markers can be used along multiple stages of disease progression, performing different roles at each stage. These clinical stages broadly depend on the stage of disease that the patient presents in and are broadly characterized in terms of the amount of circulating ctDNA, and the availability of tumour tissue material, as outlined below.

1.4.1 Screening

The first and technically most challenging setting is that of screening. In population screening programs, individuals without symptoms of cancer are periodically screened for the presence of cancer. In this setting ctDNA offers potential as a minimally invasive method for early cancer detection, potentially screening for single or multiple cancers.

A major complicating factor in this setting is that there is a low pre-test probability of each screened individual to have the disease, posing stringent criteria on the positive predictive value (PPV) of a test: Of all the positive results, how many were true positive? In other words, the false positive rate of the test must at maximum be in the same order as the disease prevalence in the intended population, to prevent anxiety in a needlessly large group of people. This stringent criterium can be partially alleviated by using a two-test strategy, where the ctDNA test is used as a pre-screening or selection test for a second test. This can be a valuable strategy if the second test is considered more reliable but also more expensive or imposes a heavier patient burden, like low dose computed tomography (LDCT) for lung cancer, or endoscopic evaluation for colorectal cancer screening.

What further complicates this setting is that it must be tumour agnostic, requiring the test to detect generic cancer-related signals, rather than detecting specific signals known to originate from a particular tumour. The development of tests that perform well in a screening setting is still an area of active research, focussing on

procedures that drastically increase the number of data points per sample, such as genome-wide methylation and fragmentation assays (41–43). Current results using Grail's Galleri test – a methylation-based multi-cancer early detection test (MCED) show a limited sensitivity for detecting early stage disease (41). These results have given rise to a debate whether or not it is at all feasible to detect early stage cancers using cfDNA (44,45).

It could be argued that even if a test does not manage to detect all the early stage cancers, it is still better than the current practice - being an absence of any screening test for most cancers. After all, detecting 27% of early stage cancers is better than not detecting anything. In this debate it is worthwhile to remember that screening programs must first show to reduce cancer-related mortality, and do this at cost-effective levels (46). "All screening programmes do harm; some do good as well, and, of these, some do more good than harm at reasonable cost." (47).

1.4.2 Local disease

When a malignancy is discovered in an early stage, before it metastasises to distant organs, this presents opportunities for treatments with curative intent. The tumours in this stage are typically small and localised, therefore allowing surgery or radiotherapy as viable treatment options to cure the patient. At the same time precisely due to the limited size of the tumour - the tumour fraction of the cfDNA will typically be low, requiring sensitive technologies to detect the ctDNA.

Despite complete surgical resection of the tumour, not all patients are cured by this intervention, and a number may develop recurrence of disease. This proportion depends on the stage of the disease, and for example for NSCLC the 5-year recurrence free survival ranges from 81% in stage I disease to 34% in stage III (48). In lieu of better predictive biomarkers, adjuvant chemotherapy is offered to all patients diagnosed with stage II or III NSCLC, and withheld from patients with stage I disease (49). This leads to overtreatment in the first group, and undertreatment in the second group, highlighting a need for better biomarkers to select patients who will benefit from adjuvant treatment.

Post-surgical detection of ctDNA could identify patients with minimal residual disease (MRD), revealing the persistent presence of micrometastases that are invisible with radiographic imaging. Such patients could benefit from adjuvant chemotherapy, while patients without MRD could benefit from treatment de-escalation (50-53). Detection of MRD is analytically challenging due to the extremely low TF, requiring the tracking of many mutations at once with state-of-the-art technology.

When surgery is part of the multimodal treatment of these patients, this allows tissue-informed MRD testing where prior knowledge of the tumour's mutations can facilitate easier recall of these variants in the plasma cfDNA (54,55). While tissueinformed approaches can be highly sensitive, they are also expensive, laborious, and time-consuming, and ideally tumour-agnostic MRD tests are developed that reach the requisite analytical and clinical sensitivity. Beyond this, clinical utility must be shown by demonstrating that earlier detection of recurrence does lead to better outcomes for the patients (56).

In a slightly different clinical environment, an increasing number of NSCLC patients is treated with neo-adjuvant immune therapy before any surgery is conducted (57). Approximately 24% of patients respond so well to this treatment that the tumours are entirely gone by the time the surgery is performed. This is called pathological complete response (pCR), indicating that no viable tumour cells are seen in the resected tissue. These patients could have been spared the surgery, and detection of pCR before the surgery is a special form of MRD detection that is gaining interest (58).

1.4.3 Metastatic disease

In metastatic disease, the tumour load in the patient is typically high and this is reflected in the cfDNA. cfDNA measurements in this stage are often performed to detect targetable mutations in tumour driver genes such as EGFR (primarily in lung cancer) or KRAS (primarily in colorectal cancer). The list of targetable mutations that needs to be tested differs per disease, but includes mutations in EGFR, BRAF, KRAS, ERBB2, fusions in ALK, ROS1, RET, and amplification and exon 14-skipping in MET for NSCLC. For CRC, the list includes KRAS, NRAS, and BRAF, as well as mismatch repair deficiency and microsatellite instability (6,7,10,11,59).

Detection of specific EGFR mutations in patients with NSCLC makes them eligible for systemic treatment with small molecule inhibitors (SMIs), which selectively target cells presenting the mutation while leaving healthy cells without the mutation unaffected (59-61). Conversely, detection of KRAS mutations in patients with CRC makes them ineligible for treatment with monoclonal antibodies (mAbs) directed against EGFR (62-64). Eligibility for these therapies is tested in tissue biopsies from one of the metastatic lesions, but when these cannot be obtained due to patient condition or site of the lesions, national and international recommendations prescribe detection of these mutations in cfDNA since 2022 (65,66).

1.4.4 Recurrence

Patients with metastatic disease treated with targeted therapies like SMIs or mAbs often show clinical response to therapy: Tumour lesions shrink, sometimes even to undetectable levels. However, in many cases the disease will reappear later, even while the patient remains on targeted therapy. This can be caused by resistance mutations developing in the tumour under the selective pressure of the therapy. Tumour cells that acquire a resistance mutation are immune to the targeted therapy (67-69). For this reason, patients are often monitored periodically. This is not feasible with tissue biopsies and is classically done with imaging techniques instead. However, the imaging techniques used are not sensitive enough to detect small lesions, and measuring the cfDNA in the blood often detects the recurrence earlier than imaging does. Periodically measuring the cfDNA has the added advantage that it can also detect the specific resistance mutation causing the tumour's immunity to therapy, which in turn may allow the administration of second generation targeted therapies that are specific to cells that have that specific resistance mutation (67).

A complicating factor is that in many patients, more than one resistance mutation is detected (70,71). This co-occurrence of resistance mutations, both on-target (i.e. on the same gene as targeted by the therapy) and off-target, implies that multiple escape routes are possible for the tumour, complicating the selection of the next therapy.

1.5 Current limitations

While the analysis of ctDNA holds a lot of promises, and the potential is widely recognized, there are a number of steps that still prevent the widespread application of ctDNA in daily practice (72,73). The most important steps have been summarized in the 'road to implementation' (74). Among the steps in this roadmap are for example the adoption by peripheral hospitals, quality assurance certifications, and the reimbursement by insurance companies. These challenges are subdivided into several groups and discussed below.

1.5.1 Standardization and comparability

The clinical implementation of ctDNA testing is hindered by significant variability in procedures across laboratories, impacting sample collection, processing, and analytical methods. This lack of standardization complicates the comparison of ctDNA results across studies and clinical settings, potentially leading to inconsistent or conflicting outcomes. The establishment of universal protocols could improve reproducibility, but the diversity of detection technologies makes harmonization challenging.

Furthermore, the absence of well-established reference materials, such as standardized controls or calibrators, hampers consistency across platforms and labs. Developing and adopting such materials would enable cross-laboratory comparisons and improve the reliability of ctDNA assays (75). Until these reference standards are widely accepted, variability will continue to pose a barrier to the broad clinical utility of ctDNA testing.

1.5.2 Sensitivity and specificity

While recent advancements have improved the sensitivity of ctDNA assays, there remains a delicate balance between sensitivity (detecting low ctDNA fractions) and specificity (minimizing false positives). Early-stage cancers or cancers with lowshedding tumours present particularly challenging scenarios for ctDNA detection. as ctDNA levels are minimal, requiring ultra-sensitive assays. However, as sensitivity increases, so does the risk of detecting non-specific signals, which may lead to false positives.

Advanced error-correction techniques, while improving accuracy, often require greater sequencing depth and thus increase cost. Striking the right balance between sensitivity and specificity is particularly crucial in these clinical settings where ctDNA levels are minimal, requiring highly optimized detection strategies.

1.5.3 Data interpretation

Another challenge to the clinical implementation of ctDNA testing lies in the complexity of data interpretation. The increasing sophistication of ctDNA assays often incorporating features like UMIs, error-correction algorithms, and multibiomarker integration—requires advanced bioinformatics pipelines, expertise, and significant computational resources that are not typically available in routine diagnostic laboratories.

Additionally, interpreting discrepant or ambiguous results can pose challenges for clinicians. Plasma-derived results may not always align with tissue findings or may show conflicting signals over time—for instance, one mutation increasing in abundance while another decreases. Such cases complicate treatment decisions, as they might reflect tumour heterogeneity, biological variability, or assay limitations.

Addressing these challenges requires streamlined, user-friendly bioinformatics tools, better training for clinical staff, and robust guidelines for managing discordant results. These improvements are essential for enabling accurate and actionable ctDNA analysis in clinical practice.

1.5.4 Cost and accessibility

The high costs associated with ctDNA testing—due to sequencing depth requirements, reagents, and specialized equipment—represent a major limitation, not only in low-income countries but also in well-resourced healthcare settings. Reducing costs without sacrificing test sensitivity or specificity is challenging. While some targeted approaches like droplet digital PCR can reduce expenses for known mutations, broader applications often require high-throughput sequencing and error correction, raising costs. Accessibility is further hindered by insurance and reimbursement barriers in many healthcare systems. Developing cost-effective vet robust methods is crucial for broadening ctDNA testing's accessibility and making it a viable option for routine clinical care.

1.5.5 Implementation hurdles

Successful integration of ctDNA testing into clinical practice also faces challenges in terms of validation and clinician adoption. For ctDNA assays to be trusted in treatment decisions, they must undergo extensive validation across different cancer types, stages, and patient populations to demonstrate consistent performance. This clinical validation requires robust studies, which can be resource-intensive and time-consuming.

Additionally, integrating ctDNA testing into clinical workflows demands training and education for clinicians, particularly in interpreting ctDNA results and integrating them with other diagnostic tools. Moreover, regulatory pathways and reimbursement policies for ctDNA tests vary widely, influencing the feasibility of broad clinical implementation. Overcoming these logistical and regulatory barriers is necessary for ctDNA testing to become a routine component of cancer care.

1.5.6 Rationale for optimization

Given these challenges, optimizing ctDNA detection methods presents an opportunity to address several of these barriers simultaneously. By refining the technologies and bioinformatics tools that underlie ctDNA testing, we can improve assay sensitivity and specificity, enhance data interpretation, and potentially lower costs through better use of existing ctDNA data, maximizing the insights that can be drawn from a single sample.

As the field continues to evolve, addressing these barriers will be essential for ctDNA to fulfil its potential as a widely accessible and effective tool for cancer detection and monitoring. Part of the solution may lie in the development of increasingly powerful technologies, such as dramatically cheaper sequencing or

even more accurate polymerases. However, part of the solution also lies in better usage of the data that are already available, and in combining data streams from different sources more effectively (72).

1.6 Thesis outline

In this thesis, we present multiple efforts to optimize the performance of cfDNA analysis methods in solid malignancies. These efforts include comparisons between existing methods, as well as the development of new data analysis procedures where these tools did not exist before.

One of the early workhorses of ctDNA analyses is ddPCR. Due to its ability to partition each experiment into almost 20,000 picoliter sized droplets, detection of even single molecules carrying a mutation in a much larger pool of non-mutated wildtype molecules was suddenly child's play with a relatively simple endpoint PCR reaction. However, validation efforts from most labs and the use recommendations from the vendor employed a simplistic threshold approach to distinguish positive samples from negative samples. In Chapter 2 we describe that by employing a thorough validation of our assays and a sophisticated post-hoc analysis, we were able to identify polymerase induced errors in the data. We wrote an R script termed ALPACA that corrects these errors and validate it using both synthetic samples and patient samples.

Next to ddPCR, other assays exist that aim to detect hotspot mutations. It is challenging to make a fair and unbiased comparison between these different assays, due to the different analytical and preanalytical requirements, and data processing procedures of each assay. In Chapter 3 we perform a head-on comparison between four hotspot mutation detection assays, in this case targeting the KRAS gene, in the setting of metastatic colorectal cancer. The methods compared are BEAMing, COBAS z480, ddPCR, and Idylla, each with different strengths and shortcomings.

In the setting of primary metastatic non-small cell lung cancer (mNSCLC) it's in national and international guidelines that patients receive a diagnostic test to see whether they have mutations in a number of genes. For this reason, single-locus hotspot mutation tests are not sufficient, and the tumour tissue biopsy material is usually tested with a broader targeted NGS panel. However, tissue biopsies are not always feasible, or do not yield sufficient material to perform all the different diagnostic tests that the pathologist wants to perform. In Chapter 4 we investigate how molecular profiling of the plasma ctDNA can complement the standard-ofcare tissue molecular profiling.

In localized NSCLC, patients with stage II-IIIA disease are offered surgery with curative intent. One of the great challenges of ctDNA analyses is to detect minimal residual disease (MRD) after removal of the tumour in this setting. By sequencing the cfDNA prior to surgery and after surgery, as well as the tumour resected tissue material and the hematopoietic cells, we aim to detect MRD in Chapter 5. By combining data streams from both mutation detection and fragment length analyses, we improve the performance of our method.

Finally, in **Chapter 6** we summarize, discuss and conclude the thesis, and discuss some exciting future directions that we feel the field is moving towards.

References

- International Agency for Research on Cancer. Cancer Today comprehensive assessment of cancer burden worldwide in 2022, based on GLOBOCAN estimates in 185 countries [Internet]. [cited 2024 Mar 21]. Available from: https://gco.iarc.fr/today/en
- IKNL. Nederlandse Kankerregistratie (NKR) [Internet]. [cited 2024 Oct 31]. Available from: nkr-2 cijfers.iknl.nl
- 3. Siegel RL, Giaguinto AN, Jemal A. Cancer statistics, 2024. CA Cancer J Clin. 2024 Jan;74(1):12–49.
- European Commission. European Commission Personalised medicine (website) [Internet]. [cited 4. 2024 Jun 27]. Available from: https://health.ec.europa.eu/medicinal-products/personalisedmedicine en
- Haslam A, Kim MS, Prasad V. Updated estimates of eligibility for and response to genome-targeted oncology drugs among US cancer patients, 2006-2020. Ann Oncol. 2021 Jul;32(7):926-32.
- ASCO. Molecular Testing for the Selection of Patients With Lung Cancer for Treatment With Targeted Tyrosine Kinase Inhibitors Guideline Endorsement [Internet]. [cited 2024 Jun 27]. Available from: https://society.asco.org/practice-patients/quidelines/molecular-testing-andbiomarkers#/9776
- Lindeman NI, Cagle PT, Aisner DL, Arcila ME, Beasley MB, Bernicker EH, et al. Updated Molecular Testing Guideline for the Selection of Lung Cancer Patients for Treatment With Targeted Tyrosine Kinase Inhibitors. J Thorac Oncol. 2018 Mar;13(3):323-58.
- NVALT. KNT-lijst NSCLC versie 2 2024-01-08 [Internet]. [cited 2024 Aug 8]. Available from: https:// www.nvalt.nl/vereniging/beleid/belangrijke-documenten/ /Klinische%20Noodzakelijke%20 Targets/KNT-lijst%20NSCLC%20versie%202%202024-01-08.pdf
- Integraal Kankercentrum Nederland I. Landelijke richtlijn niet kleincellig longcarcinoom. [Internet]. Available from: https://iknl.nl/nkr/evaluatie-met-nkr-data/richtlijnen
- 10. Sepulveda AR, Hamilton SR, Allegra CJ, Grody W, Cushman-Vokoun AM, Funkhouser WK, et al. Molecular Biomarkers for the Evaluation of Colorectal Cancer: Guideline Summary From the American Society for Clinical Pathology, College of American Pathologists, Association for Molecular Pathology, and American Society of Clinical Oncology. J Oncol Pract. 2017 May;13(5):333-7.
- 11. Leighl NB, Page RD, Raymond VM, Daniel DB, Divers SG, Reckamp KL, et al. Clinical Utility of Comprehensive Cell-free DNA Analysis to Identify Genomic Biomarkers in Patients with Newly Diagnosed Metastatic Non-small Cell Lung Cancer. Clin Cancer Res. 2019 Aug 1;25(15):4691-700.
- 12. Merker JD, Oxnard GR, Compton C, Diehn M, Hurley P, Lazar AJ, et al. Circulating Tumor DNA Analysis in Patients With Cancer: American Society of Clinical Oncology and College of American Pathologists Joint Review. J Clin Oncol. 2018 Jun 1;36(16):1631-41.
- 13. Cescon DW, Bratman SV, Chan SM, Siu LL. Circulating tumor DNA and liquid biopsy in oncology. Nat Cancer. 2020 Mar 20;1(3):276-90.
- 14. García-Pardo M, Makarem M, Li JJN, Kelly D, Leighl NB. Integrating circulating-free DNA (cfDNA) analysis into clinical practice: opportunities and challenges. Br J Cancer. 2022 Sep 1;127(4):592-602.
- 15. Heitzer E, Ulz P, Geigl JB. Circulating Tumor DNA as a Liquid Biopsy for Cancer. Clin Chem. 2015 Jan 1;61(1):112-23.
- 16. Nikanjam M, Kato S, Kurzrock R. Liquid biopsy: current technology and clinical applications. J Hematol Oncol J Hematol Oncol. 2022 Sep 12;15(1):131.

- 17. Tivey A, Church M, Rothwell D, Dive C, Cook N. Circulating tumour DNA looking beyond the blood. Nat Rev Clin Oncol. 2022 Sep;19(9):600-12.
- 18. Bettegowda C, Sausen M, Leary RJ, Kinde I, Wang Y, Agrawal N, et al. Detection of Circulating Tumor DNA in Early- and Late-Stage Human Malignancies. Sci Transl Med [Internet]. 2014 Feb 19 [cited 2023 Sep 7];6(224). Available from: https://www.science.org/doi/10.1126/scitranslmed.3007094
- 19. Avanzini S, Kurtz DM, Chabon JJ, Moding EJ, Hori SS, Gambhir SS, et al. A mathematical model of ctDNA shedding predicts tumor detection size. Sci Adv. 2020 Dec;6(50):eabc4308.
- 20. Boniface CT, Spellman PT. Blood, Toil, and Taxoteres: Biological Determinants of Treatment-Induced ctDNA Dynamics for Interpreting Tumor Response. Pathol Oncol Res. 2022 May 19:28:1610103.
- 21. Nabavizadeh SA, Ware JB, Guiry S, Nasrallah MP, Mays JJ, Till JE, et al. Imaging and histopathologic correlates of plasma cell-free DNA concentration and circulating tumor DNA in adult patients with newly diagnosed glioblastoma. Neuro-Oncol Adv. 2020 Jan 1;2(1):vdaa016.
- 22. Kustanovich A, Schwartz R, Peretz T, Grinshpun A. Life and death of circulating cell-free DNA. Cancer Biol Ther. 2019 Aug 3;20(8):1057-67.
- 23. Khier S, Lohan L. Kinetics of Circulating Cell-Free DNA for Biomedical Applications: Critical Appraisal of the Literature. Future Sci OA. 2018 Apr;4(4):FSO295.
- 24. Taylor SC, Laperriere G, Germain H. Droplet Digital PCR versus gPCR for gene expression analysis with low abundant targets: from variable nonsense to publication quality data. Sci Rep. 2017 May 25;7(1):2409.
- 25. Hou Y, Chen S, Zheng Y, Zheng X, Lin JM. Droplet-based digital PCR (ddPCR) and its applications. TrAC Trends Anal Chem. 2023 Jan;158:116897.
- 26. Diehl F, Li M, He Y, Kinzler KW, Vogelstein B, Dressman D. BEAMing: single-molecule PCR on microparticles in water-in-oil emulsions. Nat Methods. 2006 Jul;3(7):551–9.
- 27. Richardson AL, Iglehart JD. BEAMing Up Personalized Medicine: Mutation Detection in Blood. Clin Cancer Res. 2012 Jun 15;18(12):3209-11.
- 28. Janku F, Claes B, Huang HJ, Falchook GS, Devogelaere B, Kockx M, et al. BRAF mutation testing with a rapid, fully integrated molecular diagnostics system. Oncotarget. 2015 Sep 29;6(29):26886-94.
- 29. Newman AM, Bratman SV, To J, Wynne JF, Eclov NCW, Modlin LA, et al. An ultrasensitive method for quantitating circulating tumor DNA with broad patient coverage. Nat Med. 2014 May;20(5):548-54.
- 30. Newman AM, Lovejoy AF, Klass DM, Kurtz DM, Chabon JJ, Scherer F, et al. Integrated digital error suppression for improved detection of circulating tumor DNA. Nat Biotechnol. 2016 May;34(5):547-55.
- 31. Phallen J, Sausen M, Adleff V, Leal A, Hruban C, White J, et al. Direct detection of early-stage cancers using circulating tumor DNA. Sci Transl Med. 2017 Aug 16;9(403):eaan2415.
- 32. Paweletz CP, Sacher AG, Raymond CK, Alden RS, O'Connell A, Mach SL, et al. Bias-Corrected Targeted Next-Generation Sequencing for Rapid, Multiplexed Detection of Actionable Alterations in Cell-Free DNA from Advanced Lung Cancer Patients. Clin Cancer Res. 2016 Feb 15;22(4):915–22.
- 33. Adalsteinsson VA, Ha G, Freeman SS, Choudhury AD, Stover DG, Parsons HA, et al. Scalable whole-exome sequencing of cell-free DNA reveals high concordance with metastatic tumors. Nat Commun. 2017 Nov 6;8(1):1324.

- 34. Peng H, Lu L, Zhou Z, Liu J, Zhang D, Nan K, et al. CNV Detection from Circulating Tumor DNA in Late Stage Non-Small Cell Lung Cancer Patients. Genes. 2019 Nov 14;10(11):926.
- 35. Nassar FJ, Msheik ZS, Nasr RR, Temraz SN. Methylated circulating tumor DNA as a biomarker for colorectal cancer diagnosis, prognosis, and prediction. Clin Epigenetics. 2021 Dec;13(1):111.
- 36. Noë M. Mathios D. Annapragada AV. Koul S. Foda ZH, Medina JE, et al. DNA methylation and gene expression as determinants of genome-wide cell-free DNA fragmentation. Nat Commun. 2024 Aug 6;15(1):6690.
- 37. Che H, Jiang P, Choy LYL, Cheng SH, Peng W, Chan RWY, et al. Genomic origin, fragmentomics, and transcriptional properties of long cell-free DNA molecules in human plasma. Genome Res. 2024 Feb;34(2):189-200.
- 38. Lo YMD, Han DSC, Jiang P, Chiu RWK. Epigenetics, fragmentomics, and topology of cell-free DNA in liquid biopsies. Science. 2021 Apr 9;372(6538):eaaw3616.
- 39. Snyder MW, Kircher M, Hill AJ, Daza RM, Shendure J. Cell-free DNA Comprises an In Vivo Nucleosome Footprint that Informs Its Tissues-Of-Origin. Cell. 2016 Jan;164(1-2):57-68.
- 40. Chiu RWK, Heitzer E, Lo YMD, Mouliere F, Tsui DWY. Cell-Free DNA Fragmentomics: The New "Omics" on the Block. Clin Chem. 2020 Dec 1;66(12):1480-4.
- 41. Klein EA, Richards D, Cohn A, Tummala M, Lapham R, Cosgrove D, et al. Clinical validation of a targeted methylation-based multi-cancer early detection test using an independent validation set. Ann Oncol. 2021 Sep;32(9):1167-77.
- 42. Carroll LN, Piscitello A, Chandra T, Putcha G. Adenoma detection improves clinical outcomes across adherence scenarios for a CRC screening blood test meeting CMS performance targets: Results from the CRC-MAPS model [Internet]. Poster presented at: Digestive Disease Week (DDW); 2022 May 20; San Diego, CA, USA. Available from: https://www.freenome.com/wp-content/ uploads/1706/09/22-1207CRC-MAPSCMStargetsDDW v8.pdf
- 43. Mazzone PJ, Bach PB, Carey J, Schonewolf CA, Bognar K, Ahluwalia MS, et al. Clinical validation of a cell-free DNA fragmentome assay for augmentation of lung cancer early detection. Cancer Discov [Internet]. 2024 Jun 3 [cited 2024 Jun 6]; Available from: https://aacrjournals.org/ cancerdiscovery/article/doi/10.1158/2159-8290.CD-24-0519/745696/Clinical-validation-of-acell-free-DNA-fragmentome
- 44. Pons-Belda OD, Fernandez-Uriarte A, Diamandis EP. Can Circulating Tumor DNA Support a Successful Screening Test for Early Cancer Detection? The Grail Paradigm. Diagnostics. 2021 Nov 23;11(12):2171.
- 45. Turning the tide of early cancer detection. Nat Med. 2024 May;30(5):1217–1217.
- 46. Turnbull C, Wald N, Sullivan R, Pharoah P, Houlston RS, Aggarwal A, et al. GRAIL-Galleri: why the special treatment? The Lancet. 2024 Feb;403(10425):431-2.
- 47. Gray JAM, Patnick J, Blanks RG. Maximising benefit and minimising harm of screening. BMJ. 2008 Mar 1;336(7642):480-3.
- 48. Rajaram R, Huang Q, Li RZ, Chandran U, Zhang Y, Amos TB, et al. Recurrence-Free Survival in Patients With Surgically Resected Non-Small Cell Lung Cancer. CHEST. 2024 May;165(5):1260–70.
- Pignon JP, Tribodet H, Scagliotti GV, Douillard JY, Shepherd FA, Stephens RJ, et al. Lung Adjuvant Cisplatin Evaluation: A Pooled Analysis by the LACE Collaborative Group, J Clin Oncol, 2008 Jul 20;26(21):3552-9.
- 50. Chae YK, Oh MS. Detection of Minimal Residual Disease Using ctDNA in Lung Cancer: Current Evidence and Future Directions. J Thorac Oncol. 2019 Jan;14(1):16-24.

- 51. Chaudhuri AA, Chabon JJ, Lovejoy AF, Newman AM, Stehr H, Azad TD, et al. Early Detection of Molecular Residual Disease in Localized Lung Cancer by Circulating Tumor DNA Profiling, Cancer Discov. 2017 Dec 1:7(12):1394-403.
- 52. Leal A, Van Grieken NCT, Palsgrove DN, Phallen J, Medina JE, Hruban C, et al. White blood cell and cell-free DNA analyses for detection of residual disease in gastric cancer. Nat Commun. 2020 Jan 27;11(1):525.
- 53. Pellini B, Chaudhuri AA. Circulating Tumor DNA Minimal Residual Disease Detection of Non-Small-Cell Lung Cancer Treated With Curative Intent. J Clin Oncol. 2022 Feb 20;40(6):567–75.
- 54. Haystack Oncology, Haystack Oncology website [Internet], [cited 2024 Apr 26]. Available from: https://haystackmrd.com/biopharma/
- 55. Marsico G, Sharma G, Perry M, Hackinger S, Forshew T, Howarth K, et al. Analytical development of the RaDaR assay, a highly sensitive and specific assay for the monitoring of minimal residual disease. [Internet]. Proceedings of the Annual Meeting of the American Association for Cancer Research 2020; 2020 Apr 27-28 and Jun 22-24. Philadelphia (PA): AACR; Cancer Res 2020;80(16 Suppl): Abstract nr 3097; 2020. Available from: https://www.inivata.com/wp-content/ uploads/2020/06/AACR_2020_poster_3097.pdf
- 56. Sorscher S. Clinical Utility of Circulating Tumor DNA Assays. J Clin Oncol. 2024 Sep. 11:JCO.24.01175.
- 57. Banna GL, Hassan MA, Signori A, Giunta EF, Maniam A, Anpalakhan S, et al. Neoadjuvant Chemo-Immunotherapy for Early-Stage Non-Small Cell Lung Cancer: A Systematic Review and Meta-Analysis. JAMA Netw Open. 2024 Apr 16;7(4):e246837.
- 58. Forde PM, Spicer J, Lu S, Provencio M, Mitsudomi T, Awad MM, et al. Neoadjuvant Nivolumab plus Chemotherapy in Resectable Lung Cancer. N Engl J Med. 2022 May 26;386(21):1973-85.
- 59. IKNL. Landelijke richtlijn niet kleincellig longcarcinoom [Internet]. 2015. Available from: https:// www.oncoline.nl/niet-kleincellig-longcarcinoom
- 60. Novello S, Barlesi F, Califano R, Cufer T, Ekman S, Levra MG, et al. Metastatic non-small-cell lung cancer: ESMO Clinical Practice Guidelines for diagnosis, treatment and follow-up. Ann Oncol. 2016 Sep;27:v1-27.
- 61. Planchard D, Popat S, Kerr K, Novello S, Smit EF, Faivre-Finn C, et al. Metastatic non-small cell lung cancer: ESMO Clinical Practice Guidelines for diagnosis, treatment and follow-up. Ann Oncol. 2018 Oct;29:iv192-237.
- 62. Biller LH, Schrag D. Diagnosis and Treatment of Metastatic Colorectal Cancer: A Review. JAMA. 2021 Feb 16:325(7):669.
- 63. Douillard JY, Oliner KS, Siena S, Tabernero J, Burkes R, Barugel M, et al. Panitumumab-FOLFOX4 Treatment and RAS Mutations in Colorectal Cancer. N Engl J Med. 2013 Sep 12;369(11):1023–34.
- 64. Cervantes A, Adam R, Roselló S, Arnold D, Normanno N, Taïeb J, et al. Metastatic colorectal cancer: ESMO Clinical Practice Guideline for diagnosis, treatment and follow-up. Ann Oncol. 2023 Jan;34(1):10-32.
- 65. cieBOD. CieBOD advies ctDNA in bloedplasma voor primaire predictieve analyse bij NSCLC [Internet]. 2024 [cited 2024 Aug 1]. Available from: https://pathologie.nl/wp-content/ uploads/2024/07/CieBOD-advies-ctDNA-bij-NSCLC-versie-1-12062024-voor-publicatie.pdf
- 66. Pascual J, Attard G, Bidard FC, Curigliano G, De Mattos-Arruda L, Diehn M, et al. ESMO recommendations on the use of circulating tumour DNA assays for patients with cancer: a report from the ESMO Precision Medicine Working Group. Ann Oncol. 2022 Aug;33(8):750-68.
- 67. Passaro A, Jänne PA, Mok T, Peters S. Overcoming therapy resistance in EGFR-mutant lung cancer. Nat Cancer. 2021 Apr 15;2(4):377-91.

- 68. Recondo G, Bahcall M, Spurr LF, Che J, Ricciuti B, Leonardi GC, et al. Molecular Mechanisms of Acquired Resistance to MET Tyrosine Kinase Inhibitors in Patients with MET Exon 14-Mutant NSCLC. Clin Cancer Res. 2020 Jun 1;26(11):2615-25.
- 69. Yang Y, Li S, Wang Y, Zhao Y, Li Q. Protein tyrosine kinase inhibitor resistance in malignant tumors: molecular mechanisms and future perspective. Signal Transduct Target Ther. 2022 Sep. 17;7(1):329.
- 70. Chmielecki J, Mok T, Wu YL, Han JY, Ahn MJ, Ramalingam SS, et al. Analysis of acquired resistance mechanisms to osimertinib in patients with EGFR-mutated advanced non-small cell lung cancer from the AURA3 trial. Nat Commun. 2023 Feb 27;14(1):1071.
- 71. Enrico DH, Lacroix L, Rouleau E, Scoazec JY, Loriot Y, Tselikas L, et al. Multiple synchronous mechanisms may contribute to osimertinib resistance in non-small cell lung cancer (NSCLC) patients: Insights of the MATCH-R study. Ann Oncol. 2019 Oct;30:v627.
- 72. Heitzer E, Van Den Broek D, Denis MG, Hofman P, Hubank M, Mouliere F, et al. Recommendations for a practical implementation of circulating tumor DNA mutation testing in metastatic nonsmall-cell lung cancer. ESMO Open. 2022 Apr;7(2):100399.
- 73. Abbosh C, Birkbak NJ, Swanton C. Early stage NSCLC challenges to implementing ctDNAbased screening and MRD detection. Nat Rev Clin Oncol. 2018 Sep;15(9):577-86.
- 74. COIN consortium. ctDNA on the road to implementation in The Netherlands COIN website [Internet]. [cited 2024 Jun 13]. Available from: https://cfdna.nl/coin-home-english/
- 75. Stetson D, Labrousse P, Russell H, Shera D, Abbosh C, Dougherty B, et al. Next-Generation Molecular Residual Disease Assays: Do We Have the Tools to Evaluate Them Properly? J Clin Oncol. 2024 Aug 10;42(23):2736-40.



Chapter 2

An Automated Correction Algorithm (ALPACA) for ddPCR Data Using Adaptive Limit of Blank and Correction of False Positive Events Improves Specificity of Mutation Detection

D.C.L. Vessies¹, T.C. Linders¹, M. Lanfermeijer¹, K.L. Ramkisoensing¹, V. van der Noort², R.D. Schouten³, G.A. Meijer⁴, M.M. van den Heuvel⁵, K. Monkhorst⁴ & D. van den Broek¹

¹ Netherlands Cancer Institute, department of laboratory medicine, Amsterdam, the Netherlands

² Netherlands Cancer Institute, biometrics department, Amsterdam, the Netherlands

³ Netherlands Cancer Institute, department of pulmonology, Amsterdam, The Netherlands

⁴ Netherlands Cancer Institute, department of pathology, Amsterdam, The Netherlands

⁵ Radboud University Medical Center, department of pulmonology, Nijmegen, The Netherlands

Abstract

Background

Bio-Rad droplet-digital PCR is a highly sensitive method that can be used to detect tumor mutations in circulating cell-free DNA (cfDNA) of patients with cancer. Correct interpretation of ddPCR results is important for optimal sensitivity and specificity. Despite its widespread use, no standardized method to interpret ddPCR data is available, nor have technical artifacts affecting ddPCR results been widely studied.

Methods

False positive rates were determined for 6 ddPCR assays at variable amounts of input DNA, revealing polymerase induced false positive events (PIFs) and other false positives. An in silico correction algorithm, known as the adaptive LoB and PIFs: an automated correction algorithm (ALPACA), was developed to remove PIFs and apply an adaptive limit of blank (LoB) to individual samples. Performance of ALPACA was compared to a standard strategy (no PIF correction and static LoB = 3) using data from commercial reference DNA, healthy volunteer cfDNA, and cfDNA from a real-life cohort of 209 patients with stage IV nonsmall cell lung cancer (NSCLC) whose tumor and cfDNA had been molecularly profiled.

Results

Applying ALPACA reduced false positive results in healthy cfDNA compared to the standard strategy (specificity 98 vs 88%, $P = 10^{-5}$) and stage IV NSCLC patient cfDNA (99 vs 93%, $P = 10^{-11}$), while not affecting sensitivity in commercial reference DNA (70 vs 68% P = 0.77) or patient cfDNA (82 vs 88%, P = 0.13). Overall accuracy in patient samples was improved (98 vs 92%, $P = 10^{-7}$).

Conclusions

Correction of PIFs and application of an adaptive LoB increases specificity without a loss of sensitivity in ddPCR, leading to a higher accuracy in a real-life cohort of patients with stage IV NSCLC.

Introduction

Bio-Rad droplet-digital PCR (ddPCR) is a sensitive and quantitative method for the detection of variants with low variant allele frequencies (VAF) (1,2). For this reason, it is often used for the detection of mutations in circulating cell-free DNA (cfDNA).

The concept of ddPCR is that DNA molecules are randomly distributed over 10 000–20 000 droplets (2,3). A PCR reaction driven by Tag polymerase amplifies the target molecules, and absence or presence of the target mutation is signaled by wildtype and mutation specific tagman hydrolysis probes labeled with hexachlorofluorescein (HEX) and fluorescein amidites (FAM) fluorescence, respectively. Subsequently, each droplet's fluorescence is individually measured, allowing for the detection of minute quantities of target molecules. In this way, ddPCR can detect rare (low VAF) mutations, making it especially useful for the detection of low abundant tumor-derived cfDNA in blood samples (1,4–6).

One of the challenges of this approach is to distinguish a true positive from a false positive signal. It has been noted that mutation positive droplets (events) can occur in wildtype-only experiments (2,3,7), underlining the need for an optimal cutoff that prevents false positive results yet preserves a high analytical sensitivity. Different strategies have been described in literature and recommendations are given by the manufacturer (2,8–13), but none of these strategies takes into account technical artifacts and concentration dependent effects.

In this study, we report the occurrence of polymerase induced false positive events (PIFs) and an input dependent increase in PIFs in ddPCR experiments. Based on this observation, we developed a novel ddPCR data interpretation algorithm (adaptive LoB and PIFs: an automated correction algorithm, ALPACA) that combines corrections for assay specific error rates and technical artifacts. Its performance was compared to the standard ddPCR data analysis strategy suggested by the manufacturer.

Materials and methods

Healthy Donors and Patient Enrollment

Plasma and serum from healthy donors were obtained under informed consent, in accordance with the declaration of Helsinki and as approved by the medical ethics committee (METC) of the Netherlands Cancer Institute (NKI; Amsterdam, the Netherlands). All patients were enrolled with written informed consent as part of the Lung Cancer Early Molecular Assessment Trial (LEMA; ClinicalTrials.gov NCT02894853), which was reviewed and approved by METC of the NKI. A subgroup of the LEMA cohort, consisting of the first consecutive cohort of 209 patients with confirmed stage IV nonsmall cell lung cancer (NSCLC) for whom pretreatment plasma was available, was used in this study.

Blood collection, cfDNA isolation, and ddPCR procedure are described in the online Supplemental Methods, and dMIOE2020 adherence in Table 4 in the online Data Supplement (14). Briefly, cfDNA was isolated using the QIAsymphony (Qiagen) and ddPCR was performed using the QX100 instruments (Bio-Rad Laboratories Inc.).

Phase 1: Designing the ALPACA Algorithm

Experiments

The ALPACA algorithm was designed using EP17 experiments (15), as follows: commercial wildtype DNA (Horizon Discovery Ltd) or mutant DNA (gBlock Gene Fragments, Integrated DNA Technologies Inc.) was measured in 60-fold in 2-4 concentrations per assay, ranging from 5 to 472 copies/µL (0.4–24.5 ng/well). Droplet counts from 60 wells were combined and analyzed as a single result.

PIF correction

The EP17 results were corrected for PIFs as follows: assuming that mutant molecules are randomly distributed over the droplets, the ratio of FAM-only vs FAM&HEX positive droplets was expected to be equal to the ratio of empty vs HEX-only positive droplets (2, 3). The cumulative binomial probability (P) to observe each ratio of FAM vs FAM&HEX given the ratio of empty vs HEX droplets was calculated. For any experiment where P was smaller than 0.1, the maximum number of FAM&HEX droplets was calculated for which we would have $P \ge 0.1$. All excess FAM&HEX droplets (the difference between the observed number and the calculated maximum expected number) were defined as PIFs and were treated as HEX-only droplets in all further analyses. The limit of P = 0.1 was determined based on performance on the EP17 training data.

Adaptive LoB

Any FAM-positive droplets remaining after PIF correction were considered false positive droplets in the EP17 experiments. The false positive rate (FPR) was calculated as the number of mutant molecules per wildtype molecule for each assay at 2-4 concentrations per assay.

For all subsequent experiments, the droplet counts from each replicate were added up and the PIFs were removed as described. The adaptive LoB was calculated as 99.9% binomial upper confidence limit of the expected number of false positive droplets, given the FPR of the EP17 experiment with the concentration closest to the concentration of the sample. This limit was determined based on performance on the EP17 training data.

A mutation was called positive if the number of remaining FAM-positive droplets after PIF removal was equal to or greater than the adaptive LoB. PIF removal and the adaptive LoB were applied sequentially in an R algorithm called ALPACA, made available in GitHub: https://github.com/DCLVessies/ALPACA.git (Fig. 1).

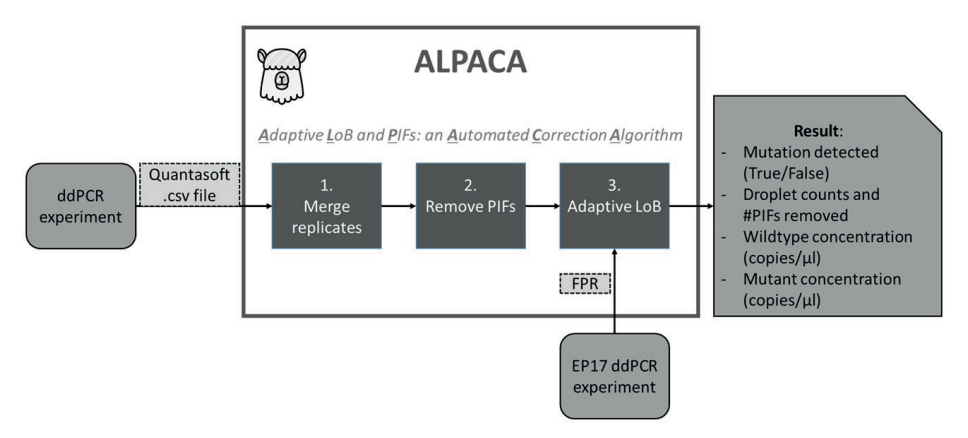


Figure 1. ALPACA is an automated algorithm in R that takes the .csv files generated by QuantaSoft as input, merges replicates, removes PIFs, and applies an adaptive LoB based on the sample-specific FPR.

Phase 2: Validation of ALPACA

The analytical performance of ALPACA was compared to the manufacturer's standard strategy (2), which used no PIF correction and called a mutation when 3 or more FAM-positive droplets were present in a duplicate experiment and the corresponding blank experiment had no positive droplets. Three data sets were used for the evaluation: (a) commercial reference DNA to assess sensitivity of the 2 strategies; (b) cfDNA from healthy donors to assess specificity; and (c) stage IV NSCLC patient cfDNA to assess diagnostic accuracy in a real-world setting.

Commercial reference DNA

Wildtype (catalog no. HD124, HD249) and mutant DNA for EGFR p. E746-A750del (HD251), EGFR p. T790M (HD258), EGFR p. L858R (HD254), and BRAF p. V600E (HD238) were acquired commercially (Horizon Discovery Ltd). Wildtype and mutant DNA were mixed to obtain different levels of mutant DNA: 4.0, 0.3, 0.1, and 0.02 mutant copies/µL in a final concentration of about 11 wildtype copies/µL (0.7 ng/ well), and 0.3, 0.03, and 0 mutant copies/µL in a final concentration of 300 wildtype copies/µL (20 ng/well). Five duplicates (10 wells) of each sample were measured with the relevant ddPCR assay (Bio-Rad, Supplemental Methods). Each duplicate was considered a single result, for a total of n = 30 results per assay. Sensitivity of ALPACA and the standard strategy was defined as the fraction of results in which the mutation was detected.

Healthy cfDNA

Healthy donor plasma and serum cfDNA was acquired as described in the Supplemental Methods. The cfDNA yield was not determined, and 9 µL of sample was used as input for ddPCR, leading to a median plasma/serum equivalent input of 0.5 mL (IQR 0.5-0.5 mL). Specificity was defined as the fraction of results in which no mutation was detected.

NSCLC patient cfDNA

Patient enrolment, blood collection, and cfDNA isolation are described in the online Supplemental Methods. Plasma cfDNA molecular profiling (PMP) was performed with the AVENIO ctDNA Targeted kit (Roche), using up to 50 ng cfDNA input (median 39 ng, IQR 28-50 ng). 17 genes were enriched with capture hybridization and sequenced to median 19000 depth (IQR 17000-22000), median 5900 unique depth after deduplication (IQR 4300–7600).

Decentralized tissue molecular profiling (TMP) was performed according to the standard of care in the hospital of enrolment. According to national and international quidelines TMP should include known NSCLC oncodriver genes, including among others KRAS and EGFR (16-18). The methods of TMP were dependent on the quantity and quality of available tumour tissue and local laboratory preferences. TMP results were obtained from the clinical pathology reports.

Mutations detected with either PMP or TMP were considered true mutations. Mutations not detected with either method were considered true negatives. An independent sample of up to 4 mL of plasma (from the same blood draw as PMP) was used for ddPCR as described in the Supplemental Methods. This cfDNA was measured with 4 ddPCR assays [EGFR p. L858R, EGFR p. T790M, KRAS p. G12/ G13 screening (Bio-Rad), and EGFR exon19 del drop-off (IDT) (19)], such that the equivalent of median 1 mL of plasma was used per assay (IQR 0.88-1 mL). The median concentration in ddPCR was 71 copies/μL (IQR 49–146 copies/μL), corresponding to median 4.8 ng/well (IQR 3.3-9.7 ng/well). 49 patients (24%) had cfDNA concentration greater than 10 ng/well. Accuracy of ALPACA and the standard strategy were calculated as agreement with the molecular profiling (PMP+TMP) results.

Statistical Methods

ddPCR results were analyzed in QuantaSoft (Bio-Rad) as described in the Supplemental Methods. Mutation calls were interpreted by the ALPACA algorithm or the standard strategy where 3 FAM-positive droplets constitute a positive mutation call.

Statistical significance levels of the differences in sensitivity, specificity, and accuracy were assessed using the McNemar test with continuity correction. Statistical significance of differences in negative and positive predictive values were assessed using a weighted generalized score using compbdt (20). ALPACA and all statistical tests were performed in R v.3.6.0. (21).

Results

Polymerase Induced FAM&HEX Positive Droplets (PIFs)

The FPR of EGFR p. T790M, EGFR p. L858R, EGFR p. E746 A750del, BRAF p. V600E, KRAS G12/G13 screening, and EGFR exon 19 deletion drop-off assays were determined according to the CLSI EP17 protocol using different amounts of wildtype reference DNA (range 0.4-24.5 ng/well). The number of mutant positive droplets differed per assay and increased with the amount of wildtype reference DNA present in the PCR reaction.

Mutant positive droplets showed a skew toward FAM&HEX vs FAM-only droplets (examples in Fig. 2, A, B). This skew was not due to stochastic distribution of mutant molecules over the droplets. For example (Fig. 2, A), the probability to observe 188 or more FAM&HEX droplets out of 193 total mutant droplets, given 67% HEXnegative droplets, is $P = 10^{-82}$. P values for all experiments ranged from P = 1 to $P = 10^{-82}$ (Table 1).

We hypothesized that the skew could be caused by Tag polymerase PCR errors introduced in originally wildtype DNA present in a droplet (Fig. 2, C). This hypothesis was based on the observations that first the FAM&HEX droplets appear in a "fan-like pattern" (Fig. 2 A, C, Supplemental Figs. 1-3) reminiscent of discrete processes such as consecutive PCR cycles. Second, the skew was absent in the EGFR p. E746 A750del (c.2235 2249del15) assay (Fig. 2, B, Table 1), a mutation unlikely to be caused by PCR error. Third, the skew correlated with the DNA concentration in the analysis (Table 1). Fourth, the skew and fan pattern were more prominent in the EGFR p. T790M (c.2369C>T) assay than in the EGFR p. L858R (c.2573T>G) and BRAF p. V600E (c.1799T>A) assays (Table 1), which is in line with the base specific error rates of Tag polymerase (22,23). The fan pattern was subsequently confirmed in KRAS p. G12D (c.35G>A) and KRAS p. G13D (c.38G>A) assays, providing a similar pattern to EGFR p. T790M (Supplemental Figs. 2 and 3). Fifth, FAM&HEX positive droplets were never observed in No Template Control wells, indicating they require wildtype target molecules to arise. Last, the skew could not be caused by nonspecific probebinding of the mutant probe to wildtype sequence, as this would result in a little FAM fluorescence in all wildtype droplets [i.e., an upward leaning wildtype cloud (14)] rather than maximum FAM fluorescence in a minority of wildtype droplets.

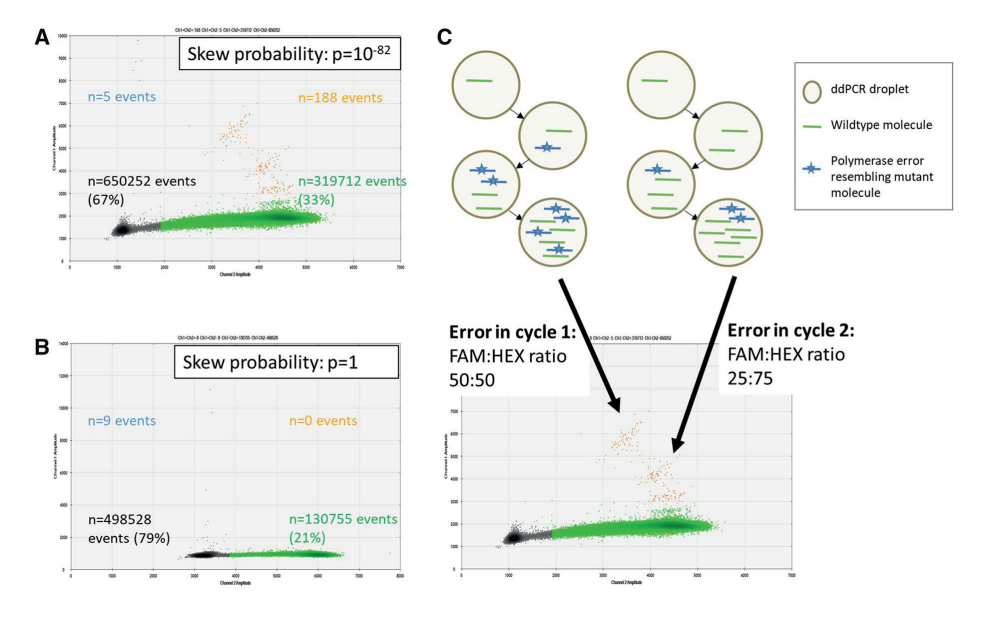


Figure 2. Polymerase induced false positive events (PIFs). Example of the combined results (A) (60 individual PCR reactions) obtained from a CLSI EP17 protocol of wildtype reference DNA with the Bio-Rad EGFR p. T790M assay. Example of EP17 combined result with Bio-Rad EGFR p. E746_A750del assay (B). Proposed mechanism of PIF occurrence: polymerase errors are introduced during ddPCR (C). The timing of the polymerase error determines the wave-like appearance of PIFs.

To verify this hypothesis 100% EGFR p. T790M mutant DNA (gBlock Gene Fragment, IDT) was used to measure the skew for the T > C transition, for which Tag polymerase has a higher error rate than for the original C>T transition (22, 23). This resulted in a 30 times higher number of FAM&HEX droplets compared to the EGFR p. T790M wildtype experiments (Supplemental Fig. 1), supporting the hypothesis that the excess FAM&HEX droplets do not represent original mutant DNA fragments and should be considered polymerase induced false positive events (PIFs) instead.

To address the occurrence of PIFs an in silico correction algorithm was developed. Briefly, this algorithm removes excess PIFs based on the likelihood of observing that distribution of FAM&HEX vs FAM-only droplets. The effect of removing PIFs is shown in Table 1.

Adaptive Limit of Blank

PIFs are a source of false positive droplets that will result in FAM&HEX droplets. In the EP17 experiments we also observed FAM-only false positive droplets, resulting in an FPR after PIF correction (Table 1). Since the FPR increased with the amount of input DNA, we developed an adaptive LoB that scales with the concentration and the number of wells analyzed. Briefly, the adaptive LoB is calculated for each experiment (all replicates of a single sample) individually. It uses the assay and concentration dependent FPR to determine the maximum expected number of FAM-positive droplets in a wildtype-only experiment after PIF removal. Only experiments that have a number of FAM-only + FAM&HEX positive droplets equal to or greater than the LoB are considered mutation positive. PIF correction and the adaptive LoB were applied sequentially in the ALPACA algorithm (Fig. 1).

Validation of ALPACA

To evaluate the performance of ALPACA we compared the results obtained by ALPACA to Bio-Rad's standard strategy (no PIF correction and static LoB = 3) (2). The validation was performed using 3 data sets: commercial reference DNA to evaluate sensitivity, healthy donor cfDNA to evaluate specificity, and NSCLC patient cfDNA as evaluation in a real-life cohort.

Commercial reference DNA

Commercial reference DNA harboring the mutation was spiked into wildtype reference DNA at various VAFs and measured in 5 duplicates. The sensitivity of ALPACA vs the standard strategy was 70 vs 68%, n = 120 (P = 0.77, Supplemental Table 1). Subgroup analysis of low-input samples (0.7 ng/well) containing 4.0, 0.3, 0.1, and 0.02 variant copies/µL likewise showed no difference in sensitivity:

Table 1. Results of the	ne EP17 e	experiments	(60	replicates	of	wildtype-only	DNA)	for	different	assays	at
2–4 different concentra	tions per d	assay.									

ddPCR assay	Mutation c annotation	Number of wells	Concentration (copies/µL)	FAM& HEX	FAM- only	HEX- only
		60	5	2	1	3725
EGFR T790M	c.2369C>T	60	34	5	0	29071
EGFR 1790M	C.2369C>1	60	144	19	6	105 418
		60	471	188	5	319712
EGFRT790M	c.2369T>C	60	59	140	45 043	13
		60	34	1	1	25838
EGFR E746- A750del	c.2235_2249del15	60	210	0	9	146 825
777 Jodel		60	270	0	1	179 864
		60	34	1	0	28018
FCED LOCOD	c.2573T>G	60	173	7	1	134469
EGFR L858R		60	309	16	0	217 063
		60	441	12	0	289718
		60	19	2	0	15387
BRAF V600E	c.1799T>A	60	297	5	4	192 957
		60	472	5	0	300 515
		60	33	0	4	32206
EGFR exon19 DEL drop-off	various deletions	60	77	2	1	65 649
		60	235	0	8	180 515
KRAS G12/G13		60	25	10	5	19971
screening	various SNVs	60	250	68	5	169 337

^a Cumulative binomial probability of observing this distribution of FAM&HEX vs FAM-only positive droplets.

75 vs 70%, n = 80, P = 0.22. Similarly, at high input and low VAF (0.3 and 0.03 variant copies/ μ L in 20 ng/well) no differences were found: 60 vs 65%, n=40, P=0.68. Meanwhile, the standard strategy had 2 false positive results in the high-input wildtype-only samples versus 0 for ALPACA.

In addition to analyzing the results as duplicates, ALPACA allows for merging a variable number of replicates and analyzing them as a single result, using the same rules for setting the adaptive LoB as it does for single wells, duplicates, or more

^b The number of FAM&HEX positive droplets that were calculated to be PIFs, and were considered HEX-only positive in downstream analysis.

^c False positive rate (FPR) calculated as the number of detected mutant molecules (after PIF removal) per wildtype molecule in the EP17 experiments.

^d The average number of false positive droplets per well that remain after PIF removal.

Empty	Skew probability (P) ^a	PIFs removed ^b	FPR (variant copies/ wildtype copy) ^c	False positive droplets per well ^d
867 076	5×10 ⁻⁵	2	3×10 ⁻⁴	0.02
978 906	2×10^{-8}	4	3×10^{-5}	0.02
809352	1×10^{-13}	15	9×10 ⁻⁵	0.17
650 252	7×10^{-83}	179	4×10 ⁻⁵	0.23
877 351	3×10 ⁻¹⁶⁶	138	3×10 ⁻⁴	0.25
864660	6×10 ⁻²	0	8×10 ⁻⁵	0.03
751 363	$1 \times 10^{\circ}$	0	6×10^{-5}	0.15
697 747	$1 \times 10^{\circ}$	0	5×10^{-6}	0.02
954099	3×10 ⁻²	0	4×10 ⁻⁵	0.02
851717	3×10^{-4}	5	2×10^{-5}	0.05
723 472	6×10^{-11}	15	4×10^{-6}	0.02
636 082	9×10 ⁻⁷	11	3×10^{-6}	0.02
936 393	3×10 ⁻⁴	1	6×10 ⁻⁵	0.02
671 975	3×10^{-2}	0	4×10 ⁻⁵	0.15
607 953	4×10^{-3}	3	5×10 ⁻⁶	0.03
1117630	9×10 ⁻¹	0	1×10 ⁻⁴	0.06
974 298	1×10 ⁻²	1	3×10 ⁻⁵	0.03
818 161	2×10^{-1}	0	4×10 ⁻⁵	0.12
935 196	4×10 ⁻¹⁴	9	3×10 ⁻⁴	0.10
716744	7×10^{-43}	65	4×10^{-5}	0.13

replicates. In contrast to strategies with a static LoB (such as the standard strategy), it therefore requires no separate validation for each different number of replicates analyzed. This feature can be used to increase the sensitivity of the approach. When data from 5 duplicates (10 wells) were merged into 1 result ALPACA's sensitivity improved from 70% (n=120) to 92% (n=24), without calling a variant in the wildtype-only samples (Supplemental Table 1).

Healthy donor cfDNA

Healthy donor cfDNA was isolated from plasma and serum, and measured in duplicates using the EGFR T790M (n=79), EGFR L858R (n=28), KRAS G12/G13 screening (n=40), and EGFR exon19 deletion (n=40) assays. Combined specificity (n=187) was significantly greater for ALPACA vs the standard strategy (98 vs 88%, $P=10^{-4}$, Supplemental Table 2). Most differences were seen in serum samples with concentration greater than 10 ng/well (94 vs 74%, n=72, $P=10^{-4}$) confirming our observation that samples with high concentration have more false positive droplets. No false positive results were seen for either strategy when using EGFR L858R or EGFR exon19 deletion drop-off, while EGFR T790M (95 vs 85%, P=0.01) and KRAS G12/G13 screening (100 vs 75%, P=0.004) showed large differences in specificity, again fitting with earlier observations.

NSCLC patient cfDNA

Last, both strategies were evaluated using a real-life cohort of stage IV NSCLC patient samples (n = 209). For all patients, molecular profiling results for plasma and tissue were available, which served as the gold standard. Comparing the ddPCR results from 4 assays (EGFR exon 19 deletion drop-off assay, EGFR L858R, EGFR T790M, and KRAS G12/G13 screening) to the gold standard, we observed overall accuracy of ALPACA vs standard strategy of 98 vs 92% ($P = 10^{-8}$, Supplemental Table 3). The accuracy for each individual assay was improved when using ALPACA (Fig. 3, A). Combining results of the 4 assays, ALPACA and the standard strategy correctly identified 61 and 65 out of 74 positive mutations (sensitivity 82 vs 88%, P = 0.13), and 730 and 683 out of 735 negative results (specificity 99 vs 93%, $P = 10^{-11}$), respectively. The negative predictive value (NPV) was 98 vs 99% (P = 0.10), and positive predictive value (PPV) was 92 vs 56% (P < 0.001).

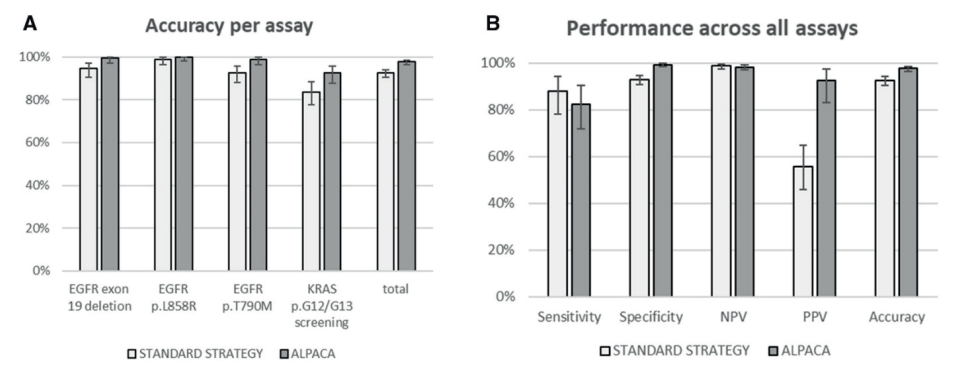


Figure 3. Patient results. Accuracy for the individual assays (A). Sensitivity, specificity, negative predictive value (NPV), positive predictive value (PPV), and accuracy for all assays combined (B). Error bars indicate exact binomial confidence intervals.

Discussion and Conclusion

Bio-Rad ddPCR is a highly sensitive method that is used in clinical and research settings to detect mutations in cfDNA (1,2). Highly sensitive methods can be hindered by the occurrence of false positive results. Yet, the manufacturer's recommendations for data processing are rather straightforward. As a consequence, it copes poorly with high-concentration samples and technical artifacts, which ultimately may cause false positive mutation calls. This can be especially relevant when therapeutic choices are based on these results and can impact patient treatment and outcome

We observed that FAM&HEX false positive droplets (PIFs) were introduced during ddPCR experiments (Fig. 2, Table 1). Our results show that the Tag polymerase, which is prone to base substitution errors (22,23), is the most likely source of PIFs. Since Tag polymerase is an irreplaceable component of Bio-Rad ddPCR Supermix, PIFs are likely to occur more generally when using this platform and the effects will be most significant for assays designed to detect C > T/G > A or T > C/A > G base substitutions. This may explain why others have found reduced specificity for the EGFR T790M (C > T) ddPCR assay compared to other assays (24).

PIFs can potentially lead to false positive ddPCR results and affect the quantification of ctDNA. We designed a statistical model to estimate the number of PIFs and exclude them from downstream analyses. In addition to PIFs, all ddPCR assays studied showed FPR increasing with DNA concentration (Table 1). The adaptive LoB sets a threshold for individual ddPCR results, considering assay characteristics, the concentration dependent FPR, and the number of wells analyzed. PIF correction and adaptive LoB were combined into the ALPACA algorithm.

In cfDNA from healthy donors ALPACA improved specificity compared to the manufacturer's standard strategy (98 vs 88%, P = 10⁻⁴), especially among samples with high cfDNA concentration (94 vs 74%, $P = 10^{-4}$). In contrast, sensitivity was not different in spiked commercial reference samples (70 vs 68%, P=0.77), either among samples with low input (75 vs 70%, P = 0.22) or with high input (60 vs 65%, P = 0.68).

Together, these results show that ddPCR produces false positive results, particularly at high DNA input concentration. These are prevented by ALPACA, leading to improved confidence in positive results. This can be especially relevant in settings seeking low VAF variants, such as detection of minimal residual disease or samples with high wildtype DNA contamination such as serum cfDNA.

Confirming our findings in cfDNA from 209 patients with stage IV NSCLC, ALPACA improved diagnostic accuracy (98 vs 92%, $P = 10^{-8}$), specificity (99 vs 93%, $P = 10^{-11}$), and PPV (92 vs 56%, P < 0.001), while not affecting sensitivity (82 vs 88%, P = 0.10) or NPV (98 vs 99%, P = 0.10) (Fig. 3, B). Importantly, the patients in this study represent a real-life cohort of patients with stage IV NSCLC, allowing to extrapolate these results to a real-life setting. In total, 47 false positive results in 41 patients (19.6%) could be avoided by applying ALPACA. False positive results were obtained by the standard strategy in KRAS (22x), EGFR p. T790M (13x), EGFR exon 19 deletion (10x) and EGFR p. L858R (2x). Vice versa, only 4 false negative results in 4 patients (1.9%) were obtained by ALPACA compared to the standard strategy, all in KRAS. Since these false positive results all can have clinical and therapeutic consequences, avoiding false positive results is crucial.

For applications where optimal sensitivity is required, it is desirable to analyze more DNA by merging data from multiple replicates. In contrast to approaches with a static LoB, ALPACA's adaptive LoB scales with the number of replicates analyzed. In this manuscript, by merging data from 10 replicates of the commercial reference samples, sensitivity for ALPACA was improved from 70 to 92%. This shows that merging replicates can be a powerful tool to improve sensitivity for ddPCR, provided the specificity is maintained by application of an adaptive LoB.

Apart from the effect on sensitivity and specificity, ALPACA will also affect the quantification of results. Differences in quantification are especially relevant when mutations are monitored longitudinally, and additional research will be required to determine the effects of ALPACA on the precision of quantification.

Another approach for preventing false positive results can be to standardize the total DNA input per reaction. Decreased specificity due to high input is circumvented that way, and no adaptive LoB is required. However, samples that do not meet the input requirement cannot be analyzed and high-concentration samples need to be diluted, decreasing the theoretical sensitivity of the method (25).

In conclusion, ddPCR causes assay specific and input dependent false positive events (coined PIFs in this study). Even after PIF correction samples with higher DNA concentrations still can have more false positive events, requiring an adaptive LoB to distinguish positive from negative results. ALPACA is a novel algorithm that applies PIF correction and an adaptive LoB to individual and merged ddPCR results. The algorithm prevents false positive results especially in samples with a high concentration. Application of ALPACA to a real-life cohort of stage IV NSCLC plasma samples significantly improved the overall accuracy, specificity, and PPV while not significantly affecting the sensitivity and NPV.

Acknowledgements

The authors thank the Core Facility Molecular Pathology and Biobanking (CFMPB) at the NKI for archiving patient material. The authors thank Tiny Korse for help in identifying and retrieving plasma and serum samples from the biobank.

Supplementary information

Supplemental tables and datasets are available at Clinical Chemistry online at DOI: 10 1093/clinchem/hyab040

References

- Postel M, Roosen A, Laurent-Puig P, Taly V, Wang-Renault SF. Droplet-based digital PCR and next generation sequencing for monitoring circulating tumor DNA: a cancer diagnostic perspective. Expert Rev Mol Diagn. 2 januari 2018;18(1):7-17.
- Bio-Rad Laboratories Inc. Droplet digital PCR applications guide (bulletin 6407 ver B) [Internet]. 2020. Beschikbaar op: https://www.bio-rad.com/webroot/web/pdf/lsr/literature/Bulletin_6407.pdf
- Milbury CA, Zhong Q, Lin J, Williams M, Olson J, Link DR, e.a. Determining lower limits of detection of digital PCR assays for cancer-related gene mutations. Biomol Detect Quantif. september 2014;1(1):8-22.
- Liang Z, Cheng Y, Chen Y, Hu Y, Liu WP, Lu Y, e.a. EGFR T790M ctDNA testing platforms and their role as companion diagnostics: Correlation with clinical outcomes to EGFR-TKIs. Cancer Lett. september 2017;403:186-94.
- Ma M, Zhu H, Zhang C, Sun X, Gao X, Chen G. 'Liquid biopsy'-ctDNA detection with great potential and challenges. Ann Transl Med. september 2015;3(16):235.
- Normanno N, Denis MG, Thress KS, Ratcliffe M, Reck M. Guide to detecting epidermal growth factor receptor (EGFR) mutations in ctDNA of patients with advanced non-small-cell lung cancer. Oncotarget. 14 februari 2017;8(7):12501-16.
- Bio-Rad Laboratories Inc. Rare mutation detection best practices guidelines (bulletin 6628) [Internet]. 2020. Beschikbaar op: https://www.bio-rad.com/webroot/web/pdf/lsr/literature/ Bulletin_6628.pdf
- Jacot W, Dalenc F, Lopez-Crapez E, Chaltiel L, Durigova A, Gros N, e.a. PIK3CA mutations early persistence in cell-free tumor DNA as a negative prognostic factor in metastatic breast cancer patients treated with hormonal therapy. Breast Cancer Res Treat. oktober 2019;177(3):659-67.
- Huang R, Xu X, Li D, Chen K, Zhan Q, Ge M, e.a. Digital PCR-Based Detection of EGFR Mutations in Paired Plasma and CSF Samples of Lung Adenocarcinoma Patients with Central Nervous System Metastases. Target Oncol. juni 2019;14(3):343-50.
- 10. Jiang X, Liu W, Zhu X, Xu X. Evaluation of EGFR mutations in NSCLC with highly sensitive droplet digital PCR assays. Mol Med Rep [Internet]. 21 mei 2019 [geciteerd 12 september 2023]; Beschikbaar op: http://www.spandidos-publications.com/10.3892/mmr.2019.10259
- 11. Milosevic D, Mills JR, Campion MB, Vidal-Folch N, Voss JS, Halling KC, e.a. Applying Standard Clinical Chemistry Assay Validation to Droplet Digital PCR Quantitative Liquid Biopsy Testing. Clin Chem. 1 december 2018;64(12):1732-42.
- 12. Oxnard GR, Paweletz CP, Kuang Y, Mach SL, O'Connell A, Messineo MM, e.a. Noninvasive Detection of Response and Resistance in EGFR -Mutant Lung Cancer Using Quantitative Next-Generation Genotyping of Cell-Free Plasma DNA. Clin Cancer Res. 15 maart 2014;20(6):1698-705.
- 13. Rowlands V, Rutkowski AJ, Meuser E, Carr TH, Harrington EA, Barrett JC. Optimisation of robust singleplex and multiplex droplet digital PCR assays for high confidence mutation detection in circulating tumour DNA. Sci Rep. 2 september 2019;9(1):12620.
- 14. The dMIQE Group, Whale AS, De Spiegelaere W, Trypsteen W, Nour AA, Bae YK, e.a. The Digital MIQE Guidelines Update: Minimum Information for Publication of Quantitative Digital PCR Experiments for 2020. Clin Chem. 1 augustus 2020;66(8):1012-29.
- 15. Institute CaLS. EP17: Evaluation of detection capability for clinical laboratory measurement procedures; approved guideline. 2nd Ed. 2012.

- 16. Novello S, Barlesi F, Califano R, Cufer T, Ekman S, Levra MG, e.a. Metastatic non-small-cell lung cancer: ESMO Clinical Practice Guidelines for diagnosis, treatment and follow-up. Ann Oncol. september 2016;27:v1-27.
- 17. Planchard D, Popat S, Kerr K, Novello S, Smit EF, Faivre-Finn C, e.a. Metastatic non-small cell lung cancer: ESMO Clinical Practice Guidelines for diagnosis, treatment and follow-up. Ann Oncol. oktober 2018;29:iv192-237.
- 18. IKNL. Landelijke richtlijn niet kleincellig longcarcinoom [Internet]. 2015. Beschikbaar op: https://www.oncoline.nl/niet-kleincellig-longcarcinoom
- 19. Wei J, Rybczynska AA, Meng P, Terpstra M, Saber A, Sietzema J, e.a. An All-In-One Transcriptome-Based Assay to Identify Therapy-Guiding Genomic Aberrations in Nonsmall Cell Lung Cancer Patients. Cancers. 1 oktober 2020;12(10):2843.
- 20. Roldán-Nofuentes JA. Compbdt: an R program to compare two binary diagnostic tests subject to a paired design. BMC Med Res Methodol. december 2020;20(1):143.
- 21. R Development Core Team. R: a language and environment for statistical computing. R Foundation for Statistical Computing, Vienna, Austria; 2019.
- 22. McInerney P, Adams P, Hadi MZ. Error Rate Comparison during Polymerase Chain Reaction by DNA Polymerase. Mol Biol Int. 17 augustus 2014;2014:1-8.
- 23. Potapov V, Ong JL. Examining Sources of Error in PCR by Single-Molecule Sequencing. Kalendar R, redacteur. PLOS ONE. 6 januari 2017;12(1):e0169774.
- 24. Sacher AG, Paweletz C, Dahlberg SE, Alden RS, O'Connell A, Feeney N, e.a. Prospective Validation of Rapid Plasma Genotyping for the Detection of EGFR and KRAS Mutations in Advanced Lung Cancer. JAMA Oncol. 1 augustus 2016;2(8):1014.
- 25. Zhang Y, Xu Y, Zhong W, Zhao J, Chen M, Zhang L, e.a. Total DNA input is a crucial determinant of the sensitivity of plasma cell-free DNA EGFR mutation detection using droplet digital PCR. Oncotarget. 24 januari 2017;8(4):5861-73.

Supplemental materials

Supplemental methods

Blood collection and cfDNA isolation

Blood was collected in 10ml K₂-EDTA tube or 10 ml cell-stabilizing tubes (STRECK, Omaha, USA). Cell-free plasma was obtained from the K₃-EDTA tube within four hours by a two-step centrifugation at room temperature: 20 minutes at 380g followed by 10 minutes at 20,000×g. Cell-stabilizing tubes were centrifuged at room temperature for 10 minutes at 1700×q, and 10 minutes at 20,000×q within seven days. Cell-free plasma was stored in 1-4 ml aliquots at -80°C. Blood for serum was collected in 8.5ml SST tubes which were mixed gently and allowed to clot for 30 minutes at room temperature. After clotting the tube was centrifuged for 10 minutes at 1700g at room temperature and the serum was stored in 1-4 ml aliquots at -30°C.

For ddPCR up to 4 ml cell-free plasma or serum was used for isolation of cfDNA, while for Next Generation Sequencing (NGS) up to 8 ml cell-free plasma (median 5 ml, inter-quartile range 4-6 ml) was used in a single replicate. Isolation was done using the QIAsymphony Circulating DNA kit (article number 1091063, Qiagen, Dusseldorf, Germany) with the QIAsymphony (Qiagen). No extraction blanks were used in this study. Elution volume was set to 60 µl and samples were stored at 4°C for use within one week.

Plasma cfDNA was not quantified prior to ddPCR (instead using a set volume of sample as described below). Plasma cfDNA was quantified prior to NGS, using the Qubit dsDNA HS Assay kit (catalogue number Q32851), and up to 50ng was used as input as described in the main methods section. Serum cfDNA was quantified prior to ddPCR, using the same Qubit kit and diluted to fall within the range of 1.5-2.5 ng/µl.

ddPCR procedure

ddPCR was performed on the Bio-Rad QX100 system (Bio-Rad Laboratories Inc, Hercules, California, USA). Two No Template Control (NTC) and Positive Control (PC) wells were included with each experiment for each assay. EP17 experiments were performed in 60 replicates, all other experiments in duplicates. For each replicate 9µl sample, 1µl each of mutant and wildtype probes and 11µl ddPCR Supermix for Probes (no dUTP) (Bio-Rad, cat# 186-3023) were used. No denaturation or restriction was performed prior to droplet assembly. Droplets were generated with QX100 Droplet Generator, thermal cycling was performed as described in **Supplemental** Methods table 1 below and droplet fluorescence was measured with QX100 Droplet Reader. Data were analysed with QuantaSoft (Bio-Rad, version 1.7.4.0917), thresholding was performed manually by experienced technicians guided by NTC and PC sample wells. Mutation calls were interpreted as described in the main text.

Supplemental Methods table 1: ddPCR cycling conditions

Cycling step	Temperature (°C)	Time	# Cycles	Ramp Rate
Enzyme activation	95	10 min	1	2 °C/sec
Denaturation	94	30 sec	40	
Annealing/extension	55	1 min		
Enzyme deactivation	98	10 min	1	
Hold (optional)	4	Infinite	1	1 °C/sec

ddPCR assays used

See online supplemental data.

Supplemental tables 1-4

See online supplemental data

Supplemental figures

See online supplemental data



Chapter 3

Performance of four platforms for *KRAS* mutation detection in plasma cell-free DNA: ddPCR, Idylla, COBAS z480 and BEAMing

D.C.L. Vessies¹, M.J.E. Greuter², K.L. van Rooijen³, T.C. Linders¹, M. Lanfermeijer¹, K.L. Ramkisoensing¹, G.A. Meijer⁴, M. Koopman³, V.M.H. Coupé², G.R. Vink^{3,5}, R.J.A. Fijneman⁴ & D. van den Broek¹

¹ Netherlands Cancer Institute, department of laboratory medicine, Amsterdam, the Netherlands

² Amsterdam University Medical Centers, location VUmc, department of epidemiology and biostatistics, Amsterdam, The Netherlands

³ University Medical Center Utrecht, department of medical oncology, Utrecht University, Utrecht, The Netherlands

⁴ Netherlands Cancer Institute, department of pathology, Amsterdam, The Netherlands

⁵ Netherlands Comprehensive Cancer Organisation, department of research, Utrecht, The Netherlands

Abstract

Multiple platforms are commercially available for the detection of circulating cellfree tumour DNA (ctDNA) from liquid biopsies. Since platforms have different input and output variables, deciding what platform to use for a given clinical or research question can be daunting. This study aimed to provide insight in platform selection criteria by comparing four commercial platforms that detect KRAS ctDNA hotspot mutations: Bio-Rad droplet digital PCR (ddPCR), BioCartis Idylla, Roche COBAS z480 and Sysmex BEAMing. Platform sensitivities were determined using plasma samples from metastatic colorectal cancer (mCRC) patients and synthetic reference samples, thereby eliminating variability in amount of plasma analysed and ctDNA isolation methods. The prevalence of KRAS nucleotide alterations was set against platform-specific breadth of target. Platform comparisons revealed that ddPCR and BEAMing detect more KRAS mutations amongst mCRC patients than Idylla and COBAS z480. Maximum sample throughput was highest for ddPCR and COBAS z480. Total annual costs were highest for BEAMing and lowest for Idylla and ddPCR. In conclusion, when selecting a platform for detection of ctDNA hotspot mutations the desired test sensitivity, breadth of target, maximum sample throughput, and total annual costs are critical factors that should be taken into consideration. Based on the results of this study, laboratories will be able to select the optimal platform for their needs.

Introduction

Patients with metastatic colorectal cancer (mCRC) may be treated with targeted therapies directed against epidermal growth factor receptor (EGFR). However, presence of a Kirsten rat sarcoma (KRAS) mutation in the tumour confers resistance to this type of therapy (1). In the current standard of care the presence of KRAS mutations is determined in tissue biopsies obtained from the tumour. Obtaining such biopsies is invasive to the patient, may not fully represent tumour heterogeneity (2), and is cost and time intensive. Detection of KRAS mutations in circulating cell-free DNA (cfDNA) from liquid biopsies offers an attractive alternative (3). Yet, cfDNA testing has its challenges, including the small amounts of available cfDNA and low fractions of circulating tumour DNA (ctDNA) (4). Multiple commercial ctDNA detection platforms are available, ranging from PCR based hotspot analysis to broad targeted NGS applications. These platforms show considerable differences in the amount of plasma required as input, the DNA isolation method, quantitative versus semi-quantitative results, the breadth of target and the total cost per sample analysed. These differences complicate a straightforward comparison of platforms, which results in a knowledge gap in cfDNA testing (5). Attempts to perform such comparisons have been made (6-9), but it cannot be excluded that the results were biased by using different amounts of plasma or cfDNA, different isolation methods (10) and/or the use of tissue biopsy results as the gold standard. In addition these studies did not evaluate factors influencing the choice for a platform in daily practice such as the costs of analysis, the maximum annual throughput and the differences in the number of mutations targeted by a platform. Four commercially available PCR-based platforms for detection of hotspot mutations in KRAS (Bio-Rad droplet digital PCR (ddPCR), BioCartis Idylla, Roche COBAS z480 and Sysmex BEAMing) were compared in this study, while limiting or eliminating the impact of factors that affect a direct comparison of platforms. Furthermore the costs of analysis and the impact of the choice for a platform on detection of KRAS mutations in mCRC patients were investigated.

Materials and methods

Patient selection and blood collection

Seventeen patients with histopathologically confirmed mCRC were included between July 2017 and February 2018 through the nationwide Prospective Dutch Colorectal Cancer cohort (PLCRC) (11). PLCRC was approved by the Medical Ethical Committee (METC) of the University Medical Center Utrecht. The review board at each participating institution approved the study, which was conducted according to the principles of the Declaration of Helsinki and the International Conference on Harmonisation Good Clinical Practice guidelines. All patients provided written informed consent to participate in the study. Patients were selected based on their KRAS mutation status as determined in tissue biopsies. Two patients without a KRAS mutation (of whom one with a KRAS amplification) were also included. Mutations in tissue were determined as part of routine diagnostics, using the method of choice for each including hospital. Specifically this was the lon Torrent Hotspot panel v2plus (14×), the Therascreen KRAS extension pyro kit (1x) and unknown (2x). Clinical data for each patient at the time of liquid biopsy are summarised in Supplemental Table 1. Blood was collected at a single time point during treatment for metastatic disease in four 10 ml Cell-free DNA BCT tubes (Streck, La Vista, NE, USA) and shipped to the Netherlands Cancer Institute (NKI, Amsterdam, the Netherlands). Cell-free plasma was obtained by a two-step centrifugation protocol (10 minutes at 1700g, followed by 10 minutes at 20000 g). Cell-free plasma was stored at -80 °C.

cfDNA isolation

CfDNA was isolated using the isolation method provided with each platform or with the QIAsymphony Circulating DNA kit (Qiagen, Düsseldorf, Germany) on the QIAsymphony (Qiagen). For the latter 4 ml of plasma was isolated and the elution volume set to 60 µl.

Construction of synthetic reference samples

Full length genomic DNA (gDNA) (Promega, Madison, WI, USA), containing no mutations in KRAS, was fragmented enzymatically with dsDNA Fragmentase [#M0348] (New England Biolabs, Ipswich, MA, USA) according to manufacturer instructions. Briefly, 60 µg gDNA was incubated with dsDNA Fragmentase and incubated for 30 minutes at 37 °C, in 30 reactions of 2 µg gDNA each. The product of the 30 reactions was pooled and double-sided SPRI cleanup was performed with Agencourt AMPure XP beads [#A63881] (Beckman Coulter Life Sciences, Indianapolis, IN, USA), using 0.8x and 2.5x ratios according to manufacturer instructions. The resulting pool of cfDNA-like wildtype DNA was analysed on the Agilent 2100 BioAnalyzer system (Agilent, Santa Clara, CA, USA) using a High Sensitivity kit (#5067–4626) (Supplemental Fig. 1).

Seven synthetic DNA fragments containing mutations in the KRAS gene (KRAS p.G12A, p.G12C, p.G13D, p.A59T, p.Q61H, p.K117N or p.A146V) were ordered as gBlocks Gene Fragments with a length of 973-999 bp from IDT (Integrated DNA Technologies Inc, Skokie, IL, USA). The sequences are provided in Supplemental sequences 1. These were fragmented sonically on a Covaris ME220 Focusedultrasonicator (Covaris inc, Woburn, MA, USA) using microTUBE AFA Fiber Pre-Slit Snap-Cap (PN 520045) vessels, with the following settings: Duration 100s, Peak Power 75 W, Duty Factor 25% and 1000 Cycles per Burst. No BioAnalyzer results are available for the fragmented oligos, as the DNA concentration is below the limit of detection for that device. The sheared synthetic DNA fragments were pooled equimolarly and spiked into the cfDNA-like wildtype DNA to achieve mutant allele frequencies (mAF) of 0.50%, 0.04%, 0.02% and 0% (i.e. no synthetic DNA spiked, wildtype control). In total six different constructed reference samples were used in this study: 50 ng input with 0.50%, 0.02% and 0% mAF, and 10 ng input with 0.50%, 0.04% and 0% mAF. Four replicates of every constructed reference sample were measured to assess the sensitivity of each platform.

Bio-Rad ddPCR

For Bio-Rad ddPCR the KRAS G12/G13 screening kit (#1863506, Bio-Rad) was used according to manufacturer's instructions. All measurements were performed in duplicate, using an 18 ul sample, 2 ul ddPCR KRAS G12/G13 Screening Multiplex Assay and 22 µl ddPCR Supermix for Probes (no dUTP) (catalogue number 186–3023). Droplets were generated with QX100 Droplet Generator and measured with QX100 Droplet Reader. Data were analysed with QuantaSoft (Bio-Rad) version 1.7.4.0917. When analysing constructed reference samples containing three mutations in KRAS codons 12 and 13, the three mutant droplet clouds were identified and analysed independently.

For data interpretation we applied a dynamic limit of blank (LoB) that is dependent on the assay used and the concentration of the sample being analysed. The false positive rate (FPR) for the ddPCR KRAS G12/G13 Screening kit had previously been determined using 60-fold measurement of Horizon KRAS Wild Type Reference Standard DNA (#HD710, Horizon) at 25 and 250 copies/µl. FPR was defined as the ratio of false positive mutant molecules over wildtype molecules, and used to determine the LoB in each sample using a binomial model with 0.1% cut-off. For example, in a duplicate experiment where 6000 wildtype molecules are observed and FPR at that concentration being 10⁻⁴, the binomial probability for observing more than three (false positive) mutant events by chance is 0.4%, and therefore cannot be excluded as a random chance event. By contrast, if more than four mutant positive events are observed (p < 0.1%) this is considered to be a true biological signal, and the sample is interpreted as positive for that mutation.

Idylla

Biocartis Idylla™ (Biocartis NV, Mechelen, Belgium) was used with the Idylla™ ctKRAS Mutation Test (REF A0081/6) according to manufacturer instructions unless otherwise indicated. Where previously isolated DNA was used with Idylla, it was diluted in nuclease free H₂O (NF-H₂O) to 1 ml and loaded onto the cartridge. This procedure was previously determined to not impact the performance of the system negatively (data not shown). Results were obtained and analysed in the IdyllaExplore environment, allowing for the identification of multiple mutations per sample.

COBAS z480

Roche COBAS z480 (Roche Molecular System Inc, Pleasanton, CA, USA) was used with the KRAS Mutation Test v2 LSR kit (material number 07989270001) according to manufacturer instructions unless otherwise indicated. Where previously isolated DNA was used with COBAS z480, it was diluted in NF-H₂O to 70 µl prior to PCR setup. Data was analysed according to instructions by uploading the ixo files to the online LSR Data Analysis tool (https://lifescience.roche.com/en nl/brands/oncology-research-kits.html).

BEAMing

Sysmex Inostics BEAMing Digital PCR (Sysmex Inostics GmbH, Hamburg, Germany) was used with the OncoBEAM™ RAS CRC kit RUO (ZR150001) and the CyFlow Cube 6i and Robby instruments according to manufacturer instructions unless otherwise indicated. Where previously isolated DNA was used with BEAMing, it was diluted in NF-H₃O to 123 µl prior to pre-amplification. Data was analysed for the KRAS variants only (ignoring NRAS variants), using the BEAMing software according to instructions. Technical performance data for all four platforms are provided in Supplemental Table 2.

Breadth of target

The point mutations in KRAS that are targeted by each platform were evaluated from the respective product specifications. These were compared to publicly available tissue biopsy mutation profiles for 1099 mCRC patients (12), that were accessed through the cBioPortal for Cancer Genomics (13,14) on December 14th, 2018.

Total annual costs

We determined the total annual cost according to the Activity Based Costing (ABC) model (15), including all reagents costs, hands-on time costs, maintenance costs and depreciation costs for all equipment used. The material costs include costs for cfDNA isolation, kit costs, control samples and additional materials. Hands-on time per sample was determined for two scenario's: High throughput (maximum number of samples per week based on maximal occupancy of the machine) and low throughput (5 samples per week). Intermediate throughput was modelled by linear interpolation of those results. Equipment depreciation was calculated by applying an annuity factor based on equipment depreciation in 10 years with an interest rate of 4.2%. Maintenance was incorporated by applying a fixed annual cost for maintenance contracts for each platform. Costs were included as raw list price costs, including all relevant taxes and were analysed as a function of annual sample throughput for each platform. To determine what factors have a large or small effect on the total cost per year we performed cost sensitivity analyses for the following parameters: 1) Equipment depreciation in 5 years rather than 10 years and 2) Manual cfDNA isolation for ddPCR, with the QIAamp Circulating Nucleic Acid Kit (Ojagen) rather than the OlAsymphony.

Results

The experimental set-up to determine the sensitivity of each platform is shown in Fig. 1, steps one to three. cfDNA from six mCRC patients was analysed following the manufacturer's instructions as indicated in the first step of Fig. 1. Tissue mutation analysis was performed as part of routine clinical care and in five of the six patients a KRAS mutation was reported. The time between the tissue analysis and the collection of the plasma ranged from 0 to 39 months. The amount of isolated cfDNA ranged from 4.3 to 53.1 ng/ml plasma. In two out of five KRAS positive patients all platforms detected the KRAS mutation. For two KRAS positive patients a KRAS mutation was detected by three of the four platforms and in one KRAS positive patient no KRAS mutation was detected in plasma by any of the platforms. For the sixth patient, for whom tissue analysis did not identify a KRAS mutation, two platforms did report a KRAS mutation. Results are shown in Table 1.

Table 1. Mutations detected by four commercially available ctDNA detection platforms in cfDNA from 6 patients with mCRC and corresponding tissue results.

Tissue KRAS result ^a	Months between tissue biopsy and blood collection	Concentration cfDNA in plasma (ng/ml) ^b	Reported mutant copies (mAF) ^c
KRAS wildtype	39	4.3	75 (0.24%)
KRAS p.G12S	10	5.5	nd
KRAS detected	Unknown	53.1	49 (0.05%)
KRAS p.G12D	1	14.1	5323 (12.51%)
KRAS p.G12D	0	5.6	172 (0.67%)
KRAS p.G12S	4	17.0	279 (0.62%)

^aTissue KRAS result is based on the standard of care test at the hospital of inclusion.

Analysis of patient derived cfDNA at equal inputs per platform

A number of confounding factors could have influenced the results from the comparison per manufacturer's instructions, including different volumes of plasma and different cfDNA isolation methods used (Fig. 1). Analysis of cfDNA from 11 mCRC patients with tissue-confirmed KRAS mutations using a single isolation method and distributing the DNA equally over the platforms allowed us to eliminate these differences, indicated in Fig. 1 step two. Time between tissue biopsy and liquid biopsy ranged from 0 to 22 months. The amount of isolated cfDNA ranged from 4.7 to 185.6 ng/ml plasma. In six out of 11 patients (54%) the results from all four platforms were concordant. KRAS p.A146T in one patient was detected by all platforms with the exception of ddPCR which did not target this mutation. Idylla reported a KRAS mutation in two patients, concordant with the KRAS mutation that had been detected in tissue, which was not detected by the other platforms. In two patients the mutations (KRAS p.G12 G12insAG and a KRAS amplification) were not targeted by any platform, but BEAMing did report the presence of a KRAS p.G12X mutation for the patient with a KRAS p.G12 G12insAG mutation. The KRAS amplification was not detected by any of the platforms as expected. When 10 ng or more input of cfDNA (n = 8) was used, the detected KRAS mutations were concordant across all platforms when considering only mutations

^b cfDNA concentration in plasma is based on Qubit measurement of cfDNA isolated by QIAsymphony using the Circulating DNA kit, and is reported in ng cfDNA per ml plasma isolated.

^cReported mutant copies and mutant allele frequency (mAF) are based on BEAMing results.

^dResults are based on 1 ml of plasma.

^eResults are based on 2 ml of plasma.

^fResults are based on 3 ml of plasma.

gnd=not detected

h KRAS p.G12X = any variant at amino acid position G12 of the KRAS gene. The result is not further specified by BEAMing or COBAS z480 platforms.

KRAS p.G12X/G13X = any variant at amino acid positions G12 or G13 of the KRAS gene. The resultis not further specified by ddPCR platform.

ddPCR ^d	Idylla ^d	COBAS z480°	BEAMing ^f
nd ^g	KRAS p.G12R	nd	KRAS p.G12Xh
nd	nd	nd	nd
KRAS p.G12X/G13X ⁱ	KRAS p.G12S	nd	KRAS p.G12X
KRAS p.G12X/G13X	KRAS p.G12D	KRAS p.G12X	KRAS p.G12X
KRAS p.G12X/G13X	nd	KRAS p.G12X	KRAS p.G12X
KRAS p.G12X/G13X	KRAS p.G12S	KRAS p.G12X	KRAS p.G12X

Sensitivity

Step 1: Analysis of plasma ctDNA from 6 KRAS positive mCRC patients.

Aim of the comparison:

- Method prescribed by manufacturer
- Patient derived ctDNA

Confounding factors:

- Four different isolation methods
- Different volumes of plasma analysed (1-3 ml)
- True mutation status of plasma sample not known
- Variable time between tissue and liquid biopsy

Step 2: Analysis of equal amounts of plasma ctDNA from 11 KRAS positive mCRC patients.

Aim of the comparison:

- Equal input of ctDNA (same plasma volume and isolation method)
- Patient derived ctDNA

Confounding factors:

- Samples not isolated using the prescribed isolation
- True mutation status of plasma samples not known
- Variable time between tissue and liquid biopsy

Step 3: Analysis of constructed reference samples.

Aim of the comparison:

- Identical constructed samples
- Spiked mutations at known mAF
- All samples measured in 4 replicates

Confounding factors:

- Artificial ctDNA samples
- Seven mutations in one analysis

Breadth of target

Step 4: Assessment of breadth of target.

Comparison based on:

- Technical data sheets and communication material
- Comparison to mutation frequencies in a cohort of metastatic colorectal cancer patients

Total costs

Step 5: Total annual cost analysis.

Comparison based on:

- Technician hands-on time
- Consumables costs
- Equipment depreciation
- Maintenance costs

Figure 1. Graphical representation of the five step approach for comparison of four commercially available ctDNA platforms.

that can be detected by all platforms. For five samples we could determine the mAF of the KRAS mutation by ddPCR and/or BEAMing. These ranged from 0.12%-15.4% (9-4656 copies/ml) (Table 2). All variants detected by all platforms were present with 39 mutant copies per platform or more.

Table 2. Mutations detected by four commercially available ctDNA detection platforms in cfDNA from 11 patients with mCRC isolated with the QIAsymphony and distributed equally over all platforms.

Tissue KRAS result ^a	Months between tissue biopsy and blood collection	total cfDNA analysed (ng) ^b	Reported mutant copies (mAF) ^c	
KRAS p.G12_G12insAG	Unknown	23.7	9 (0.12%)	
KRAS p.G12V	Unknown	23.0	1167 (15.4%)	
KRAS p.A146T	9	17.3	106 (1.7%)	
KRAS p.G12D	0	94.4	39 (0.13%)	
KRAS p.G13D	Unknown	8.1	nd	
KRAS p.G12V	Unknown	167.0	4656 (8.5%)	
KRAS p.G12C	5	10.1	nd	
KRAS p.G12D	9	13.7	nd	
KRAS p.G12D	20	8.2	nd	
KRAS p.G13D	22	10.2	nd	
KRAS amplification	Unknown	4.2	nd	
Overall sensitivity (%)				

Sensitivity of KRAS detection based on synthetic reference samples

Analysing four replicates of synthetic reference samples harbouring multiple KRAS mutations allowed us to eliminate the effect of not knowing the true mutation status of the samples, and limit the effects of sampling errors due to replicate measurements, as outlined in step three of Fig. 1. Overall, more mutations were detected at higher total input and higher mAF, validating the successful construction of the synthetic reference samples. At 10 ng DNA input valid results were obtained for 0% and 38% of COBAS z480 and BEAMing measurements, respectively. At 50 ng this increased to 83% and 93% of measurements, respectively.

^aThe KRAS mutation status was determined in tissue using the method of choice of the hospital of inclusion.

^bTotal cfDNA input per method is based on Qubit measurement of cfDNA isolated by QIAsymphony using the Circulating DNA kit.

^cReported mutant copies and mutant allele frequency (mAF) are based on BEAMing results.

dnt = not targeted.

end = not detected.

fdetected mutations divided by the total number of mutations detectable by that platform.

ddPCR	Idylla	COBAS z480	BEAMing
nt ^d	nt	nt	KRAS p.G12X
KRAS p.G12X/G13X	KRAS p.G12V	KRAS p.G12X	KRAS p.G12X
nt	KRAS p.A146T	KRAS p.146×	KRAS p.A146T
KRAS p.G12X/G13X	KRAS p.G12D	KRAS p.G12X	KRAS p.G12X
nd ^e	KRAS p.G13D	nd	nd
KRAS p.G12X/G13X	KRAS p.G12V	KRAS p.G12X	KRAS p.G12X
nd	nd	nd	nd
nd	nd	nd	nd
nd	KRAS p.G12D	nd	nd
 nd	nd	nd	nd
nt	nt	nt	nt
38% ^f	67%	44%	50%

ddPCR and Idylla did not report any invalid results. The sensitivity depended on the total amount of input for each platform. At a mAF of 0.5%, 62 mutations were detected with 50 ng input, compared to 29 mutations for 10 ng input. At 50 ng input the COBAS z480 reported a KRAS p.A59X variant in all valid replicates of the wildtype control samples. The percentage of all mutations detected ranged from 39% (BEAMing) to 13% (Idylla) (Table 3).

For comparison of platform sensitivities we evaluated a subset of three mutations (KRAS p.G12A, p.G12C and p.G13D) that were targeted by all four platforms. Sensitivity over all mAFs ranged from 10% (COBAS z480) to 65% (ddPCR). Considering only samples with 0.5% mAF (15 and 75 mutant copies/reaction) sensitivities ranged between 19% (COBAS z480) and 100% (ddPCR) (Table 3). Raw reported mutation detection values are provided in Supplemental data set 1.

Input DNA (ng)	Mutant allele	Mutant copies	ddPCR				
	frequency (%)	per analysis ^a	All mutations (%)	KRAS p.G12/G13 (%)			
10	0.00 ^d	0	nd ^e	nd			
10	0.04	1	nd	nd			
10	0.50	15	43	100			
50	0.00 ^d	0	nd	nd			
50	0.02	3	25	58			
50	0.50	75	43	100			
Overall sensitivity (%)			28	65			
Sensitivity 50 ng (%)			34	79			

22

50

Table 3. Mutations detected in constructed reference samples by four commercially available ctDNA detection platforms.

Sensitivity 10 ng (%)

Impact of breadth of target detection

To determine the impact of having a broader panel when analysing cfDNA, the number of mutations targeted per platform were compared to publicly available tissue biopsy mutation profiles of 1099 mCRC patients (12). Of 1099 patients, 46% (505/1099) had a mutation in KRAS. ddPCR targets 82% of those (413/505), Idylla and COBAS z480 both 96% (485/505) and BEAMing 94% (477/505). To estimate the effect of platform sensitivity superimposed on platform breadth on the detection of KRAS mutations in a general mCRC population, the sensitivities determined on synthetic reference samples at 50 ng input with 0.5% or 0.02% mAF were included. Based on these assumptions ddPCR and BEAMing were likely to detect KRAS mutations at a mAF of 0.5% in respectively 38% and 32% of mCRC patients, compared to 22% and

^a Average number of mutant copies per analysis was calculated as Input DNA (ng) * 300 (Genome Equivalents/ng) * Mutant allele frequency (Mutant copies/Genome Equivalent).

^b For COBAS z480, invalid results were obtained at 10 ng DNA input for all replicates, at 50 ng of DNA input invalid results were obtained in 25% of the replicates at 0 and 75 mutant copies. Invalid results were counted as not detected.

For BEAMing, invalid results were obtained at 10 ng DNA input in 88%, 54% and 46% of the replicates at 0, 1 and 15 mutant copies respectively. At 50 ng input 7% of all replicates were reported as invalid. Invalid results were counted as not detected.

^d Wildtype control samples without synthetic mutant fragment spike-in.

end = not detected.

Detected mutations divided by the total number of mutations present over four replicates. Not all platforms target all mutations, and will have lower reported sensitivity as a result.

⁹ A false positive KRAS A59X was reported in all wildtype replicates. These false positives were based on a software error (personal communication with Roche Diagnostics).

Idylla		COBAS z480 ^b		BEAMing	
All mutations (%)	KRAS p.G12/ G13 (%)	All mutations (%)	KRAS p.G12/ G13 (%)	All mutations (%)	KRAS p.G12/ G13 (%)
nd	nd	nd	nd	nd	nd
nd	nd	nd	nd	4 ^f	12
11	16	nd	nd	54	62
nd	nd	12 ⁹	nd	nd	nd
4	8	17	nd	8	25
36	50	62	38	92	75
13	19	20	10	39	44
20	29	40	19	50	50
6	8	0	0	27	37

17% for Idylla and COBAS z480. At 0.02% mAF, ddPCR showed to detect 22% of patients, Idylla 8%, COBAS z480 0%, and BEAMing 11% (Table 4).

Total cost analysis

The total annual cost of the platforms correlated linearly to the number of samples analysed per year (R2 for linearity between 0.9973 and 1.000) (Fig. 2 and Supplemental data set 2). Total annual costs were highest for BEAMing, while ddPCR was found to be the least expensive platform to use when more than 110 samples were analysed per year. At lower throughput Idylla was found to be slightly less expensive due to lower fixed annual costs.

Table 4. Estimation of the impact of the breadth of target and sensitivity of platforms at two different mutant allele fraction levels in the detection of KRAS mutations in a mCRC population.

	Prevalence of <i>KRAS</i> mutations in mCRC	Breadth of <i>KRAS</i> targets	Sensitivity at 50 ng DNA mAF 0.50% ^a
ddPCR	46%	82%	100%
Idylla	46%	96%	50%
COBAS z480	46%	96%	38% ^b
BEAMing	46%	94%	75% ^c

^a Sensitivity was based on the detection of KRAS p.G12 and p.G13 mutations in synthetic reference samples at the indicated input and mAF.

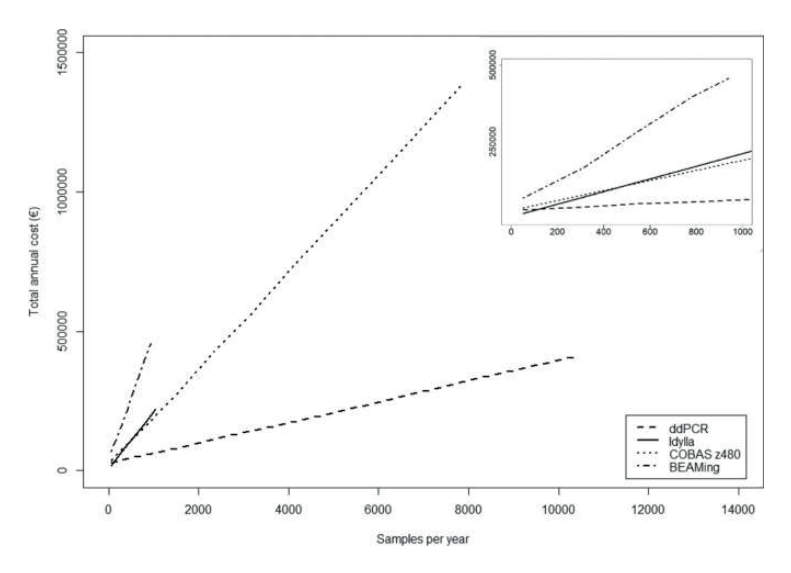


Figure 2. Total annual costs as a function of the number of samples analysed per year. The width on the x-axis is determined by the maximum number of samples that can be analysed per year based on optimal platform occupancy.

^b Invalid result were obtained for 25% of the results.

^cInvalid result were obtained for 25% of the results.

d Invalid result were obtained for 12% of the results.

Sensitivity at 50 ng DNA mAF 0.02% ^a	Estimated % of KRAS positive patients detected (50 ng, mAF 0.50%)	Estimated % of <i>KRAS</i> positive patients detected (50 ng, mAF 0.02%)
58%	38%	22%
8%	22%	4%
0%	17%	0%
25% ^d	32%	16%

For all platforms, the material costs per sample were the largest contributor to the total annual costs. The higher the throughput the greater the relative contribution of the material costs became for all platforms, up to 80% for BEAMing (940 samples per year) and 95% for COBAS z480 (7800 samples per year) (Supplemental data set 2).

Given the rapidly developing field of ctDNA detection, the impact of an instrument depreciation time of 5 instead of 10 years was evaluated. This increased the fixed annual costs with 31% (COBAS z480) to 73% (Idylla). A limited effect of using manual cfDNA isolation with the QIAamp Circulating DNA Kit versus automated cfDNA isolation with QIAsymphony was observed (Supplemental data set 2).

Conclusion/discussion

We show that performing a systematic comparison is complicated by multiple factors, all of which can impact the sensitivity. By understanding, eliminating or limiting these factors an unbiased comparison of the four platforms was performed, showing that ddPCR and BEAMing have a higher sensitivity for KRAS hotspot mutations than Idylla and COBAS z480. In addition it was shown that Idylla has the lowest annual cost at low sample throughput, while ddPCR is least expensive at higher sample throughput. BEAMing is the most expensive platform overall.

To compare the sensitivity of each platform in this study a number of factors were considered: The volume of plasma used, the total DNA input, and the isolation method. By performing the sensitivity comparison in three steps we could eliminate the impact of each of these factors. In the first step 6 patient samples were analysed following the protocols of the respective platforms (Table 1). Several factors could have influenced these results, hampering a direct link to the performance of the platforms (Fig. 1). To eliminate possible effects from different plasma volumes and isolation methods, patient plasma was isolated using a single method and the isolated cfDNA was distributed equally over the platforms. The results were fully concordant for samples with at least 39 mutant copies per reaction, which was in line with results obtained with synthetic reference samples. Compared to the other platforms Idvlla detected two additional mutations in samples with less than 8 ng cfDNA input (Table 2). Since Idylla does not report mAFs we cannot exclude that this is the result of sampling distribution errors. All patient samples in this study were obtained during treatment, and time between tissue and liquid biopsy differed greatly between patients. This complicates the interpretation of the results, as the true mutation status of these plasma samples is unknown at the time of the liquid biopsy.

In order to limit the effects of sampling errors and eliminate the unknown true mutation status of patient plasma cfDNA, synthetic reference samples were constructed and measured in four replicates, ddPCR and BEAMing performed better than Idylla and COBAS z480 (Table 3), both overall and among a limited number of mutations that were targeted by all platforms. This is in line with previous reports (6-9).

Sensitivity is not the only factor that defines the performance of a platform. The detection of KRAS mutations in a real life mCRC population will depend on the sensitivity of the platform, the prevalence of specific KRAS mutations in the population, and the number of mutations analysed by the platform. Since few publications report the mAF of KRAS mutations detected in the cfDNA of mCRC cohorts (16-18), some assumptions were required to extrapolate the data from the synthetic reference samples to a general mCRC cohort. Here we assumed 0.50% mAF and 50 ng cfDNA input, leading to a predicted detection rate of KRAS mutations amongst a total mCRC patient population of 17-22% for the non-digital platforms, versus 32–38% for the digital platforms (Table 4). The main factor driving this difference was the sensitivity of BEAMing and ddPCR, while the breadth of target and mutation prevalence in the target population had a more limited impact. Although no cohort of mCRC patients will have exactly 0.50% mAF and 50 ng cfDNA input, this example still provides insight in the interplay between sensitivity, breadth of target and prevalence of the mutations in the intended population, thereby further aiding future users in comparing these platforms.

For application of a platform in daily practice the total annual costs are a highly relevant factor. The costs per platform differed greatly. At low sample throughput Idylla was least expensive, while ddPCR was less expensive for higher throughput. BEAMing was the most expensive across the whole range of throughput investigated. Out of the factors investigated, the material cost per sample was the largest contributor to the total annual cost.

Overall the effectiveness of a platform to detect mutations in a patient population depends on its performance characteristics. The performance of a platform is affected by sensitivity - which depends on the amount of plasma analysed, isolation method, and PCR technique -, the character of the result (quantitative or qualitative), the number of mutations targeted, the population under investigation, and the cost of analysis. The decision which platform to use in a specific clinical or research setting will often be based on the expected population and number of samples, and the performance of the platforms in the intended situation. A direct comparison of the platforms is hampered by the lack of a gold standard and any harmonisation between the platforms.

A number of studies have compared cell-free DNA mutation detection platforms (6–9). For example, Garcia et al. (6) reported the highest sensitivity for BEAMing in a comparison of BEAMing, ddPCR and an NGS approach. In this comparison the amount of total cfDNA input for BEAMing (123 µl) was substantially higher than for ddPCR (8 µl) and NGS (10 µl). Since the amount of plasma or cfDNA analysed will affect sensitivity of the analysis this might have introduced a bias. Vivancos et al. (7) reported increased detection of KRAS mutations in a comparison of BEAMing and BioCartis Idylla. In this study BEAMing was used to select KRAS positive samples to be tested on the Idylla platform. By re-testing samples, different volumes of plasma were analysed (3 ml vs 1 ml). Furthermore, samples that were negative by BEAMing were not tested using Idylla, introducing a bias by design of the study. Thress et al. (8) found higher sensitivity for two digital platforms (BEAMing and ddPCR) than for two non-digital platforms (COBAS and Therascreen). In this case equal volumes of plasma were used for all platforms, but having used mutations detected in tissue as the sole reference value to calculate sensitivity and specificity might still introduce discrepancies and/or biases. Wang et al. (9) compared ddPCR and ARMS, finding higher sensitivity for the digital approach (ddPCR). In this study the amount of cfDNA used for each platform was not specified, complicating the interpretation of their results.

Apart from the four platforms compared in this study, other methods for the detection of mutations in cfDNA are available. Further research using patient samples, equal input and reference samples as well as total cost analyses will be required to learn how other platforms compare to the platforms included in this study.

In conclusion, our results show that multiple factors affect the performance of a specific platform in daily practice. For the detection of KRAS mutations in a cohort of mCRC patients, the sensitivity of a platform was the most important differentiating factor compared to the number of mutations targeted and their prevalence in the target population. Idylla was the least expensive platform at low throughput, while ddPCR was less expensive at higher annual sample throughput. BEAMing was the most expensive across the whole range investigated. Selecting an optimal platform depends on the patient or study population, the yearly sample throughput, the required sensitivity in relation to the clinical or scientific question at hand and available funds.

Acknowledgements

The collaboration project is co-funded by the PPP Allowance (grant LSHM16047-H005) made available by Health~Holland, Top Sector Life Sciences & Health, to stimulate public-private partnerships. We thank Rianne van der Wiel for performing part of the analyses and Boris van Doorn and Flore Grijseels for helpful discussions.

Data availability

All data generated during this study are included in this published article (and its Supplemental Information files), and/or are available from the corresponding author on reasonable request.

References

- Sorich MJ, Wiese MD, Rowland A, Kichenadasse G, McKinnon RA, Karapetis CS. Extended RAS mutations and anti-EGFR monoclonal antibody survival benefit in metastatic colorectal cancer: a meta-analysis of randomized, controlled trials. Ann Oncol. januari 2015;26(1):13-21.
- Sveen A, Løes IM, Alagaratnam S, Nilsen G, Høland M, Lingjærde OC, e.a. Intra-patient Intermetastatic Genetic Heterogeneity in Colorectal Cancer as a Key Determinant of Survival after Curative Liver Resection. Maley CC, redacteur. PLOS Genet. 29 juli 2016;12(7):e1006225.
- Spindler KLG, Boysen AK, Pallisgård N, Johansen JS, Tabernero J, Sørensen MM, e.a. Cell-Free DNA in Metastatic Colorectal Cancer: A Systematic Review and Meta-Analysis. The Oncologist. 1 september 2017;22(9):1049-55.
- Bettegowda C, Sausen M, Leary RJ, Kinde I, Wang Y, Agrawal N, e.a. Detection of Circulating Tumor DNA in Early- and Late-Stage Human Malignancies. Sci Transl Med [Internet]. 19 februari 2014 [geciteerd 7 september 2023];6(224). Beschikbaar op: https://www.science.org/doi/10.1126/ scitranslmed.3007094
- Merker JD, Oxnard GR, Compton C, Diehn M, Hurley P, Lazar AJ, e.a. Circulating Tumor DNA Analysis in Patients With Cancer: American Society of Clinical Oncology and College of American Pathologists Joint Review. J Clin Oncol. 1 juni 2018;36(16):1631-41.
- Garcia J, Forestier J, Dusserre E, Wozny AS, Geiguer F, Merle P, e.a. Cross-platform comparison for the detection of RAS mutations in cfDNA (ddPCR Biorad detection assay, BEAMing assay, and NGS strategy). Oncotarget. 20 april 2018;9(30):21122-31.
- Vivancos A, Aranda E, Benavides M, Élez E, Gómez-España MA, Toledano M, e.a. Comparison of the Clinical Sensitivity of the Idylla Platform and the OncoBEAM RAS CRC Assay for KRAS Mutation Detection in Liquid Biopsy Samples. Sci Rep. 20 juni 2019;9(1):8976.
- Thress KS, Brant R, Carr TH, Dearden S, Jenkins S, Brown H, e.a. EGFR mutation detection in ctDNA from NSCLC patient plasma: A cross-platform comparison of leading technologies to support the clinical development of AZD9291. Lung Cancer. december 2015;90(3):509-15.
- Wang W, Song Z, Zhang Y. A Comparison of ddPCR and ARMS for detecting EGFR T790M status in ctDNA from advanced NSCLC patients with acquired EGFR-TKI resistance. Cancer Med. januari 2017;6(1):154-62.
- 10. Sorber L, Zwaenepoel K, Deschoolmeester V, Roeyen G, Lardon F, Rolfo C, e.a. A Comparison of Cell-Free DNA Isolation Kits. J Mol Diagn. januari 2017;19(1):162-8.
- 11. Burbach JPM, Kurk SA, Coebergh Van Den Braak RRJ, Dik VK, May AM, Meijer GA, e.a. Prospective Dutch colorectal cancer cohort: an infrastructure for long-term observational, prognostic, predictive and (randomized) intervention research. Acta Oncol. 1 november 2016;55(11):1273-80.
- 12. Yaeger R, Chatila WK, Lipsyc MD, Hechtman JF, Cercek A, Sanchez-Vega F, e.a. Clinical Sequencing Defines the Genomic Landscape of Metastatic Colorectal Cancer. Cancer Cell. januari 2018;33(1):125-136.e3.
- 13. Gao J, Aksoy BA, Dogrusoz U, Dresdner G, Gross B, Sumer SO, e.a. Integrative Analysis of Complex Cancer Genomics and Clinical Profiles Using the cBioPortal. Sci Signal [Internet]. 2 april 2013 [geciteerd 7 september 2023];6(269). Beschikbaar op: https://www.science.org/doi/10.1126/ scisignal.2004088
- 14. Cerami E, Gao J, Dogrusoz U, Gross BE, Sumer SO, Aksoy BA, e.a. The cBio Cancer Genomics Portal: An Open Platform for Exploring Multidimensional Cancer Genomics Data. Cancer Discov. 1 mei 2012;2(5):401-4.

- 15. Lievens Y, Van Den Bogaert W, Kesteloot K. Activity-based costing: a practical model for cost calculation in radiotherapy. Int J Radiat Oncol. oktober 2003;57(2):522-35.
- 16. Tie J, Cohen JD, Wang Y, Li L, Christie M, Simons K, e.a. Serial circulating tumour DNA analysis during multimodality treatment of locally advanced rectal cancer: a prospective biomarker study. Gut. april 2019;68(4):663-71.
- 17. Schwaederle M, Chattopadhyay R, Kato S, Fanta PT, Banks KC, Choi IS, e.a. Genomic Alterations in Circulating Tumor DNA from Diverse Cancer Patients Identified by Next-Generation Sequencing. Cancer Res. 1 oktober 2017;77(19):5419-27.
- 18. Wang Y, Li L, Cohen JD, Kinde I, Ptak J, Popoli M, e.a. Prognostic Potential of Circulating Tumor DNA Measurement in Postoperative Surveillance of Nonmetastatic Colorectal Cancer. JAMA Oncol. 1 augustus 2019;5(8):1118.

Supplemental files

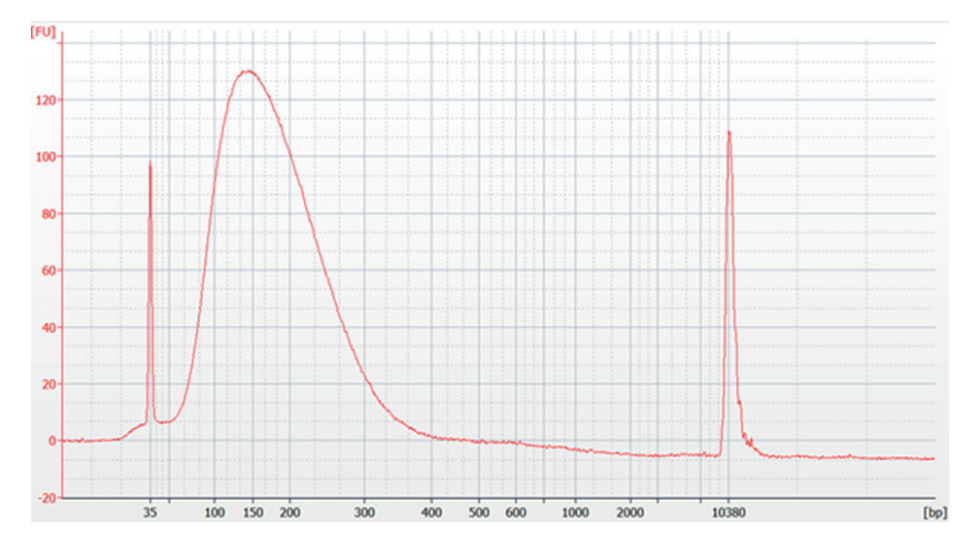
Supplemental table 1. Clinical data for patients presented in tables 1 and 2.

Patient ID (table/line)	Palliative systemic treatment agents	Palliative systemic treatment line	Previous systemic treatments
1/1	encorafenib/ binimetinib/ cetuximab	3rd line	CAPOX (6x), CAP (4x), irinotecan (3x)
1/2	CAP-B (maintainance)	1st line	Started CAPOX-B (6x), CAP-B maintainance
1/3	FOLFIRI-B	1st line	Adjuvant CAPOX (8x)
1/4	FOLFOX-B	1st line	None
1/5	start FOLFOXIRI-B	1st line	None
1/6	FOLFOXIRI-B	1st line	None
2/1	Trifluridine-tipiracil	3rd line	CAPOX/FOLFOX (10x), CAP (6x), irinotecan (2x)
2/2	CAP-B (maintainance)	1st line	CAPOX-B (2x), CAP-B reintroduction after treatment holiday
2/3	CAP-B	2nd line	CAPOX-B (6x), FOLFIRI (metastasectomy thereafter)
2/4	Not started, started CAP-B 2 months later	n.a.	None
2/5	CAP-B	1st line	None
2/6	FOLFOX-B	1st line	None
2/7	CAP-B (maintainance)	1st line	CAPOX-B (4x)
2/8	FOLFIRI-B	1st line	None
2/9	CAP-B (maintainance)	1st line	Started CAPOX-B (6x), CAP-B maintainance
2/10	FOLFIRI-B	1st line	None
2/11	FOLFOXIRI-B	1st line	CAPOX-B (4x), CAPOX (4x) and tumor debulking in ORCHESTRA

Time on treatment (months)	Disease status	First response evaluation after liquid biopsy	Metastatic site(s)
3	Partial response	RECIST PR	Liver, lymph nodes
9	Signs of progression	RECIST PD	Peritoneum
0.5	Recently started systemic therapy	RECIST SD, tumor load increasing	Lymph nodes, peritoneum
0.5	Recently started systemic therapy	RECIST PD	Liver, lymph nodes
0	At start palliative systemic treatment	RECIST SD, tumor load not altered	Liver, peritoneum, lung
2	Recently started systemic therapy	RECIST SD, tumor load decreasing	Liver
0.5	Recently started new systemic therapy	RECIST PD	Liver, lymph nodes, lung, peritoneum, subcutis
0	At start reintroduction CAP-B	RECIST SD, tumor load decreasing	Liver, bones, local recurrence primary tumor
1	Recently started new systemic therapy	RECIST PD	Liver, lymph nodes
0	Treatment naive, started CAP-B 2 months later	n.a.	Liver
3	Responsive to firstline treatment	RECIST SD, tumor load decreasing	Liver, lung, peritoneum
0	At start palliative systemic treatment	RECIST SD, tumor load not altered	Liver, lung, lymph nodes, primary tumor
5	Stable disease	RECIST SD, tumor load not altered	Liver, lung, primary tumor
1	Recently started systemic therapy	RECIST PR (metastasectomy was performed)	Liver
18	Responsive to firstline treatment	RECIST SD, tumor load increasing	Lung, primary tumor
2	Stable disease	RECIST SD, tumor load not altered	Liver, peritoneum
0	Recently started new systemic therapy	RECIST PR	Lung, bones

Supplemental table 2. Technical specifications of the compared platforms, as reported by manufacturers.

	ddPCR	Idylla	COBAS z480	BEAMing
Basic principle	droplet digital PCR	quantitative PCR	quantitative PCR	droplet multiplex PCR
Number of amino acid changes in <i>KRAS</i> detectable by platform	7	18	21	14
Plasma input volume	None specified	1 ml plasma	2 ml plasma	3 ml plasma
cfDNA isolation method	None specified	In cartridge	Column based, supplied with kit	Column based, supplied with kit
Quantitation	Quantitative (copies/μl)	Semi-quantitative (Cq values)	Semi-quantitative (SQI values)	Quantitative (mutant fraction)
Reported lower limit of detection	0.1% allele frequency	100 copies/ ml plasma	200 copies/ ml plasma	0.02% allele frequency
Hands-on time	1-3 hours	15 minutes	1-3 hours	8-9 hours
Time to result	None specified	2-3 hours	1-2 days	3 days



Supplemental figure 1. BioAnalyzer trace for enzymatically fragmented, double-sided SPRI size selected wildtype genomic DNA. The peak corresponds to 149bp, slightly smaller than for cfDNA (160-170bp).

Supplemental sequences for synthetic KRAS fragments are provided in the online supplemental files, as are supplemental data sets 1 and 2 at DOI 10.1038/s41598-020-64822-7.



Chapter 4

Clinical Utility of Plasma-Based Comprehensive Molecular Profiling in Advanced Non–Small-Cell Lung Cancer

R.D. Schouten^{1*}, D.C.L. Vessies^{2*}, L.J.W. Bosch³, N.P. Barlo⁴, A.S.R. van Lindert⁵, S.A.G.M. Cillessen⁶, D. van den Broek², M.M. van den Heuvel⁷, K. Monkhorst³

- ¹ Netherlands Cancer Institute, department of pulmonology, Amsterdam, the Netherlands
- ² Netherlands Cancer Institute, department of laboratory medicine, Amsterdam, the Netherlands
- ³ Netherlands Cancer Institute, department of pathology, Amsterdam, The Netherlands
- ⁴ Noordwest Ziekenhuisgroep, Alkmaar, the Netherlands
- ⁵ University Medical Centre Utrecht, Utrecht, the Netherlands
- ⁶ Amsterdam University Medical Centres, Amsterdam, the Netherlands
- ⁷ Radboud University Medical Centre, department of pulmonology, Nijmegen, the Netherlands

^{*} Authors contributed equally

Abstract

Purpose

Comprehensive molecular profiling (CMP) plays an essential role in clinical decision making in metastatic non-small-cell lung cancer (mNSCLC). Circulating tumor DNA (ctDNA) analysis provides possibilities for molecular tumor profiling. In this study, we aim to explore the additional value of centralized ctDNA profiling next to current standard-of-care protocolled tissue-based molecular profiling (SoC-TMP) in the primary diagnostic setting of mNSCLC in the Netherlands.

Methods

Pretreatment plasma samples from 209 patients with confirmed mNSCLC were analyzed retrospectively using the NGS AVENIO ctDNA Targeted Kit (Roche Diagnostics, Basel, Switzerland) and compared with paired prospective pretreatment tissue-based molecular profiling from patient records. The AVENIO panel is designed to detect single-nucleotide variants, copy-number variations, insertions or deletions, and tyrosine kinase fusion in 17 genes.

Results

Potentially targetable drivers were detected with SoC-TMP alone in 34.4% of patients. Addition of clonal hematopoiesis of indeterminate potential-corrected, plasma-based CMP increased this to 39.7% (P < 0.001). Concordance between SoC-TMP and plasma-CMP was 86.6% for potentially targetable drivers. Clinical sensitivity of plasma-CMP was 75.2% for any oncogenic driver. Specificity and positive predictive value were more than 90% for all oncogenic drivers.

Conclusion

Plasma-CMP is a reliable tool in the primary diagnostic setting, although it cannot fully replace SoC-TMP. Complementary profiling by combined SoC-TMP and plasma-CMP increased the proportion of patients who are eligible for targeted treatment.

Introduction

Comprehensive molecular profiling (CMP) has become a cornerstone in clinical decision making in metastatic non-small-cell lung cancer (mNSCLC). Identifying genetic biomarkers in tumor tissue allows optimal personalized treatment in the first-line setting. A distinct set of biomarkers is recommended for diagnostic testing in all patients with stage IV NSCLC (1-3).

In lung cancer, the standard diagnostic procedures are often hampered by a lack of available tumor tissue or tissue being unsuitable for molecular analysis (4–6). One of the reasons for this can be that no tumor sampling can take place because of a poor clinical condition at the time of diagnosis, and biopsies can be considered too risky. As a result, many patients will not receive optimal personalized treatment.

Analysis of circulating tumor DNA (ctDNA) from a patient's blood has provided minimally invasive possibilities for molecular tumor profiling. Various studies have shown that next-generation sequencing (NGS) of plasma ctDNA can be useful for detecting genetic biomarkers. Plasma NGS has shown high sensitivity and high concordance with standard-of-care tissue-based molecular profiling (SoC-TMP) (7-10). Here, we compared plasma-based CMP plus SoC-TMP to SoC-TMP alone. This was performed in the Dutch diagnostic landscape with a relatively high proportion of tissue profiled patients, in contrast to the diagnostic landscape in earlier studies. Additionally, plasma-CMP in those studies was often outsourced, and here we investigate the performance of in house plasma-CMP on the AVENIO platform.

Therefore, in this study, we explore the additional value of centralized, in-house plasma-CMP next to modern SoC-TMP in the Dutch diagnostic landscape. Secondary aims are to determine the concordance of plasma-CMP and SoC-TMP, and the number of targetable mutations identified by plasma-CMP only.

Materials and methods

Patients

All patients in this study consented with the use of plasma and tissue samples by providing written informed consent for participation in a larger project, namely the Lung cancer Early Molecular Assessment trial: ClinicalTrials.gov identifier: NCT02894853. This multicenter diagnostic study was reviewed and approved by the medical ethics committee of the Netherlands Cancer Institute in Amsterdam, the Netherlands. The ctDNA substudy reported here was conducted in accordance with the Declaration of Helsinki (as revised in 2013) and the guidelines for Good Clinical Practice.

Nine hospitals in the Netherlands contributed to patient enrollment. Patients were eligible if they had confirmed stage IV NSCLC, were fully treatment-naive, and had a pretreatment plasma sample taken. To exclude the risk of selection bias, the first consecutive cohort of 224 patients was included.

Study Procedures

Decentralized tissue analysis was performed according to the local standard of care in the hospital of enrollment during routine clinical diagnostic workup. SoC-TMP consisted of NGS (panels shown in Appendix Table A1) and single gene analyses for rearrangements. The results from SoC-TMP were obtained from the clinical pathology reports, or was requested from either the treating pulmonologist, the involved pathologist, or the involved clinical molecular biologist. According to national and international quidelines, molecular profiling should cover known NSCLC oncodriver genes such as KRAS, EGFR, BRAF, ERBB2, ALK, ROS1, RET, and MET (1-3).

Plasma-CMP was centrally performed retrospectively and did not affect clinical decision making. Blood samples were centrally stored and processed. Samples from patients at the site of the central laboratory were collected in K2-EDTA tubes, whereas those from patients in other hospitals were collected in cellstabilizing tubes (STRECK, Omaha, NE). All whole-blood samples were sent to the central laboratory by regular mailing services. Local sampling, central processing, and central storage of all blood samples were completed within the 5-day stabilizing period.

Blood samples were centrifuged for 10 minutes at 1,700g at room temperature. Cells were stored at -80°C and plasma was centrifuged for 10 minutes at 20,000g before storage at -80°C. Median 5 mL cell-free plasma—interguartile range 4-6 mL—was used per sample for isolation of cell-free DNA (cfDNA) using the QIAsymphony Circulating DNA Kit (article number 1091063, Qiagen, Düsseldorf, Germany) with the QIAsymphony (Qiagen). A median of 39 ng cfDNA (interquartile range 28-50 ng) was used as input for plasma-based NGS. With the exception of the cfDNA isolation methods used, all sample handlings were performed according to manufacturer guidelines.

Plasma-CMP was performed using the AVENIO ctDNA Targeted kit (11,12) (Roche Diagnostics, Basel, Switzerland), which covers hotspot regions of the aforementioned eight oncodriver genes (KRAS, EGFR, BRAF, ERBB2, ALK, ROS1, RET, and MET) and in an additional nine other genes: APC, BRCA1, BRCA2, DPYD, KIT, NRAS, PDGFRA, TP53, and UGT1A1. Single-nucleotide variants with a variant allele frequency (VAF) of 0.10% or higher have reported sensitivity and positive predictive value (PPV) of > 99% (12), and were considered in the analysis. Copy-number variations (CNV) with a test-specific CNV score lower than 5.0 are considered borderline, according to the kit manual. However, we found high variability in CNV score, and no correlation between CNV score and detection rate in tissue was seen. Additionally, a large proportion of CNVs (11 out of 30; 36.7%) that were detected in plasma were not covered in the matched tissue analysis. We considered that we could not make a reliable statement about CNV testing in this setting, and therefore we excluded all CNVs that were reported by plasma-CMP from our final analysis.

All variants were classified per level of pathogenicity using online databases at OncoKB (update September 17, 2020) (13), ClinVar (14), IARC TP53 Database (15), COSMIC (16), JaxCKB (17), and Franklin Genoox (18). The system published at OncoKB (version V2, published on December 20, 2019) (19) was used as the basis for classification of drivers. In this report, level 1 drivers are US Food and Drug Administration (FDA)-recognized biomarkers predictive of response to an FDAapproved drug in NSCLC. Level 2 or 3A drivers are biomarkers predictive of response to a drug that may be available off-label or in the setting of a clinical trial. Level 3B or 4 drivers are biomarkers for which there is an FDA-approved or investigational drug available in another indication, or for which there is compelling biologic evidence of response to a drug (13).

Genetic variants that are detected in cfDNA may not always be associated with cancer. Other studies have shown that many cfDNA mutations may be consistent with clonal hematopoiesis of indeterminate potential (CHIP) (20,21). Samples containing driver mutations in plasma but not in tissue were verified on the blood cell pellet to exclude CHIP. DNA was isolated from the cells using the QIAsymphony DSP DNA Midi Kit (article number 937255, Qiagen) with the QIAsymphony. The DNA was fragmented sonically using a Covaris ME220 Focused-ultrasonicator (Covaris Inc, Woburn, MA) in microTUBE AFA Fiber Pre-Slit Snap-Cap (PN 520045) vessels, with the following settings: duration 100 seconds, peak power 75 W, duty factor 25%, and 1,000 cycles per burst. DNA input for AVENIO ctDNA Targeted Kit (Roche) was 50 ng. Sequencing depth was identical to the plasma samples to avoid falsenegative results.

Index hopping, or index cross-talk, is a possible cause of false positives and is inherent to massively parallel sequencing methods where multiple samples are pooled (22,23). The plasma-CMP pipeline automatically flags samples that are potentially the result of index hopping. All suspect samples in our cohort were retested.

Statistical Analyses

For this exploratory study, we had a maximum of 224 plasma NGS tests available in the central laboratory. Concordance was defined as the sum of true positives and true negatives as a fraction of all tests. Sensitivity, specificity, PPV, and negative predictive value (NPV) of plasma-CMP were calculated with SoC-TMP as the gold standard. We applied McNemar's chi-square test to assess whether combined SoC-TMP plus plasma-CMP identifies more patients with driver mutations than SoC-TMP alone ($\alpha = .05$). To assess any difference in DNA input between samples in which oncogenic drivers were concordantly detected in tissue and plasma, and samples in which drivers were not detected in plasma, a Mann-Whitney U test for unpaired data with no normal distribution was used. Statistical analyses were performed using IBM SPSS Statistics version 27.

Results

Cohort Characteristics

In total, 224 patients with confirmed stage IV NSCLC were included in this study. Fifteen patients were excluded from the analysis. Three patients were not treatmentnaive at the time of tissue sampling, and no pretreatment plasma samples were available for 12 patients. In total, 209 patients were included in the analysis (Fig 1). The median time between the collection of tissue for standard diagnostic purposes and the collection of blood for plasma-CMP was 14 days (range, 0-90 days), with 84.3% of paired samples taken within 30 days.

Detection of Oncogenic Variants

In total, 363 oncogenic variants were detected in 209 patients; these are shown in graphic overviews in the Data Supplement. Routine molecular diagnostics in tissue resulted in molecular profiling of 182 patients (87.1%, Data Supplement), centralized in-house plasma-CMP was feasible in 206 patients (98.6%, Data Supplement), and combined feasibility was 85.6% (179/209 patients, Data Supplement). All detected oncogenic drivers are shown in Appendix Tables A2-A4.

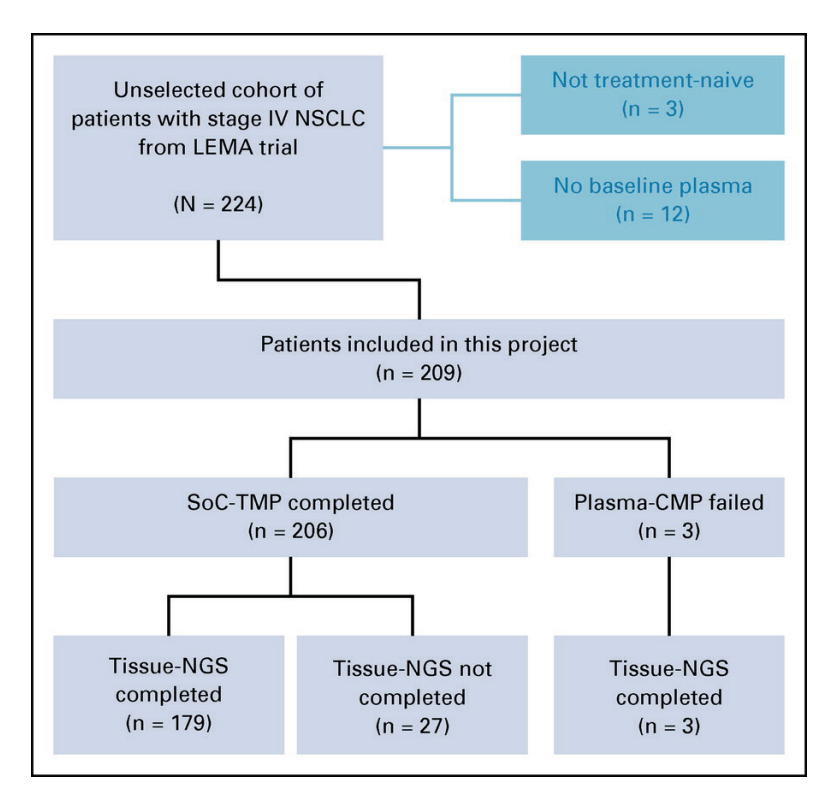


Figure 1. Flow diagram of inclusion. In total, 209 patients had CMP, either tissue-based, plasma-based, or both. Fifteen of the initially selected 224 patients were ineligible. CMP, comprehensive molecular profiling; LEMA, Lung cancer Early Molecular Assessment; NGS, next-generation sequencing; NSCLC, non-small-cell lung cancer; SoC-TMP, standard-of-care protocolled tissue-based molecular profiling.

Out of 182 patients for whom SoC-TMP was feasible, level 1 drivers were identified in 31 patients (17.0%). The number of patients identified with a potentially targetable driver (level 1, 2, or 3A) in tissue was 72 (39.6%). The total number of patients with an oncogenic driver (level 1-4, including most KRAS mutations) in tissue was 121 (66.5%). Histologic subtypes in the latter group were 112 adenocarcinomas, four squamous cell carcinomas (SCCs), two large-cell neuroendocrine carcinomas, one sarcomatoid carcinoma, and two not-otherwise-specified NSCLC. The diagnostic yield of SoC-TMP, i.e., the proportion of patients in the total cohort in whom a level 1-4 driver was found, was 57.9% (121 out of 209 patients).

Plasma-CMP identified 24 patients with a Level 1 driver (11.7% of 206), 62 patients with a level 1-3A driver (30.1%), and 103 patients with a level 1-4 driver (50.0%). The diagnostic yield of plasma-CMP was 49.3% (103 out of 209 patients).

Performance of Plasma-CMP Compared With SoC-TMP

Out of 179 patients for whom both SoC-TMP and plasma-CMP were completed, 31 were identified with a level 1 driver in either tissue, plasma, or both. Twentyone out of 31 patients were identified by both SoC-TMP and plasma-CMP (67.7%). Nine patients were identified by SoC-TMP only, and one patient was identified by plasma-CMP only. Concordance of level 1 driver detection, comprising both negative and positive cases, was 94.4% (169 out of 179 patients).

Level 1-3A drivers were detected in 75 out of these 179 patients. Fifty-one were identified by both SoC-TMP and plasma-CMP (68.0%), 19 by SoC-TMP alone, and five by plasma-CMP alone. Concordance of level 1-3A driver detection was 86.6% (155 out of 179 patients).

A total of 117 patients were identified with a level 1-4 driver: 88 by both SoC-TMP and plasma-CMP (75.2%), 24 exclusively by SoC-TMP, and five by plasma-CMP only. Concordance of level 1-4 driver detection was 83.8% (150/179).

Compared with current SoC-TMP, sensitivity of plasma-CMP was 70.0% for level 1 drivers, 72.9% for level 1-3A drivers, and 78.6% for level 1-4 drivers. Specificity of plasma-CMP was 99.3%, 95.4%, and 92.5% for level 1, level 1-3A, and level 1-4 drivers, respectively. PPV was 95.5% and NPV was 94.3% for level 1 drivers. PPV and NPV were 91.1% and 84.6% for level 1-3A drivers, respectively. Finally, for level 1-4 drivers, PPV was 94.6% and NPV was 72.1%. Full contingency tables are shown in Appendix Table A5.

Concordance between plasma-CMP and SoC-TMP might have been affected by the DNA input of plasma-CMP. When considering all oncogenic driver variants (level 1-4), the diagnostic yield was correlated with DNA input: median input from concordant samples was 42.95 ng (range, 12.7-50.0 ng), and 28.65 ng (range, 10.3-50.0 ng) in samples in which tissue-identified drivers were not detected in plasma (P = .038).

Additional Value of Plasma-CMP

Plasma-CMP identified additional driver mutations in eight patients who reported a completed SoC-TMP. One patient was identified with a KRAS G12C in plasma, whereas a KRAS G12A was also detected in both tissue and plasma. One patient was identified with a level 1 driver, six patients with a level 2-3A driver, and one with a level 4 driver.

For 27 patients (12.9% of the total cohort), SoC-TMP was not feasible because of insufficient tumor material (n = 13; 48.1%), no tumor material (n = 9; 33.3%), or for unknown reasons (n = 5; 18.5%). This involved 11 patients with adenocarcinoma, nine with SCC, one with large cell neuroendocrine carcinoma, and six with tumors of undetermined histology. A level 1 driver was detected in two of these patients (7.4%), two other patients had a KRAS G12C mutation (level 1-3A driver total n = 4; 14.8%), and another three had a level 3B-4 driver (level 1-4 driver total n = 7; 25.9%) (Data Supplement).

In total, plasma-CMP next to SoC-TMP increased the number of patients with a level 1 driver from 31 to 34 in the total cohort; from 14.8% to 16.3% of 209 patients (P = .250). For patients with level 1-3A driver, the number significantly increased from 72 to 83 patients (ie, 34.4%-39.7% of the total cohort, P < .001). Considering level 1-4 drivers, the number of patients identified also increased significantly from 121 to 135 (ie. 57.9%-64.6% of the total cohort: P < .001).

CHIP and Index Hopping

In our cohort, 18 patients (8.6%) were identified in whom a total of 23 level 1-4 driver mutations were detected in plasma that had not been detected by SoC-TMP. For seven of these 18 patients, SoC-TMP was incomplete and did not cover the variant detected in plasma. In the remaining 11 patients, SoC-TMP had not detected the mutation. WBC DNA sequencing detected one of the suspect variants (KRAS G12S, patient P177), which was considered to be a CHIP and excluded from further analyses.

The plasma-CMP pipeline flagged two variants that potentially resulted from index hopping. Both were EGFR L858R mutations and could not be reproduced by retesting; one sample was negative in the retest, and the other test failed because of technical problems. Moreover, digital droplet PCR did not confirm the L858R mutations in these samples. Therefore, both samples were considered negative for EGFR L858R in the final analysis and are not shown in figures or tables.

Discussion

We aimed to determine the value of CMP of plasma in a real-world, multicenter, clinical cohort of treatment-naive patients who presented with metastasized NSCLC. Our results show that plasma-CMP next to SoC-TMP identified significantly more patients with potentially targetable driver mutations (i.e. Level 1-3A, P < .001) and other clinically relevant drivers in the Dutch diagnostic landscape. Plasma-CMP produced reliable data in a real-world cohort with PPV and specificity of > 90%. The concordance with SoC-TMP was at least 83.8% and clinical sensitivity at least 67.7% for oncogenic drivers.

The increased number of patients with an oncogenic driver was lower than previously was published (9,10). This is primarily because the yield of potentially targetable driver mutations from SoC-TMP was higher in our cohort (34.4%) than for others (20.5% (9) and 21.3% (10)), leaving less room for improvement, given that the total number of patients identified with a potentially targetable driver after addition of plasma-CMP was comparable in our cohort (39.7%) to others (35.8% (9) and 27.3% (10)).

Another factor that helps explain the seemingly small increase of oncogenic driver mutations detected by addition of plasma-CMP is that in our cohort, the group with missing or incomplete SoC-TMP contained relatively more SCCs (nine out of 27 v 10 out of 182 in the rest of the cohort), possibly because this histologic subtype is physically harder to reach for biopsy. The prevalence of driver mutations is known to be lower in SCC, meaning that the subset of patients with missing or incomplete SoC-TMP is enriched for a group of patients for whom plasma-CMP is less likely to be of added value.

CHIPs were detected in only one patient (0.5%), contrasting starkly with other studies reporting CHIPs in 53%-62% of patients (20,24). Most importantly, we showed that CHIPs rarely occur as clinically relevant driver variants. Although other studies report all CHIPs found with sequencing panels up to 2 Mbp in size, we focused exclusively on clinical relevance and only reported variants that might affect treatment decisions. None of these variants was in the top 28 genes most affected by CHIPs. Even among variants found in plasma but not in tissue, the number of CHIPs found was comparatively low, suggesting that these variants may originate from other lesions than the one biopsied for SoC-TMP. Together, these findings indicate that routine testing of blood cell pellets with extensive NGS methods may not be necessary in the setting of treatment selection.

We postulate that plasma-CMP can be used in the clinical setting in two scenarios. First, synchronous combined SoC-TMP and plasma-CMP to increase the proportion of patients in whom a potentially targetable driver is detected. This may increase the number of patients who receives optimal personalized treatment. Our data support the potential utility of plasma-CMP in this scenario. Second, upfront plasma-CMP,

4

followed by SoC-TMP when no targetable driver is detected in plasma, might be a realistic option, given the high specificity and PPV, and lower sensitivity and NPV of plasma-CMP. However, it cannot fully replace tissue-based diagnostics as certain biomarkers (eg, histologic subtype or programmed death-ligand 1) can currently only be assessed on tumor tissue. Until alternative methods for such companion diagnostics are developed (25), the need for obtaining tumor tissue remains.

We conclude that in-house plasma-CMP improves the detection of clinically relevant oncodriver mutations in patients with mNSCLC. With an expanding palette of treatable mutations, rapid advances in molecular diagnostics, and increasing affordability and performance of plasma-CMP, this relatively new technique is establishing its role in the diagnostic workup of mNSCLC. However, analysis of the cost effectiveness is warranted to determine the optimal implementation in routine clinical care.

References

- Novello S, Barlesi F, Califano R, Cufer T, Ekman S, Levra MG, e.a. Metastatic non-small-cell lung cancer: ESMO Clinical Practice Guidelines for diagnosis, treatment and follow-up. Ann Oncol. september 2016:27:v1-27.
- Planchard D, Popat S, Kerr K, Novello S, Smit EF, Faivre-Finn C, e.a. Metastatic non-small cell lung cancer: ESMO Clinical Practice Guidelines for diagnosis, treatment and follow-up. Ann Oncol. oktober 2018;29:iv192-237.
- Integraal Kankercentrum Nederland I. Landelijke richtlijn niet kleincellig longcarcinoom. [Internet]. Beschikbaar op: https://iknl.nl/nkr/evaluatie-met-nkr-data/richtlijnen
- Rangachari D. VanderLaan PA, Le X, Folch E, Kent MS, Gangadharan SP, e.a. Experience with targeted next generation sequencing for the care of lung cancer: Insights into promises and limitations of genomic oncology in day-to-day practice. Cancer Treat Commun. 2015;4:174-81.
- Lim C, Tsao MS, Le LW, Shepherd FA, Feld R, Burkes RL, e.a. Biomarker testing and time to treatment decision in patients with advanced nonsmall-cell lung cancer. Ann Oncol. juli 2015;26(7):1415-21.
- Kuijpers C, Heuvel M, Overbeek L, van Slooten HJ, Lindert A, Damhuis R, e.a. National variation in molecular diagnostics in metastatic lung cancer. Ned Tijdschr Geneeskd. december 2018;162.
- Lovejoy A, Pati A, Muñoz A. In-depth assessment reveals powerful performance and flexibility of the AVENIO ctDNA Analysis Kits. [Internet]. 2017. Beschikbaar op: https://sequencing.roche. com/content/dam/rochesequence/worldwide/resources/SEQ100108_AVENIO%20ctDNA_ Performance_White_Paper.pdf
- Balaji SA, Shanmugam A, Chougule A, Sridharan S, Prabhash K, Arya A, e.a. Analysis of solid tumor mutation profiles in liquid biopsy. Cancer Med. november 2018;7(11):5439-47.
- Aggarwal C, Thompson JC, Black TA, Katz SI, Fan R, Yee SS, e.a. Clinical Implications of Plasma-Based Genotyping With the Delivery of Personalized Therapy in Metastatic Non-Small Cell Lung Cancer, JAMA Oncol. 1 februari 2019;5(2):173.
- 10. Leighl NB, Page RD, Raymond VM, Daniel DB, Divers SG, Reckamp KL, e.a. Clinical Utility of Comprehensive Cell-free DNA Analysis to Identify Genomic Biomarkers in Patients with Newly Diagnosed Metastatic Non-small Cell Lung Cancer. Clin Cancer Res. 1 augustus 2019;25(15):4691-700.
- 11. Newman AM, Lovejoy AF, Klass DM, Kurtz DM, Chabon JJ, Scherer F, e.a. Integrated digital error suppression for improved detection of circulating tumor DNA. Nat Biotechnol. mei 2016;34(5):547-55.
- 12. Roche Sequencing Solutions. AVENIO ctDNA Targeted Kit. [Internet]. Beschikbaar op: https:// sequencing.roche.com/content/dam/rochesequence/worldwide/resources/brochure-avenioctdna-targeted-kit-SEQ100046.pdf
- 13. Chakravarty D, Gao J, Phillips S, Kundra R, Zhang H, Wang J, e.a. OncoKB: A Precision Oncology Knowledge Base. JCO Precis Oncol. november 2017;(1):1-16.
- 14. National Library of Medicine. Variation Viewer [Internet]. Beschikbaar op: https://www.ncbi.nlm. nih.gov/variation/view/
- 15. Bouaoun L, Sonkin D, Ardin M, Hollstein M, Byrnes G, Zavadil J, e.a. TP53 Variations in Human Cancers: New Lessons from the IARC TP53 Database and Genomics Data: Human Mutation. Hum Mutat. september 2016;37(9):865-76.
- 16. Forbes SA, Beare D, Boutselakis H, Bamford S, Bindal N, Tate J, e.a. COSMIC: somatic cancer genetics at high-resolution. Nucleic Acids Res. 4 januari 2017;45(D1):D777-83.

- 17. JaxCKB [Internet]. Beschikbaar op: https://ckb.jax.org/gene/grid
- 18. Franklin Genoox [Internet]. Beschikbaar op: https://franklin.genoox.com/home
- 19. OncoKB. OncoKB Therapeutic Levels of Evidence V2 [Internet]. Beschikbaar op: https://www. oncokb.org/levels
- 20. Razavi P, Li BT, Brown DN, Jung B, Hubbell E, Shen R, e.a. High-intensity sequencing reveals the sources of plasma circulating cell-free DNA variants. Nat Med. december 2019;25(12):1928-37.
- 21. Hu Y, Ulrich BC, Supplee J, Kuang Y, Lizotte PH, Feeney NB, e.a. False-Positive Plasma Genotyping Due to Clonal Hematopoiesis. Clin Cancer Res. 15 september 2018;24(18):4437-43.
- 22. MacConaill LE, Burns RT, Nag A, Coleman HA, Slevin MK, Giorda K, e.a. Unique, dual-indexed sequencing adapters with UMIs effectively eliminate index cross-talk and significantly improve sensitivity of massively parallel sequencing, BMC Genomics, december 2018;19(1):30.
- 23. Kircher M, Sawyer S, Meyer M. Double indexing overcomes inaccuracies in multiplex sequencing on the Illumina platform. Nucleic Acids Res. 1 januari 2012;40(1):e3-e3.
- 24. Leal A, Van Grieken NCT, Palsgrove DN, Phallen J, Medina JE, Hruban C, e.a. White blood cell and cell-free DNA analyses for detection of residual disease in gastric cancer. Nat Commun. 27 januari 2020;11(1):525.
- 25. Kloten, Lampignano, Krahn, Schlange. Circulating Tumor Cell PD-L1 Expression as Biomarker for Therapeutic Efficacy of Immune Checkpoint Inhibition in NSCLC. Cells. 1 augustus 2019;8(8):809.

Appendix

Original Appendix tables are available for this paper at DOI: 10.1200/PO.20.00450

Table A1. Standard-of-Care Tissue-Based Molecular Profiling Techniques

Ion Ampliseq Cancer Hotspot Panel

Ion Ampliseq Colon and Lung Cancer Research Panel

Truseq Amplicon Cancer Panel

Single-Molecule Molecular Inversion Probes Panel

Note. Molecular profiling of tumor tissue was performed decentralized, according to the local standard of care. The participating centers used various versions of the panels shown here, including customized versions. In addition to these next-generation sequencing panels, the molecular diagnostics included single gene analyses for rearrangements and copy-number variations (eg, immunohistochemistry and fluorescent in situ hybridization).

Table A2. Level 1 Driver Mutations Detected in Tissue, Plasma, or Both

Detected	in Both	Detected in Both Tissue and Plasma		Detected in Tissue Only	in Tissue	Only		Detected in Plasma Only	in Plasm	ia Only	
Patient	Gene	Variant	VAF Plasma (%)	Patient	Gene	Variant	VAF Plasma (%)	Patient	Gene	Variant	VAF Plasma (%)
P082	ALK	Fusion EML4	No VAF	P068	BRAF	V600E	Not detected	P091	ALK	L1196M	0.1
P085	ALK	Fusion EML4	No VAF	P113	EGFR	E746_A750del	Not detected	P131a	BRAF	V600E	2
P089	ALK	Fusion EML4	No VAF	P152	EGFR	E746_AS752delinsV	Not detected	P176 ^b	EGFR	E746_A750del	6.2
P100	BRAF	V600E	49.6	P119	EGFR	L858R	Not detected	P019 ^b	MET	c.3082+3A>G	0.1
P097	BRAF	V600E	16.9	P034	EGFR	L858R	Not detected				
P053	BRAF	V600E	16.8	P191	EGFR	S752_I759del	Not detected				
P135	BRAF	V600E	1	P117	EGFR	T790M	Not detected				
P008	BRAF	V600E	6.0	P075°	MET	Y1003F	Not detected				
P150	EGFR	E746_A750del	13.1	P063	ROS1	fusion	Not detected				
P067	EGFR	E746_A750del	0.3	P009	ROS1	fusion	Not detected				
P029	EGFR	E746_S752delinsV	3								
P001	EGFR	L747_E749del	1.2								
P139	EGFR	L858R	11.4								
P157	EGFR	L858R	3.9								
P131	EGFR	L858R	3.7								
P093	EGFR	L858R	1.2								
P126	EGFR	L861Q	4.2								
P136	MET	c.3028+3A>G	5.2								
P087	MET	c.3082+1G>A	14.1								
016	RET	Fusion KIF5B	No VAF								
P057	ROS1	Fusion SLC34A2	No VAF								
Abbrevia	tions: CN	1P. comprehensive mo	olecular profiling	CNV. copy	v-numbe	Abbreviations: CMP comprehensive molecular profiling: CNV, copy-number variation: SoC-TMP standard-	andard-				

Abbreviations: CMP, comprehensive molecular profiling; CNV, copy-number variation; SoC-1MP, standardof-care protocolled tissue-based molecular profiling; VAF, variant allele frequency

^{*} EGFR L858R mutation was detected in both tissue and plasma from this patient. In retrospect, this patient had a synchronous colorectal carcinoma that might have harbored the BRAF V600E mutation. However, the patient died before this could be confirmed.

^b SoC-TMP could not be performed in these patients.

^c Plasma-CMP was not successful in this patient.

Table A3. Level 2-3A Driver Mutations Detected in Tissue, Plasma, or Both

					1						
Detected	Detected in Both	Tissue and Plasma		Detecte	Detected in Tissue Only	Only		Detected	Detected in Plasma Only	a Only	
Patient	Gene	Variant	VAF Plasma	Patient	Gene	Variant	VAF Plasma	Patient	Gene	Variant	VAF Plasma
			(%)				(%)				(%)
P141	ERBB2	A775_G776insYVMA	37.9	P081	EGFR	Exon 20 ins	Not detected	P087ª	ERBB2	R103Q	0.2
P056	KRAS	G12C	67.5	021	KRAS	G12C	Not detected	P002	ERBB2	R896C ^b	0.1
P163	KRAS	G12C	37.9	P003	KRAS	G12C	Not detected	P125	ERBB2	S310Y ^b	0.3
P180	KRAS	G12C	33.9	P048	KRAS	G12C	Not detected	P130 ^c	KRAS	G12C	10.8
P156	KRAS	G12C	20	P052	KRAS	G12C	Not detected	P175 ^d	KRAS	G12C	3
P051	KRAS	G12C	14.8	P059	KRAS	G12C	Not detected	P148 ^c	KRAS	G12C	6.0
P041	KRAS	G12C	13.9	P195	KRAS	G12C	Not detected	P151	KRAS	G12C	0.5
022	KRAS	G12C	12.9	P201	KRAS	G12C	Not detected	026	KRAS	G12C	0.2
P129	KRAS	G12C	11.3	P040	MAP2K1	K57Ne	Not detected	P047	KRAS	G12C	0.2
P183	KRAS	G12C	10.8	P155	MET	CNV	Not detected				
P077	KRAS	G12C	7.6	P121	MET	CNV	Not detected				
P122	KRAS	G12C	5.3								
P174	KRAS	G12C	3.3								
P026	KRAS	G12C	3.2								
P153	KRAS	G12C	3.1								
P078	KRAS	G12C	2.6								
P065	KRAS	G12C	2.5								
P006	KRAS	G12C	2.2								
P011	KRAS	G12C	2								
P055	KRAS	G12C	_								
P096	KRAS	G12C	0.8								
P023	KRAS	G12C	0.7								
P039	KRAS	G12C	0.7								
027	KRAS	G12C	9.0								
P098	KRAS	G12C	0.4								
P186	KRAS	G12C	0.3								

Table A3. Continued

		5									
Detecte	Detected in Both Tis	Tissue and Plasma		Detected	Detected in Tissue Only	e Only		Detected in Plasma Only	l in Plasn	na Only	
Patient Gene	Gene	Variant	VAF Plasma Patient Gene Variant	Patient	Gene	Variant	VAF Plasma Patient Gene Variant	Patient	Gene	Variant	VAF Plasma
			(%)				(%)				(%)
P038	KRAS	G12C	0.2								
P074	KRAS	G12C	0.2								
P190	KRAS	G12C	0.1								
P102	MET	CNV	No VAF								
P126 ^f	MET	CNV	No VAF								
P139 ^f	MET	CNV	No VAF								

Abbreviations: CMP, comprehensive molecular profiling; CNV, copy-number variation; SoC-TMP, standard-of-care protocolled tissue-based molecular profiling; VAF, variant allele frequency

^a MET exon 14 skipping mutation also detected in this patient. ERBB2 R103Q not covered in the SoC-TMP panel ^b ERBB2 R896C and S310Y variants were not covered in the SoC-TMP panel

^c SoC-TMP could not be performed in these patients

^d KRAS G12A was also detected in both tissue and plasma from this patient

^e MAP2K1 K57N variant was not covered in the plasma-CMP panel

^f Level 1 EGFR driver mutations were also detected in these patients

Table A4. Level 3B-4 Driver Mutations Detected in Tissue, Plasma, or Both

Dototod	I in Doth Ti	cmoold but survived at bottotto		Dototod	Jacobs Tail Lotton	,		Dototod:	I a C cm2 cla mi bottotto	, lad	
Delected	III DOCU II	ssue and Plas	ша	Delected	III IISSNe Ou	A		Delected	n Pidsma	, uniy	
Patient	Gene	Variant	VAF Plasma	Patient	Gene	Variant	VAF Plasma	Patient	Gene	Variant	VAF Plasma
			(%)				(%)				(%)
P047	BRAF	G469A	2.1	P133a	AKT1b	E17K	Not detected	P160 ^c	BRAF	G469V	11.2
P039d	BRAF	G469V	1.4	P134e	AKT1b	E17K	Not detected		NRAS	Q61H	0.1
P108	BRAF	K601E	23.3	P023 ^d	ATMb	L2890P	Not detected	$P036^a$	BRCA2	S3376*	0.2
P149	ERBB2	CNV	No VAF	P132e	ATMb	R3008C	Not detected	P131 ^f	KRAS	A146T	0.4
P131g	ERBB2	CNV	No VAF	P127	CDKN2Ab	D108Y	Not detected	P174 ^d	KRAS	G12A	0.1
P199	KRAS	G12A	67.5	P166	CDKN2Ab	E88*	Not detected	P178 ^c	KRAS	G12D	25.6
P004	KRAS	G12A	16.8	P016 ^a	CDKN2Ab	H83L	Not detected	Р104с. h	KRAS	G12D	0.3
P028	KRAS	G12A	6.2	P180 ^d	CDKN2Ab	M53I	Not detected		KRAS	A146P	0.2
P134	KRAS	G12A	5.1	013	CDKN2Ab	R87GfsTerS9	Not detected		KRAS	L19F	0.4
P175i	KRAS	G12A	9.0	027 ^d	ERBB2	CNV	Not detected		KRAS	Q61E	0.2
P132	KRAS	G12A	0.4	P099	KRAS	G12A	Not detected		KRAS	Q61H	0.1
P187	KRAS	G12A	0.2	P005	KRAS	G12F	Not detected	P052 ^j	KRAS	G12V	0.1
P072	KRAS	G12D	3.1	P016	KRAS	G12V	Not detected	P074 ^d	KRAS	G13D	0.5
P194	KRAS	G12D	0.8	P120	KRAS	G13D	Not detected	P181	KRAS	V14I	0.5
P007	KRAS	G12D	0.4	P185	KRAS	Q61H	Not detected	P199 [€]	NRAS	G12D	0.1
P070	KRAS	G12D	0.4	P075 ^k	NRAS	Q61L	Not detected	P091I	PDGFRA	D846Y	0.1
P076	KRAS	G12D	0.4	P049	PIK3CAb	E542K	Not detected				
P171	KRAS	G12D	0.2	P037	PIK3CAb	E545K	Not detected				
P092	KRAS	G12F	7.7	P184	PIK3CAb	E545K	Not detected				
P071	KRAS	G12F	5.3	P150m	PIK3CAb	E545K	Not detected				
P192	KRAS	G12F	1.1	P146	PIK3CAb	M1043V	Not detected				
P173	KRAS	G12S	15.2								
P110	KRAS	G12V	7.5								
P162	KRAS	G12V	3.2								
P167	KRAS	G12V	1.6								
P182	KRAS	G12V	1.5								

_
σ
Ф
7
-
=
Ħ
-
О.
\cup
4.
4
44
A4
e A4
le A4
rble A4
able A4

Detected	in Both T	Detected in Both Tissue and Plasma	ma	Detected	Detected in Tissue Only	ınly		Detected	Detected in Plasma Only	Only	
Patient Gene	Gene	Variant	VAF Plasma	Patient	Gene	Variant	VAF Plasma	Patient	Gene	Variant	VAF Plasma
			(%)				(%)				(%)
P133	KRAS	G12V	6.0								
P144	KRAS	G12V	0.8								
P036	KRAS	G12V	0.4								
P143	KRAS	G12V	0.2								
P095	KRAS	G13C	2.8								
P179	KRAS	G13D	0.7								
P062	KRAS	Q61H	31.5								
P022	KRAS	Q61H	14.6								
P064	KRAS	Q61H	4.4								
P172	KRAS	Q61H	0.3								
P203	KRAS	Q61H	0.2								
P170	KRAS	Q61K	0.7								
004	NRAS	Q61K	13.9								

Abbreviations: CMP, comprehensive molecular profiling; CNV, copy-number variation; SoC-TMP, standard-

of-care protocolled tissue-based molecular profiling; VAF, variant allele frequency ^a KRAS G12V also detected in both tissue and plasma from this patient

^b AKT1, ATM, CDKN2A and PIK3CA genes not covered in the plasma-CMP panel

SoC-TMP could not be performed in these patients

^d KRAS G12C also detected in both tissue and plasma from this patient

^e KRAS G12A also detected in both tissue and plasma from this patient

⁹ EGFR L858R also detected in both tissue and plasma from this patient EGFR L858R also detected in both tissue and plasma from this patient

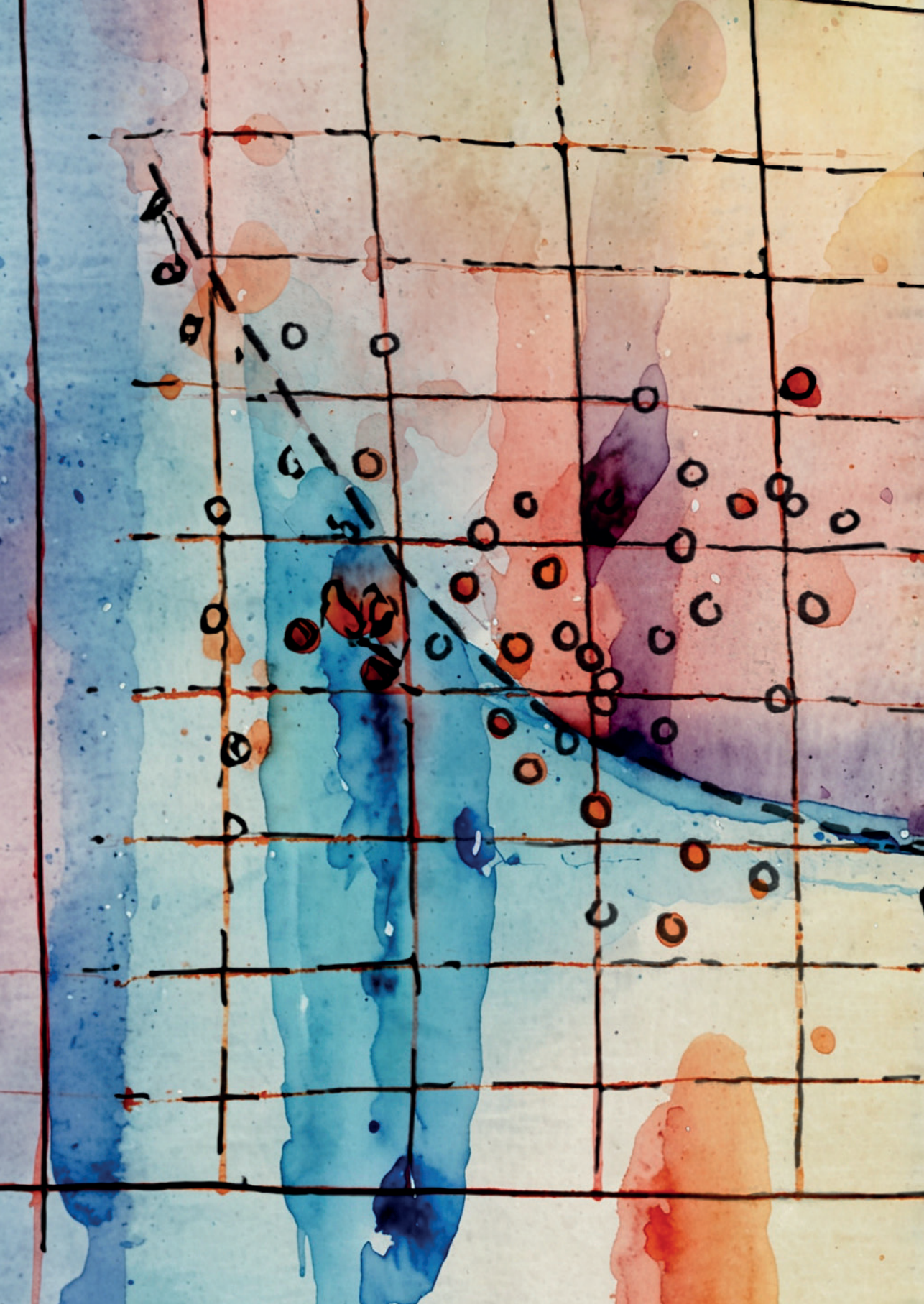
h Patient had a synchronus hepatocellular carcinoma

KRAS G12C also detected in plasma from this patient KRAS G12C also detected in tissue from this patient

* MET exon 14 skipping also detected in tissue from this patient, and plasma-CMP not successful

ALK L1196M also detected in plasma from this patient

" EGFR exon 19 deletion also detected in both tissue and plasma from this patient



Chapter 5

Combining variant detection and fragment length analysis improves detection of minimal residual disease in postsurgery circulating tumour DNA of stage II–IIIA NSCLC patients

D.C.L. Vessies¹*, M.M.F. Schuurbiers²*, V. van der Noort³, I. Schouten⁴, T.C. Linders¹, M. Lanfermeijer¹, K.L. Ramkisoensing¹, K.J. Hartemink⁵, K. Monkhorst⁶, M.M. van den Heuvel², D. van den Broek¹

^{*} Authors contributed equally

¹ Netherlands Cancer Institute, department of laboratory medicine, Amsterdam, the Netherlands

² Radboud University Medical Centre, department of pulmonary diseases, Nijmegen, the Netherlands

³ Netherlands Cancer Institute, biometrics department, Amsterdam, the Netherlands

⁴ Netherlands Cancer Institute, department of pulmonology, Amsterdam, The Netherlands

⁵ Netherlands Cancer Institute, department of surgery, Amsterdam, the Netherlands

⁶ Netherlands Cancer Institute, department of pathology, Amsterdam, the Netherlands

Abstract

Stage II-IIIA nonsmall cell lung cancer (NSCLC) patients receive adjuvant chemotherapy after surgery as standard-of-care treatment, even though only approximately 5.8% of patients will benefit. Identifying patients with minimal residual disease (MRD) after surgery using tissue-informed testing of postoperative plasma circulating cell-free tumour DNA (ctDNA) may allow adjuvant therapy to be withheld from patients without MRD. However, the detection of MRD in the postoperative setting is challenging, and more sensitive methods are urgently needed. We developed a method that combines variant calling and a novel ctDNA fragment length analysis using hybrid capture sequencing data. Among 36 stage II-IIIA NSCLC patients, this method distinguished patients with and without recurrence of disease in a 20 times repeated 10-fold cross validation with 75% accuracy (P = 0.0029). In contrast, using only variant calling or only fragment length analysis, no signification distinction between patients was shown (P = 0.24 and P = 0.074 respectively). In addition, a variant-level fragmentation score was developed that was able to classify variants detected in plasma cfDNA into tumourderived or white-blood-cell-derived variants with 84% accuracy. The findings in this study may help drive the integration of various types of information from the same data, eventually leading to cheaper and more sensitive techniques to be used in this challenging clinical setting.

Introduction

Lung cancer is the leading cause of cancer-related deaths worldwide (1). At diagnosis, 40–50% of nonsmall cell lung cancer (NSCLC) patients present with stage I–III disease (2,3). Resection is the primary treatment approach for stage I–II disease, and an important component of the multimodality approach for stage III. Based on a meta-analysis of multiple randomised controlled trials the standard of care for stage II-IIIA NSCLC includes adjuvant chemotherapy, even though the absolute disease-free survival (DFS) benefit is limited (5.8%) (4.5). Moreover, adjuvant personalised regimens have been registered recently, using targeted therapy or immune checkpoint inhibitors (6,7). Consequently, there is an unmet clinical need to identify patients who will not benefit from adjuvant therapy.

The prospect of using circulating cell-free DNA (cfDNA) to detect postoperative minimal residual disease (MRD) was met with initial optimism (8,9). However, although early detection of relapse using cfDNA has been reported in gastric cancer (10) and colon cancer (11), as well as for NSCLC post-therapy (12,13), cfDNA as a postoperative marker to identify NSCLC patients who will not benefit from adjuvant therapy is not yet reported.

Traditionally the detection of MRD is focussed on detecting somatic variants in the resected tissue material, and tracing those in the postoperative or postadjuvant therapy plasma (8-14). Approaches using the same panel for all patients can be limited by the number of variants that are available for tracking. To overcome this, tissue-informed personalised assays have been developed, tailored to every individual patient, to trace up to 48 mutations in plasma (12-15). However, designing and analysing such individualised assays is costly and time-consuming, which may be problematic in between surgery and adjuvant therapy.

More recently, other approaches have been developed using additional characteristics of cfDNA, next to mutations, to help detect the presence of circulating tumour DNA (ctDNA). One promising approach is the interrogation of cfDNA fragment length, leveraging the knowledge that ctDNA is shorter than nontumour-derived cfDNA (16-21). This has been used to infer a patient-level fragmentation-based classifier from shallow whole-genome sequencing (WGS) data (22,23), as well as to help distinguish tumour-derived mutation calls from clonal haematopoiesis-derived mutation calls in hybrid capture sequencing data (19,24,25). This mounting evidence suggests that fragment length analysis could also be used to support the classical variant-based detection of MRD. As

fragment length analysis and variant tracing are independent read-outs of the presence of ctDNA, there is an opportunity to combine the two approaches to improve the sensitivity of detecting MRD.

In this proof-of-principle study we explore the potential of combining patient-level fragment length analysis and variant calling from hybrid capture sequencing data for MRD detection in stage II-IIIA NSCLC patients.

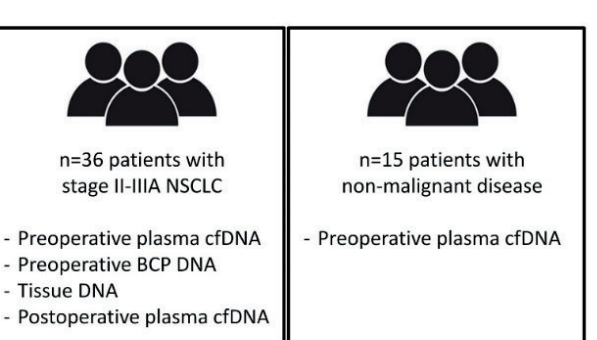
Materials and methods

A flow chart illustrating the procedures and data streams in this project is provided in Fig. 1.

Patients

All patients were enrolled with written informed consent as part of the multi-centre Lung Early Molecular Assessment trial (LEMA; ClinicalTrials.gov NCT02894853), which was in accordance with the standards set in the declaration of Helsinki and was approved by the medical ethics committee (METC) of the Netherlands Cancer Institute (NKI). Patients were only included in this MRD study if they were diagnosed with pathological stage II-IIIA NSCLC disease and if resected tissue material, preoperative plasma (0-50 days prior to surgery), preoperative BCP and postoperative plasma were available. The postoperative plasma was required to be taken at least 3 days postsurgery (26), and before adjuvant therapy, with a maximum of 36 days postsurgery. A cohort of 36 patients meeting these criteria was selected.

Also, a control group was selected from the LEMA trial and consisted of 15 riskand age-matched patients with a suspicion of lung cancer based on imaging, who subsequently underwent a tissue biopsy which proved a nonmalignant diagnosis. This cohort of risk- and age-matched controls is a reflection of daily clinical practice where we need to distinguish between patients with lung cancer and patients with nonmalignant diseases of the lung. Details of the nonmalignant control group are provided in Table S1. For the nonmalignant control group only the preoperative plasma sample was sequenced as described below.



HYBRID CAPTURE SEQUENCING

197 genes, 198kbp

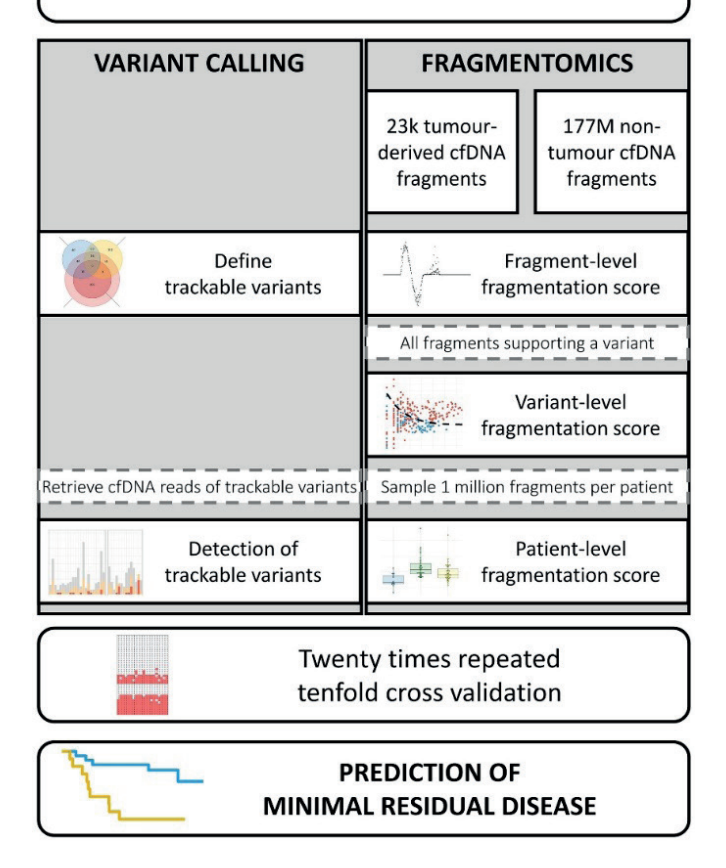


Figure 1. Flow chart illustrating the experimental procedures and data flows in this study. Blood and tissue samples from 36 NSCLC patients and plasma cfDNA from 15 risk- and age-matched patients with nonmalignant disease were sequenced with a targeted hybrid capture sequencing panel. Optimised variant calls were combined with patient-level fragmentomics, both from the hybrid capture sequencing data, to determine the presence of minimal residual disease in each patient in a 20 times repeated 10-fold cross validation.

Samples

Blood was collected in two hospitals, either using 10 mL K2-EDTA tubes or 10 mL cell-stabilising tubes (CST; STRECK, Omaha, NE, USA). Cell-free plasma was obtained from the K2-EDTA tube within 4h by a two-step centrifugation at room temperature: 20 min at 380 g followed by 10 min at 20 000 g. Cell-stabilising tubes were centrifuged at room temperature for 10 min at 1700 g and 10 min at 20 000 g within 7 days. Cell-free plasma was stored in 1–4 mL aliquots at $-80\,^{\circ}$ C. cfDNA isolation was performed using the QlAsymphony Circulating DNA kit (article number 1091063, Qiagen, Dusseldorf, Germany) with the QlAsymphony (Qiagen). No extraction blanks were used in this study. Elution volume was set to 60 μ L and samples were stored at 4 °C until use. No significant differences were observed in the fragmentation scores of samples collected in EDTA tubes or CST (data not shown). To confirm this, a pilot experiment was performed with nine patients with metastatic NSCLC. Blood was concurrently drawn in both CST and EDTA tubes, and patient-level FS was determined. Based on a Passing Bablok regression we conclude that the type of tube does not influence the patient-level FS (Fig. S1B).

DNA from BCP was isolated from a 1 mL pellet using the QIAsymphony DSP DNA Midi Kit (article number 937255, Qiagen). Elution volume was set to $400\,\mu\text{L}$ and samples were stored at 4°C until use. DNA was fragmented sonically on a Covaris ME220 Focused-ultrasonicator (Covaris Inc., Woburn, MA, USA) using microTUBE AFA Fibre Pre-Slit Snap-Cap (PN 520045) vessels, with the following settings: Duration 70 s, Peak Power 70 W, Duty Factor 20% and 1000 Cycles per Burst.

DNA from tissue was obtained from FFPE slides. The pathologist scored tumour percentage and indicated most tumour-dense region for isolation on an H&E slide. Five to 10 (depending on tumour size) FFPE 10 µm slides were used. DNA and RNA were isolated simultaneously with the AllPrep DNA/RNA FFPE isolation kit (Qiagen, #80234) by using the QIAcube, according to the manufacturer's protocol. DNA input into the AVENIO library preparation phase was determined according to the protocol (median 37.3 ng, IQR 32.6–46.3 ng). Fragmentation of the FFPE tissue DNA was performed enzymatically, according to the AVENIO library preparation protocol.

Sequencing and variant calling

Fourteen preoperative samples were sequenced with a large capture panel comprising 1.1 Mb as described earlier (27), which fully overlaps the AVENIO Surveillance Panel and only the overlapping regions were used. All other samples (22/36 preoperative plasma, BCP, tissue and postoperative plasma of 36 NSCLC patients, as well as the preoperative plasma samples of patients with nonmalignant

disease) were sequenced in-house using the AVENIO Surveillance Panel (for Research Use Only; not for use in diagnostic procedures, Roche Sequencing Systems, Inc. Pleasanton, CA, USA), covering hypermutated regions or full exonic sequences of 197 genes, total size 198kb (28). Handling in accordance with the predefined protocol, we isolated cfDNA from all available plasma and used 50 µL of the eluate as input for the AVENIO library preparation. Median cfDNA input for preoperative samples was 24.4 ng (IQR: 17.4-38.5 ng), for postoperative samples was 50.0 ng (IQR: 49.4–50.0 ng).

Samples were multiplexed and sequenced on an Illumina NextSeg550, generating median 30 m reads per sample (IQR: 27-34 m). Median unique sequencing depth in preoperative samples was 3678× (IOR: 2495–4758×), in postoperative samples 6289× (IQR: 5081-6980×), in BCP 3428× (IQR: 3162-3684×) and in tissue 1938× (IQR: 1573-2819×).

Variant calling was performed using the AVENIO pipeline, using the unfiltered called variants. All variants that were detected in blood cell pellet were considered to be germline if they were also detected in tumour tissue. They were considered to be CHIP if they were not detected in tumour tissue. Germline variants and CHIPs were removed from downstream analysis. All variants except germline variants are reported in Table S2. Raw data read counts were extracted from the .freq files of the postoperative plasma for all variants detected in any sample of that patient.

Variant calling cut-offs in the postoperative plasma were optimised. Specifically, the cut-offs were lowered for tumour-informed and preoperative plasma-informed variants. We iteratively lowered the cut-offs to requiring one to eight reads. Additionally, the cut-off for calling a patient MRD-positive varied from requiring at least one to six baseline-informed variants detected in the postoperative plasma. The best combination of cut-offs was selected based on the highest concordance with recurrence status of the patients.

Fragmentation score

To calculate the FS, we first built a reference database of reads that contained tumourinformed mutations, and stored their respective lengths from the deduplicated BAM files, in total 21 705 fragments. For the nontumour reads we collected reads from 15 patients with nonmalignant disease (177.6 million fragments).

First, we randomly sampled 10000 reads from each set and calculated the probability density for each fragment length to occur in tumour- and nontumourderived cfDNA (Fig. 2A). Next, we calculated the log-2 of the ratio of these densities, maxed at +5 and -5 for lengths that had a count of 0 in either group. Additionally, fragment lengths that had a total of 20 reads or fewer were given a score of 0. This process was bootstrapped over 1000 iterations to smooth out any noisy areas and reduce the impact of sampling errors.

Thus, each fragment length was allocated a per-fragment fragmentation score in this reference set, illustrated in Fig. S2A. In order to translate this per-fragment score into a per-patient score, we randomly sampled 1 million fragments from each patient and reported the mean fragmentation score per million fragments (Fig. 2A,B and Fig. S3A). Patients who had an FS greater than the mean FS plus two times the standard deviation among 15 plasma samples from patients with nonmalignant disease were considered positive for MRD detection. Technical reproducibility of the FS was shown by 10 times repeated subsampling of one million, hundred thousand, ten thousand or one thousand reads per sample (Fig. S4A). The confidence interval of the calculated FS was consistently smaller than 0.01 when one million reads were sampled, indicating very consistent patient-level FS reproducibility at this sampling size (Fig. S4B).

The per-fragment score was translated to a per-variant score (VFS) by averaging the scores of all fragments supporting a specific variant (Fig. 3A). If the same variant was detected in both the preoperative and postoperative plasma, the fragments were analysed collectively in order to obtain more fragments per variant, resulting in a better score. The nonmalignant cfDNA threshold was established by randomly sampling each number of reads from 15 patients with nonmalignant disease 1000 times, and calculating the VFS. The threshold was set at the mean plus two times the standard deviation in nonmalignant reads. The minimum number of reads to include a variant was determined by assessing the best performance by assigning a score of 1 for each correctly classified variant, -1 for incorrectly classified variants and 0 for indeterminate variants below the cut-off, and resulted in a cut-off of eight reads. The same cut-offs were applied to the validation data in the MSKCC/Grail cohort (Fig. S3B).

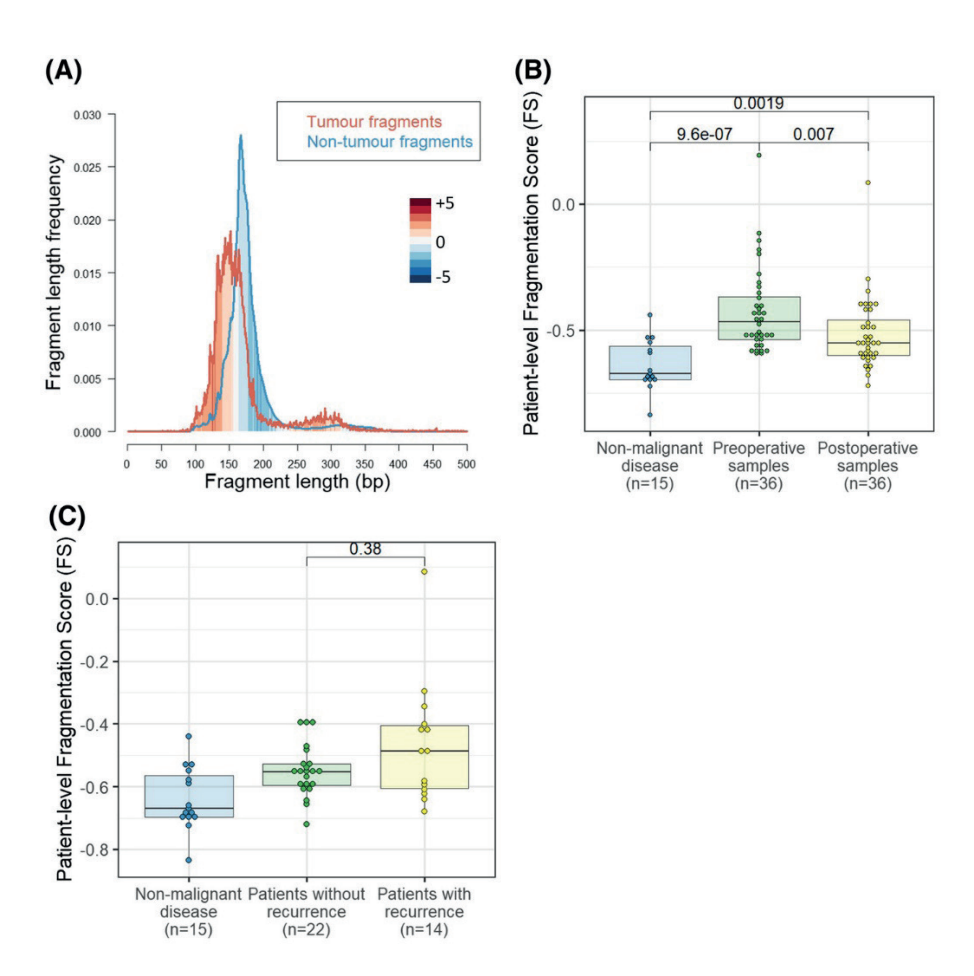


Figure 2. Fragment length analysis. (A) Fragment length density in the perspective of fragment length in base pairs (bp) including tumour fragments (red, n = 21705 fragments), defined by containing a tumourderived mutation, and nontumour fragments (blue, n = 177.6 million fragments) from patients with nonmalignant disease. Red shaded areas indicate fragment lengths that are more prevalent in tumour cfDNA, while blue shaded areas are more prevalent in nontumour cfDNA. The intensity of colours corresponds to the log-2 of the relative ratio of tumour- to nontumour-derived fragments. (B) Patient-level fragmentation score (FS) for age-matched nonmalignant patients (i.e. control group, n = 15), and paired preoperative and postoperative plasma samples from NSCLC patients (n = 36). Fragmentation score was significantly higher in both preoperative patient samples and postoperative patient samples when compared to nonmalignant patients (P < 0.001 and P = 0.002 respectively, Wilcoxon rank sum test). FS was significantly higher in preoperative patient samples compared to paired postoperative patient samples (P = 0.007, paired t-test). (C) Patient-level FS for age-matched nonmalignant patients (i.e. control group, n = 15), and postoperative plasma samples from NSCLC patients, categorised in patients with (n = 14) versus without recurrence of disease (n=22). There was no statistically significant difference between the postoperative FS of patients with recurrence and patients without recurrence of disease (P = 0.38, Wilcoxon rank sum test).

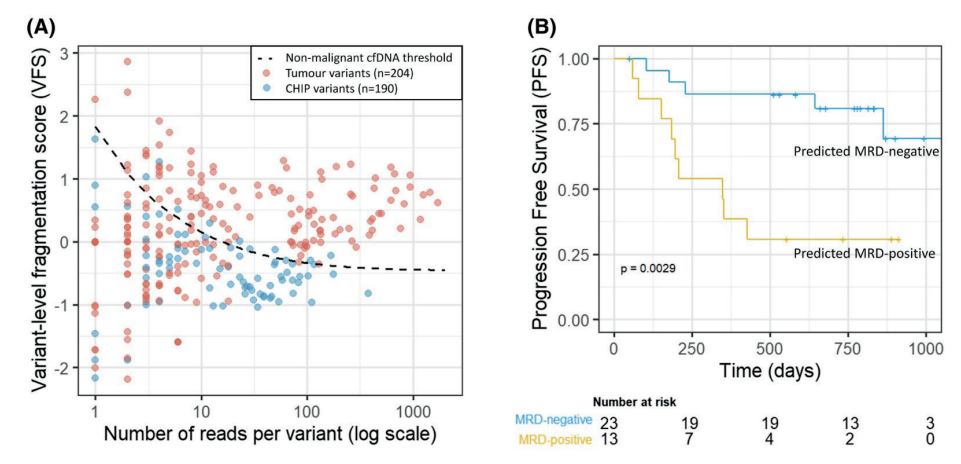


Figure 3. Variant level fragment length analysis and Kaplan–Meier curve of the combined MRD-model. (A) Variant-level fragmentation score (VFS) versus number of reads per variant for all tumour-informed variants (n = 204, red) and CHIP variants (n = 190, blue) in the LEMA-MRD cohort. Reads from preoperative and postoperative plasma for the same variant were added up for this analysis. The black dashed line represents the mean plus two times standard deviation of fragments randomly sampled from 15 patients with nonmalignant disease and is used as a nonmalignant cfDNA threshold. (B) Performance of a combined MRD model including fragment length analysis and variant calling. Kaplan–Meier curve with progression-free survival (PFS) of MRD-positive (yellow) and MRD-negative patients (blue) based on the combined variant calling and patient-level fragmentation score (FS) model in a 20 times repeated 10-fold cross validation. Patients were labelled as MRD-positive or -negative by the majority result of the cross validation. The model was able to differentiate between patients with recurrence of disease and those without (P = 0.0029, log-rank test).

The algorithm to calculate the FS and VFS was written in R (29) and has been made publicly available (https://github.com/DCLVessies/Fragmentomics) for other researchers to evaluate, along with the established fragment length reference set. The FS and VFS presented in this work could in principle be used in any cfDNA sequencing method that preserves the fragment length information, such as hybrid capture sequencing and (shallow) whole-genome sequencing, but not in PCR-based amplicon sequencing.

Cross validation

The applicability of the combined variant calling and FS model for predicting recurrence was validated using a 20 times repeated 10-fold cross validation. For each repeat, the 36 patients were randomly divided into 10 folds of three or four patients. In each iteration the model was trained on nine folds, and the training algorithm was applied on the remaining fold until each fold had been applied once. In total, this process of cross validation was repeated 20 times.

For each fold, the reference set for the FS was rebuilt using only the mutation reads in the 90% of the data used for training, and all FS including the FS for patients with nonmalignant disease were recalculated. Cut-offs for the variant calling were determined likewise based on the training data. The variant calling and FS each provided a true or false call based on their respective cut-offs as described above. Based on the best fit of the training data to the status of disease recurrence, the model determined whether both outcomes had to be positive or whether one positive outcome was sufficient. Subsequently, this algorithm was applied to the one remaining fold that was not included in the training data. The final performance of the model was determined by the majority call for each patient among the 20 repeats – that is, a patient was counted as predicted positive if it was predicted positive at least 11 times (Fig. S5).

For the randomly assigned patient-level FS as shown in Fig. S6C, the FS and variant calls were determined as described above, but subsequently, the patient-level FS was assigned to a randomly determined other NSCLC patient.

Potential clinical implications

Based on the Lung Adjuvant Cisplatin Evaluation (LACE) meta-analysis of five randomised controlled trials (4), adjuvant chemotherapy after complete resection of stage II and III NSCLC was established as the standard of care (5). The absolute disease-free survival benefit of adjuvant chemotherapy was determined to be 5.8% in the meta-analysis, and this was assumed to be the case in our simulations.

In order to estimate the fraction of patients that benefit from adjuvant chemotherapy in the MRD-positive and -negative groups, we assumed that the sensitivity of detecting recurrence is the same as the sensitivity for detecting patients who would benefit from chemotherapy. While this assumption is not ideal, this is the closest estimate we have based on the data generated in this study.

In a 10 000 times repeated bootstrap simulation 36 patients were randomly drawn from our cohort, with replacement. Next, each of the 36 patients was randomly assigned a prediction: MRD-positive or MRD-negative with probability equal to the results of the TTF-CV (Fig. S5, rightmost column). In each iteration the 5.8% of people who benefit from adjuvant chemotherapy were distributed between the MRD-negative and -positive groups proportionally to the sensitivity for detecting recurrence in that iteration (e.g. if sensitivity for detecting recurrence was 80% in that iteration, then likewise 80% of the 5.8% of patients who would benefit from adjuvant chemotherapy were allocated to the MRD-positive group). The fraction of MRD-positive and -negative patients who would benefit from adjuvant chemotherapy was reported.

Results

In total 36 stage II-IIIA NSCLC patients with available preoperative blood cell pellet (BCP) and plasma, resected tissue material and postoperative plasma between 3 and 36 days postsurgery were included in this study. In addition, 15 patients with nonmalignant disease and with available preoperative blood plasma were selected as a control group. All patients were selected from the larger Lung Early Molecular Assessment trial (LEMA; ClinicalTrials.gov NCT02894853).

Patient characteristics

In this cohort six patients (17%) were diagnosed with pathological stage IIA, 18 patients (50%) with stage IIB and 12 patients (33%) with stage IIIA disease. In total, recurrence of disease occurred in 14 patients (39%) with a median followup of 23 months (IOR 19-30 months). The clinical characteristics of the assessed cohort are represented in Table 1. A total of 16 patients (44%) had squamous cell carcinoma, in line with national prevalence of this histological subtype in stage II (35%) and III (36%) NSCLC patients in the Netherlands (30).

Somatic variants

To detect MRD using variant calling, we first identified tumour-related variants in the preoperative setting using tissue and plasma and subsequently sought whether these variants could be traced in the postoperative plasma. After removing clonal haematopoiesis of indeterminate potential (CHIP) and germline variants, a median of 8 (range 3-34) tissue-informed or preoperative plasma-informed variants per patient remained that could be tracked in the postoperative plasma. As such, variants that were only detected in postoperative plasma were considered uninformative and were removed from analysis. In total, 389 trackable variants were identified in 36 patients, of which 154 variants (40%) in the postoperative plasma were directly reported by the AVENIO pipeline or had reads in the deduplicated BAM files (Fig. 4A).

Table 1. Clinical characteristics of NSCLC patients in this cohort. LCNEC, Large-cell neuroendocrine carcinoma; NSCLC-NOS, Nonsmall cell lung cancer – not otherwise specified.

· · · · · · · · · · · · · · · · · · ·	All patients	Stage II	Stage III
	N=36	N=24	N=12
Age, median years (IQR)	68 (62–76)	69 (62–75)	67 (61–76)
Sex, n (%)			
- Male	23 (64)	15 (63)	8 (67)
- Female	13 (36)	9 (37)	4 (33)
Smoking status, n (%)			
- Active	11 (31)	8 (33)	3 (25)
- Former	25 (69)	16 (67)	9 (75)
Pack years, median (IQR)	38 (20–57)	37 (20–55)	43 (23–70)
Tumour histology, n (%)			
- Adenocarcinoma	18 (50)	13 (54)	5 (42)
- Squamous cell carcinoma	16 (44)	10 (42)	6 (50)
- NSCLC-NOS	1 (3)	1 (4)	0
- LCNEC	1 (3)	0	1 (8)
Recurrence of disease, n (%)*			
- Yes	14 (39)	7 (29)	7 (58)
- No	22 (61)	17 (71)	5 (42)
Adjuvant chemotherapy			
- Yes, completed	7 (19)	5 (21)	2 (17)
- Yes, partially completed	7 (19)	3 (12)	4 (33)
- No	22 (61)	16 (67)	6 (50)
Days between baseline plasma and surgery, median (IQR)	8 (6–14)	8 (6–14)	9 (6–15)
Days between surgery and postoperative plasma, median (IQR)	10 (6–23)	13 (6–25)	6 (4–20)
Months follow-up, median (IQR)	23 (19–30)	26 (22–30)	19 (7–23)

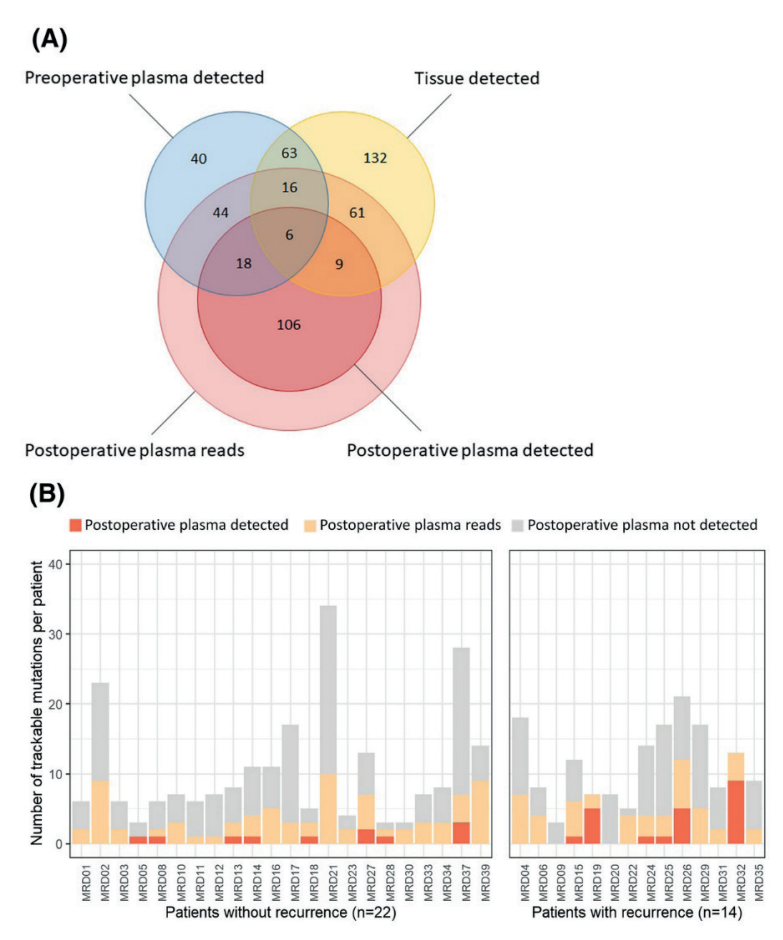


Figure 4. Variants detected in tumour tissue and pre- and postoperative plasma. (A) Total number of absolute variants across 36 patients detected in tumour tissue (yellow), preoperative plasma (blue) and/ or postoperative plasma (red), including a differentiation in variants called by the Avenio pipeline or only with supporting reads. (B) Number of trackable variants per patient that were detected or had supporting reads in the postoperative plasma, categorised in patients with (n = 14) versus patients without recurrence of disease (n = 22). Trackable variants are defined as detected variants in the preoperative setting in either plasma or tumour tissue. Trackable variants in dark orange were detected by the Avenio pipeline, trackable variants in light orange were not detected by Avenio but did have reads in the alignment files. Trackable variants in grey did not have reads in the postoperative plasma alignment files.

When considering the prognostic power of MRD detection using only variants, a median of 3 variants per patient (range 1-10) were detected or had reads in the postoperative plasma of patients who did not develop recurrence, in comparison to a median of 4 variants (range 0-13) in patients who did develop recurrence (Fig. 4B). Defining disease recurrence as a surrogate endpoint for the presence of MRD postsurgery, we performed a 20 times repeated 10-fold cross validation (TTF-CV, described in Materials and methods) to evaluate the performance of variant calling for detecting MRD. Using only variant calling with optimised variant call thresholds we were unable to accurately distinguish patients with and without recurrence (P = 0.24, log-rank test, Fig. S6A).

Fragment length analysis

We investigated differences between ctDNA and nontumour cfDNA fragment lengths. ctDNA fragments were defined by containing a tumour tissue-informed mutation, of which 21705 fragments were detected in the plasma of 36 patients. In line with what others found, these ctDNA fragments were shorter than cfDNA fragments from patients with nonmalignant disease (control group), including both the mononucleosomal and the dinucleosomal fragments (Fig. 2A) (16.18,20). Correspondingly, the relative abundance of each fragment length in ctDNA versus nontumour cfDNA fragments indicates the likelihood of each fragment originating from a tumour cell or a nontumour cell. As described in the Materials and methods section, this property was used to calculate an aggregated patientlevel Fragmentation Score (FS) from 1 million fragments per patient, derived from the same hybrid capture sequencing data as the variant calling.

Median patient-level FS in the preoperative samples was -0.47 (IQR -0.54 to -0.37), which was higher than observed in the postoperative samples with a median of -0.55 (IQR -0.60 to -0.46, P=0.007, paired t-test, Fig. 2B). FS among 15 patients with nonmalignant disease (median -0.67, IQR -0.70 to -0.56) was lower than in preoperative samples (P < 0.001, Wilcoxon rank sum test) and in postoperative samples (P=0.002, Wilcoxon rank sum test, Fig. 2B). Applying a cut-off at the mean plus two times standard deviation of the patient-level FS for patients with nonmalignant disease, we reached 100% specificity (95% CI 72%-100%), and sensitivity of 44% (95% CI 28%-62%) and 25% (95% CI 12%-42%) in preoperative and postoperative samples respectively. Subsequently, the performance of the patient-level FS was validated in the DELFI cohort (22). We applied a cut-off of the mean plus two times standard deviation of the patient-level FS among 213 samples from healthy individuals. This resulted in 98.6% specificity (95% CI 95.9%–99.7%) and 58% sensitivity among lung cancer cases (n = 12, 95% CI 28%-85%), confirming the performance of the patient-level FS (Fig. S3A). However, the difference in postoperative FS between patients with and without recurrence was not significant (median -0.49 versus -0.55, P=0.38, Wilcoxon rank sum test, Fig. 2C) and using only the FS we were unable to accurately distinguish patients with and without recurrence (P = 0.07, log-rank test, Fig. S6B).

Additionally, a variant-level fragmentation score (VFS) was developed to differentiate tumour-informed variants from nontumour variants (e.g. CHIPs) based on the fragment length of the supporting reads. The VFS distinguished tumour-informed variants from CHIPs with 84% specificity (159/190 CHIPs classified correctly) and 55% sensitivity (113/204 tumour variants classified correctly; Fig. 3A). When considering only variants with at least eight reads, the specificity was 82% (131/159 CHIPs) and sensitivity was improved to 86% (93/108 tumour variants). The performance of the VFS was validated in an independent cohort with high confidence calls of CHIPs and biopsy-matched variants from Grail/MSKCC (31). Using the exact same criteria and cut-offs as established in our own cohort, we reached 93% specificity (106/114 CHIPs) and 82% sensitivity (263/319 tumour variants: Fig. S3B), confirming the robustness and generalisability of the VFS classification. However, including this classifier in the MRD detection model did not improve its ability to distinguish patients with and without recurrence since the variants were already correctly classified by having sequenced the tumour tissue and BCP.

Combined variants and FS model

To improve the accuracy of the MRD model we explored the possibility of combining the variant detection and FS approach. The method of combination and the TTF-CV used to evaluate the performance of this combined model are described in Materials and methods. The clinical sensitivity of the combined variant calling and FS approach for detecting ctDNA in preoperative plasma was 75% (95% CI 58%–88%) at 100% specificity (95% CI 78%–100%), compared to 44% for FS alone (95% CI 28%–62%) and 47% for variant detection alone (95% CI 30%–64%), highlighting the complementarity of these approaches (Fig. S1A).

When applied to detect MRD, the combined model was able to differentiate patients with disease recurrence from those without with an accuracy of 75% (Fig. 3B, P = 0.0029, log-rank test). The negative predictive value (NPV) was 78% (95% CI 56%–92%). The performance of this combined model was significantly superior in comparison to the model using only variant calling (Fig. S6A, P = 0.24, log-rank test), only FS (Fig. S6B, P = 0.07, log-rank test), or a model combining variant calling and randomly generated FS (Fig. S6C, P = 0.18, log-rank test), indicating the addition of FS is truly informative.

Due to the small cohort size and limited number of events (n = 14), it was not possible to perform a multivariate Cox proportional hazards analysis. Instead, we evaluated the bivariate Cox hazard ratios of the MRD prediction model using each of the

following factors as a covariate: disease stage (stage II versus stage IIIA), simultaneous secondary malignancies (yes versus no), completion of adjuvant chemotherapy (not started versus not completed versus completed) and the time between surgery and postoperative blood draw (in days). This revealed the MRD prediction model was a significant predictor of progression-free survival (PFS) in all bivariate analyses, and only tumour stage was found to be a significant covariate (Table S3).

Potential clinical implications

To explore the potential effect of implementing an MRD test with similar performance in a larger setting, we simulated the hypothetical effect on clinical decision making (Materials and methods). Therefore, the following assumptions were made: first, 5.8% of patients potentially benefit from adjuvant chemotherapy (4,5). Second, the MRD test's sensitivity for detecting those patients that benefit is equal to the sensitivity for detecting patients who will develop recurrence of disease. This simulation estimated a decrease in benefit of adjuvant chemotherapy in the MRD-negative group to 3.7% (95% CI: 1.4%-5.6%). On the other hand, in the MRD-positive group the expected benefit of adjuvant chemotherapy was hypothesised to increase to a median of 9.0% (95% CI: 6.1%–13.3%; Fig. S7).

Discussion

There is an unmet clinical need to identify stage II-IIIA NSCLC patients who have been successfully cured by surgery alone and will not benefit from adjuvant therapy. Detection of postoperative MRD may help guide adjuvant treatment decisions and reduce overtreatment. Although studies in other types of cancer have demonstrated the ability to detect postoperative MRD (10,11), and post-therapy detection of MRD in NSCLC (12,13), no studies to date have reported postsurgery detection of MRD in stage II-IIIA NSCLC patients with the intent of withholding adjuvant therapy in the MRD-negative group.

Here we present a combined variant calling and fragment length model to detect postoperative MRD and predict recurrence of disease which reached 75% accuracy in cross-validation (P = 0.0027, log-rank test). The analyses presented in this work may help drive the integration of various types of information from the same data, ultimately leading to cheaper and more sensitive techniques for detecting postoperative MRD in this setting.

Study design limitations

While the present results are hopeful, they need to be critically nuanced. First and most importantly, this study was designed as an explorative proof-of-concept study, and the results should be interpreted as such.

Second, in this study both patients with and without adjuvant chemotherapy were included. Disease recurrence was used as a surrogate endpoint to identify patients with MRD postsurgery. One drawback of this approach is that patients who were cured by adjuvant therapy will show up as false-positive results in this study design (i.e. MRD-positive but no recurrence), and skew the model towards more cautious calling of MRD. Since only 14 patients in our cohort started adjuvant chemotherapy, of whom only seven patients completed it, and because of the minimal cure rate of adjuvant chemotherapy, we do not expect this to have a large effect on the results.

Along the same lines, it is important to consider that asking who will develop recurrent disease is not the same as asking who will benefit from adjuvant therapy. By extension, the clinical implications simulated in this study should be interpreted as a best estimate based on the data we have, and not as actual data generated by this study. This estimate might be used to generate hypotheses or inform the design of a follow-up study.

Model performance

Despite these limitations, this study supplied valuable insights. In order to get an indication of the clinical sensitivity of the combined model we applied it to preoperative plasma samples and patients with nonmalignant disease, using the confirmed presence or absence of a tumour as a clinical gold standard to evaluate the performance of the test. We reached a sensitivity of 75% at 100% specificity, comparable to the performance of other methods that combine mutation detection with fragmentation patterns. For example, in a cohort of 85 stage I-III lung cancer patients Lung-CLiP reached sensitivities of 54% and 67% in stage II and III respectively, at 98% specificity (24). MRDetect reached 67% sensitivity for 39 patients with lung adenocarcinoma, of whom 78% with stage I-IIA, at 96% specificity (32). INVAR reports a sensitivity of 63% in 19 NSCLC patients with stage I-III (25). DELFI is a different model that uses shallow whole-genome sequencing combined with artificial intelligence to detect genome-wide fragmentation patterns (23). Among 24 stage II-IIIA lung cancer patients, this model reached 96% sensitivity at 80% specificity, and 71% sensitivity at 98% specificity. This indicates that the combined variant detection and fragmentation pattern model developed in this study performs comparably to other state-of-theart models.

When comparing the performance for detecting MRD, the present model had an accuracy of 75% (95% CI 58%-88%) in cross-validation, with an NPV of 78% (95% CI 56%–92%). This was comparable to an accuracy of 77% (95% CI 55%–92%) among 22 stage I-III lung adenocarcinoma patients for MRDetect (32), with an NPV of 100% (95% CI 74%-100%). It should be noted that in the MRDetect study only five patients developed recurrent disease, compared to 14 patients in our study, leaving little room for false-negative results. This is probably caused by a high proportion of stage I disease (14 out of 22 patients), and a comparatively short follow-up for the negatively tested stage II and III patients in their cohort (n=4). When only considering stage II-III patients in the MRDetect study (n = 8) the accuracy was 88% (95% CI 48%–100%) and the NPV 100% (95% CI 40%–100%).

We speculate that while our model shows a highly significant distinction between patients with a high or low risk of developing recurrence (P = 0.0029, Fig. 3B), the sensitivity and NPV of our and similar methods will not be sufficient to ethically withhold adjuvant therapy in the clinical application of a postoperative MRD-test in stage II-III NSCLC. For that reason, the field is working towards increasingly sensitive techniques, and to that end it will be important to obtain as much information as possible from data that is already generated in current and future diagnostic procedures. By combining hybrid capture variant calling data, which can be used for molecular profiling, with fragmentation analyses from the same data, our method is another step in that direction.

Additionally, the postoperative samples in this cohort were obtained relatively soon after surgery (median 6 days). Considering that three out of four falsepositive patients in our cohort had their blood collected within 5 days after surgery and had elevated levels of cfDNA in their blood (Fig. S5), this might indicate a failure of clearance of ctDNA of the primary tumour after surgery. Performance characteristics of the method might be improved by obtaining the blood with a longer interval after surgery to make sure any residual ctDNA from the primary tumour has cleared, although definitive evidence about the optimal timepoint for blood draw after surgery is still lacking (33).

Fragmentation score

To the best of our knowledge the fragmentation score (FS) presented in this work is the first method that derives both a patient-level and variant-level fragmentation score from hybrid capture sequencing data. In our model the predictive weight of each fragment is determined by the relative abundance in ctDNA versus nontumour cfDNA. As a consequence, fragments of 130–150 bp and 250–300 bp are given higher predictive weight towards ctDNA, while fragments of 180–210 bp are given higher predictive weight towards healthy cfDNA (Fig. 2A, Fig. S2A).

This method provides several advantages compared to other studies that use fragment length analysis to detect ctDNA. Other models most often define one or several 'windows' of fragment lengths that are enriched for ctDNA, such as the window of 100–150 bp (22), 90–150 bp (19) or < 160 bp and 230–310 bp (24). However, these windows allocate the same predictive weight to each fragment within that window, and the boundaries of the windows may change between different research groups. This is especially detrimental in the 150–160 bp range, which is the most abundant in cfDNA and would have a large impact on the model, even though fragments in that range are abundant in both ctDNA and nontumour cfDNA and therefore poor predictors.

Applying our model to patients with nonmalignant disease, the patient-level FS was significantly lower than in both preoperative and postoperative patient samples (Fig. 2B). This finding was reproduced in publicly available data of the DELFI cohort, highlighting the reproducibility and broader applicability of the approach (Fig. S3A). The DELFI data were generated from shallow WGS data, confirming that the patient-level FS performance does not depend on the target area of the sequencing data. However, based on patient-level FS alone we were unable to reliably distinguish patients with and without recurrence (Fig. S6B), underlining the finding that patient-level FS is not a silver bullet solution and should be used in conjunction with other means of MRD detection like variant calling.

To reduce the need for BCP-paired sequencing, methods are needed to distinguish CHIPs from tumour-derived mutations (34). To that end we developed a VFS. Since we had access to a rich dataset containing tumour tissue, BCP and plasma sequencing data we were able to report the performance of the VFS on an individual variant level, which has not been reported before. The VFS was capable of distinguishing tumour-derived variants from nontumour-derived variants (i.e. CHIPs) with high specificity (84%) and reasonable sensitivity (55%). Sensitivity in variants with at least eight reads improved to 86%, with comparable specificity (82%), at the cost of inconclusive results for 32% of variants (Fig. 3B). Validation of the trained model in a highly characterised public dataset of Grail/MSKCC reached an even superior performance with 82% sensitivity and 92% specificity (Fig. S3B).

Since variants were already classified based on tumour tissue and BCP sequencing, the VFS was not of added value in our current MRD model. We speculate that the VFS could be applied in future studies to filter nontumour-derived variants with high accuracy, and thereby reduce or eliminate the need to sequence tumour tissue and/or BCP alongside plasma samples.

Clinical implications

In an exploratory hypothesis-generating simulation we estimated the potential clinical consequences of implementing the MRD prediction model in clinical practice. In the MRD-negative group we hypothesised that only 3.7% of patients would benefit from adjuvant chemotherapy, potentially tipping the debate towards withholding adjuvant chemotherapy for these patients. However, the simulated data does not correct for chemotherapy undergone by patients in our cohort and represents data from only a small cohort. As such these simulated estimates should be treated as hypothesis generating based on the data we have and not as a prediction of the clinical impact of our model.

At present, adjuvant targeted therapy and immunotherapy are being integrated in early-stage NSCLC to improve cure rates and long term overall survival (7,35,36). Extensive molecular testing at diagnosis can identify oncogenic drivers and therefore presents an opportunity for targeted treatment in the adjuvant setting. Epidermal growth factor receptor tyrosine kinase inhibitors (EGFR-TKI) have shown promising efficacy in clinical trials for resected EGFR mutant NSCLC (7). A plausible future scenario would be the incorporation of precision medicine into treatment of earlier stages of NSCLC. Since this presented MRD model is based on hybrid capture NGS data, this method would provide both a molecular analysis to guide treatment and the identification of MRD as regards which patients would benefit. A recent study with patients who received adjuvant anti-PD-1 immunotherapy after melanoma resection showed that nearly half of the patients (43%) developed chronic anti-PD-1 related adverse events, defined as persistent symptoms 12 weeks after anti-PD-1 discontinuation (37). Since chronic adverse events can severely impact quality of life in the long term, it will become increasingly important to guide physicians and patients towards informed decisions about adjuvant treatment.

Conclusion

In conclusion, we present an explorative study to detect postsurgery MRD in stage II-IIIA NSCLC patients, prior to adjuvant therapy. Using only variant calling or only fragment length analysis, we were unable to distinguish patients with or without recurrence of disease with sufficient accuracy. The combined model was capable of stratifying patients after surgery into high versus low risk of developing recurrent disease in a cross-validation setting. The performance of this model was comparable to other methods that employ combined fragmentation and variant calling. The results of this model could be used as a stepping stone towards a more sensitive model to detect MRD in stage II–IIIA NSCLC patients.

Data availability

The datasets generated during this study are included in this published article and its supplementary information files are available from the corresponding author on reasonable request. The patient-level fragmentation score (FS) was validated in the DELFI cohort (22), accessed through FinaleDB (38). The performance of the VFS was validated in the Grail/MSKCC cohort (31), accessed through EGA data accession number EGAD00001005302 (39).

Acknowledgements

All kits and reagents in this research were funded by Roche Diagnostics, as agreed in OVK-16830. The funder had no influence on the conception and design of the study, on the data analysis or interpretation, or on the writing or decision to publish this manuscript. We thank the Core Facility of Molecular Pathology and Biobanking (CFMPB) of the Netherlands Cancer Institute, and in particular Maartje Alkemade for her help in retrieving materials from the biobank and isolating the tissue DNA. Additionally we thank Robert Schouten for his work in the LEMA study. Ruben Moritz of the NKI pathology IT department was instrumental in collecting the data from the European Genome-phenome Archive (EGA). We thank Pedram Razavi and Jorge Reiss (MSKCC) for allowing us access to their well curated dataset at the EGA. And lastly, we are grateful to the people of EGA and FinaleDB for setting up archives of publicly available data for researchers to use.

Supplementary information

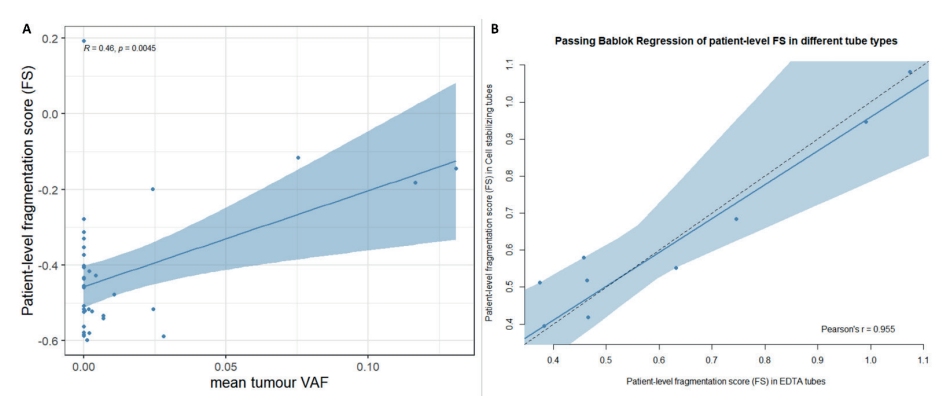
is available for this paper at DOI: https://doi.org/10.1002/1878-0261.13267.

References

- Goldstraw P, Chansky K, Crowley J, Rami-Porta R, Asamura H, Eberhardt WEE, e.a. The IASLC Lung Cancer Staging Project: Proposals for Revision of the TNM Stage Groupings in the Forthcoming (Eighth) Edition of the TNM Classification for Lung Cancer. J Thorac Oncol. januari 2016;11(1):39-51.
- 2. Netherlands Cancer Registry (NKR). Aantal nieuwe gevallen longkanker 2018.
- 3. McPhail S, Johnson S, Greenberg D, Peake M, Rous B. Stage at diagnosis and early mortality from cancer in England. Br J Cancer. maart 2015;112(S1):S108-15.
- Pignon JP, Tribodet H, Scagliotti GV, Douillard JY, Shepherd FA, Stephens RJ, e.a. Lung Adjuvant 4. Cisplatin Evaluation: A Pooled Analysis by the LACE Collaborative Group. J Clin Oncol. 20 juli 2008:26(21):3552-9.
- Pirker R. Adjuvant chemotherapy in patients with completely resected non-small cell lung cancer. Transl Lung Cancer Res. oktober 2014;3(5):305-10.
- Wakelee HA, Altorki NK, Zhou C, Csőszi T, Vynnychenko IO, Goloborodko O, e.a. IMpower010: Primary results of a phase III global study of atezolizumab versus best supportive care after adjuvant chemotherapy in resected stage IB-IIIA non-small cell lung cancer (NSCLC). J Clin Oncol. 20 mei 2021;39(15_suppl):8500-8500.
- Wu YL, Tsuboi M, He J, John T, Grohe C, Majem M, e.a. Osimertinib in Resected EGFR -Mutated Non-Small-Cell Lung Cancer. N Engl J Med. 29 oktober 2020;383(18):1711-23.
- Abbosh C, Birkbak NJ, Swanton C. Early stage NSCLC challenges to implementing ctDNA-8 based screening and MRD detection. Nat Rev Clin Oncol. september 2018;15(9):577-86.
- Chae YK, Oh MS. Detection of Minimal Residual Disease Using ctDNA in Lung Cancer: Current Evidence and Future Directions. J Thorac Oncol. januari 2019;14(1):16-24.
- 10. Leal A, Van Grieken NCT, Palsgrove DN, Phallen J, Medina JE, Hruban C, e.a. White blood cell and cell-free DNA analyses for detection of residual disease in gastric cancer. Nat Commun. 27 januari 2020;11(1):525.
- 11. Tie J, Wang Y, Tomasetti C, Li L, Springer S, Kinde I, e.a. Circulating tumor DNA analysis detects minimal residual disease and predicts recurrence in patients with stage II colon cancer. Sci Transl Med [Internet]. 6 juli 2016 [geciteerd 28 september 2023];8(346). Beschikbaar op: https://www. science.org/doi/10.1126/scitranslmed.aaf6219
- 12. The TRACERx consortium, The PEACE consortium, Abbosh C, Birkbak NJ, Wilson GA, Jamal-Hanjani M, e.a. Phylogenetic ctDNA analysis depicts early-stage lung cancer evolution. Nature. 25 mei 2017;545(7655):446-51.
- 13. Chaudhuri AA, Chabon JJ, Lovejoy AF, Newman AM, Stehr H, Azad TD, e.a. Early Detection of Molecular Residual Disease in Localized Lung Cancer by Circulating Tumor DNA Profiling. Cancer Discov. 1 december 2017;7(12):1394-403.
- 14. McDonald BR, Contente-Cuomo T, Sammut SJ, Odenheimer-Bergman A, Ernst B, Perdigones N, e.a. Personalized circulating tumor DNA analysis to detect residual disease after neoadjuvant therapy in breast cancer. Sci Transl Med. 7 augustus 2019;11(504):eaax7392.
- 15. Marsico G, Sharma G, Perry M, Hackinger S, Forshew T, Howarth K, e.a. Analytical development of the RaDaR assay, a highly sensitive and specific assay for the monitoring of minimal residual disease. [Internet]. Proceedings of the Annual Meeting of the American Association for Cancer Research 2020; 2020 Apr 27-28 and Jun 22-24. Philadelphia (PA): AACR; Cancer Res 2020;80(16 Suppl):Abstract nr 3097; 2020. Beschikbaar op: https://www.inivata.com/wp-content/ uploads/2020/06/AACR_2020_poster_3097.pdf

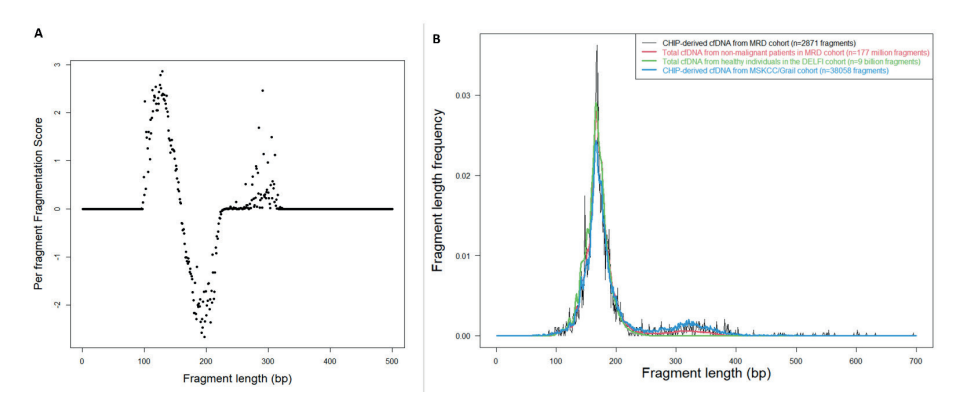
- 16. Chiu RWK, Heitzer E, Lo YMD, Mouliere F, Tsui DWY. Cell-Free DNA Fragmentomics: The New "Omics" on the Block. Clin Chem. 1 december 2020;66(12):1480-4.
- Jiang P, Chan CWM, Chan KCA, Cheng SH, Wong J, Wong VWS, e.a. Lengthening and shortening of plasma DNA in hepatocellular carcinoma patients. Proc Natl Acad Sci [Internet]. 17 maart 2015 [geciteerd 28 september 2023];112(11). Beschikbaar op: https://pnas.org/doi/full/10.1073/ pnas.1500076112
- 18. Lo YMD, Han DSC, Jiang P, Chiu RWK. Epigenetics, fragmentomics, and topology of cell-free DNA in liquid biopsies. Science. 9 april 2021;372(6538):eaaw3616.
- 19. Mouliere F, Chandrananda D, Piskorz AM, Moore EK, Morris J, Ahlborn LB, e.a. Enhanced detection of circulating tumor DNA by fragment size analysis. Sci Transl Med. 7 november 2018;10(466):eaat4921.
- Underhill HR. Leveraging the Fragment Length of Circulating Tumour DNA to Improve Molecular Profiling of Solid Tumour Malignancies with Next-Generation Sequencing: A Pathway to Advanced Non-invasive Diagnostics in Precision Oncology? Mol Diagn Ther. juli 2021;25(4):389-408.
- 21. Underhill HR, Kitzman JO, Hellwig S, Welker NC, Daza R, Baker DN, e.a. Fragment Length of Circulating Tumor DNA. Kwiatkowski DJ, redacteur. PLOS Genet. 18 juli 2016;12(7):e1006162.
- 22. Cristiano S, Leal A, Phallen J, Fiksel J, Adleff V, Bruhm DC, e.a. Genome-wide cell-free DNA fragmentation in patients with cancer. Nature. juni 2019;570(7761):385-9.
- 23. Mathios D, Johansen JS, Cristiano S, Medina JE, Phallen J, Larsen KR, e.a. Detection and characterization of lung cancer using cell-free DNA fragmentomes. Nat Commun. 20 augustus 2021;12(1):5060.
- 24. Chabon JJ, Hamilton EG, Kurtz DM, Esfahani MS, Moding EJ, Stehr H, e.a. Integrating genomic features for non-invasive early lung cancer detection. Nature. 9 april 2020;580(7802):245-51.
- 25. Wan JCM, Heider K, Gale D, Murphy S, Fisher E, Mouliere F, e.a. ctDNA monitoring using patient-specific sequencing and integration of variant reads. Sci Transl Med. 17 juni 2020;12(548):eaaz8084.
- Chen K, Zhao H, Shi Y, Yang F, Wang LT, Kang G, e.a. Perioperative Dynamic Changes in Circulating Tumor DNA in Patients with Lung Cancer (DYNAMIC). Clin Cancer Res. 1 december 2019;25(23):7058-67.
- 27. Schuurbiers M, Huang Z, Saelee S, Javey M, De Visser L, Van Den Broek D, e.a. Biological and technical factors in the assessment of blood-based tumor mutational burden (bTMB) in patients with NSCLC. J Immunother Cancer. februari 2022;10(2):e004064.
- Roche Sequencing Solutions. AVENIO ctDNA Surveillance Kit [Internet]. Beschikbaar op: https://sequencing.roche.com/content/dam/rochesequence/worldwide/resources/brochure-avenio-ctdna-surveillance-kit-SEQ100046.pdf
- 29. R Development Core Team. R: a language and environment for statistical computing. R Foundation for Statistical Computing, Vienna, Austria; 2019.
- 30. Evers J, De Jaeger K, Hendriks LEL, Van Der Sangen M, Terhaard C, Siesling S, e.a. Trends and variations in treatment of stage I–III non-small cell lung cancer from 2008 to 2018: A nationwide population-based study from the Netherlands. Lung Cancer. mei 2021;155:103-13.
- 31. Razavi P, Li BT, Brown DN, Jung B, Hubbell E, Shen R, e.a. High-intensity sequencing reveals the sources of plasma circulating cell-free DNA variants. Nat Med. december 2019;25(12):1928-37.
- 32. Zviran A, Schulman RC, Shah M, Hill STK, Deochand S, Khamnei CC, e.a. Genome-wide cell-free DNA mutational integration enables ultra-sensitive cancer monitoring. Nat Med. juli 2020;26(7):1114-24.

- 33. Pellini B, Chaudhuri AA. Circulating Tumor DNA Minimal Residual Disease Detection of Non-Small-Cell Lung Cancer Treated With Curative Intent. J Clin Oncol. 20 februari 2022;40(6):567-75.
- 34. Heitzer E, Van Den Broek D, Denis MG, Hofman P, Hubank M, Mouliere F, e.a. Recommendations for a practical implementation of circulating tumor DNA mutation testing in metastatic nonsmall-cell lung cancer. ESMO Open. april 2022;7(2):100399.
- 35. Bai R, Li L, Chen X, Chen N, Song W, Cui J. Neoadjuvant and Adjuvant Immunotherapy: Opening New Horizons for Patients With Early-Stage Non-small Cell Lung Cancer. Front Oncol. 9 oktober 2020:10:575472.
- 36. Hendriks LEL, Van Meerbeeck J, Cadranel J. Targeted adjuvant therapy in non-small cell lung cancer: trick or treat? Eur Respir J. oktober 2021;58(4):2101637.
- 37. Patrinely JR, Johnson R, Lawless AR, Bhave P, Sawyers A, Dimitrova M, e.a. Chronic Immune-Related Adverse Events Following Adjuvant Anti–PD-1 Therapy for High-risk Resected Melanoma. JAMA Oncol. 1 mei 2021;7(5):744.
- 38. Zheng H, Zhu MS, Liu Y. FinaleDB: a browser and database of cell-free DNA fragmentation patterns [Internet]. Bioinformatics; 2020 aug [geciteerd 28 september 2023]. Beschikbaar op: http://biorxiv.org/lookup/doi/10.1101/2020.08.18.255885
- 39. Freeberg MA, Fromont LA, D'Altri T, Romero AF, Ciges JI, Jene A, e.a. The European Genomephenome Archive in 2021. Nucleic Acids Res. 7 januari 2022;50(D1):D980-7.



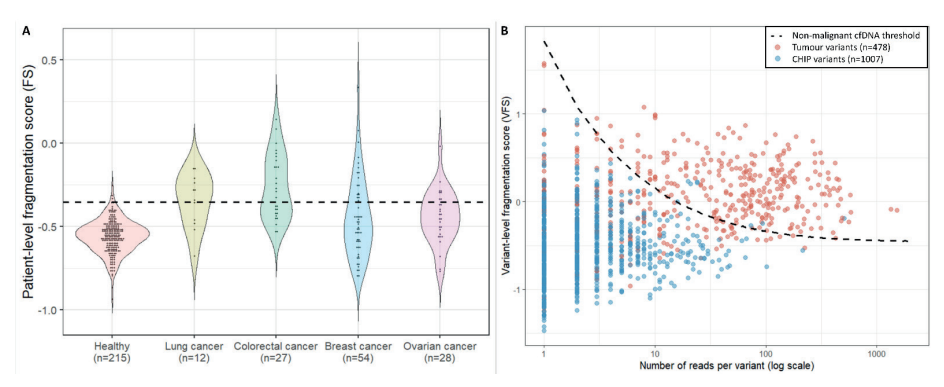
Supplemental figure \$1. Analytical validation of patient-level FS

A. Patient-level FS versus the mean tumour variant allele frequency (VAF) in all preoperative samples (n=36). Line and shaded area represent Pearson correlation and corresponding confidence interval. **B.** Passing-Bablok regression of patient-level FS in biological replicates (n=9) sampled in EDTA tubes or Cell stabilizing tubes.



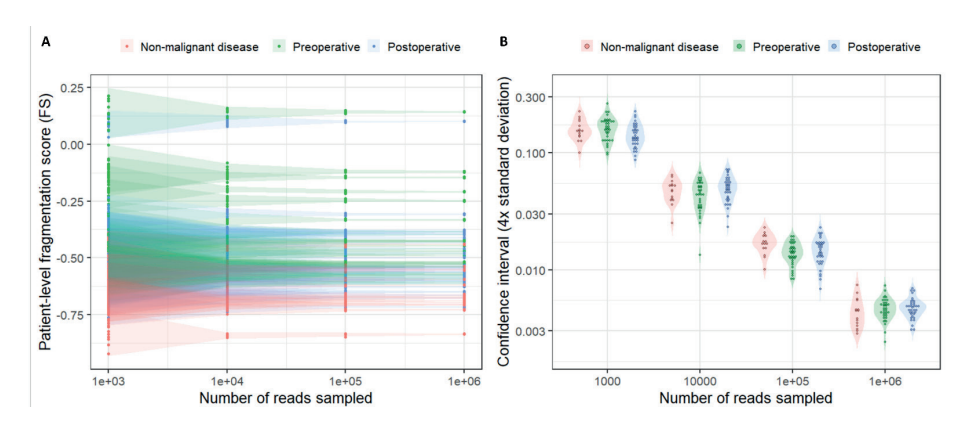
Supplemental figure S2. Fragment level fragmentation

A. The per-fragment fragmentation score for various fragment lengths, corresponding to the log-2 of the ratio of tumour-fragments to non-tumour-fragments (**figure 2A**). The per-fragment fragmentation score was bootstrapped over 1,000 iterations and regions with an insufficient number of fragments were given a score of 0 (**Methods**) To translate the per-fragment score to the per-patient fragmentation score (FS), we used the average per-fragment score of 1 million randomly drawn fragments per patient. To translate the per-fragment score to a per-variant fragmentation score (VFS) we averaged the per-fragment score of all fragments supporting a variant. **B.** Fragment length frequencies of various cohorts of non-tumour cfDNA: CHIP-derived cfDNA in the MRD cohort (black), cfDNA from patients with non-malignant disease in the MRD cohort (red), cfDNA from healthy donors from the DELFI cohort (green) and CHIP-derived cfDNA in the MSKCC/Grail cohort (blue). The peaks for all these sources of non-tumour cfDNA are overlapping, indicating that cfDNA from non-malignant patients does not have a different fragmentation pattern compared to other established sources of non-malignant cfDNA, despite underlying disease in these patients.



Supplemental figure S3. Validation of patient-level fragmentation score (FS) and variant-level fragmentation score (VFS) in the DELFI and MSKCC/Grail cohorts, respectively

A. Patient-level FS applied to the DELFI cohort. Horizontal dashed line indicates the mean plus two times standard deviation of the FS amongst n=215 Healthy volunteers in this cohort. This corresponds to a specificity of 98.6% and sensitivity of 58% amongst n=12 lung cancer patients. B. Variant-level fragmentation score (VFS) applied to the MSKCC/Grail cohort. The black dashed line corresponds to the non-malignant cfDNA threshold as determined in figure 2A. Limiting the analysis to only variants with at least 8 reads, tumour variants were detected with 82% sensitivity (263/319 tumour variants, red) and CHIP variants with 93% specificity (106/114 CHIP variants, blue).

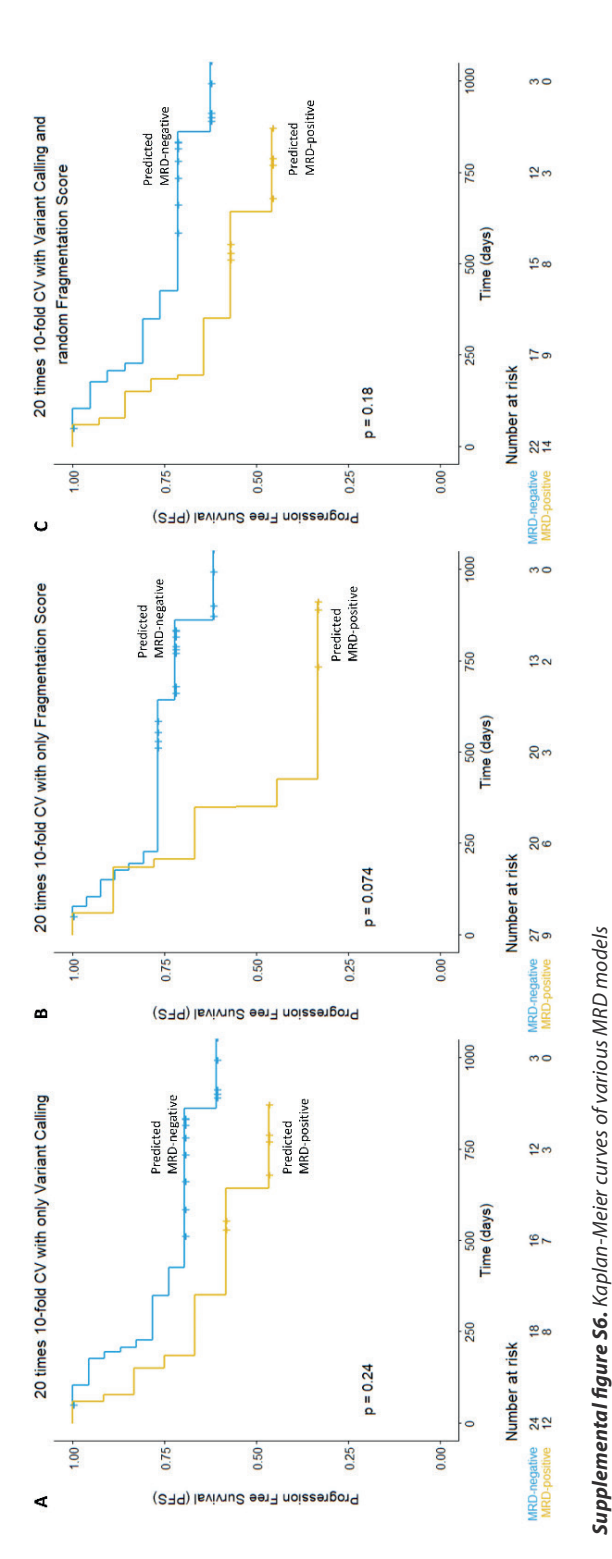


Supplemental figure S4. Technical reproducibility and downsampling of patient-level FS

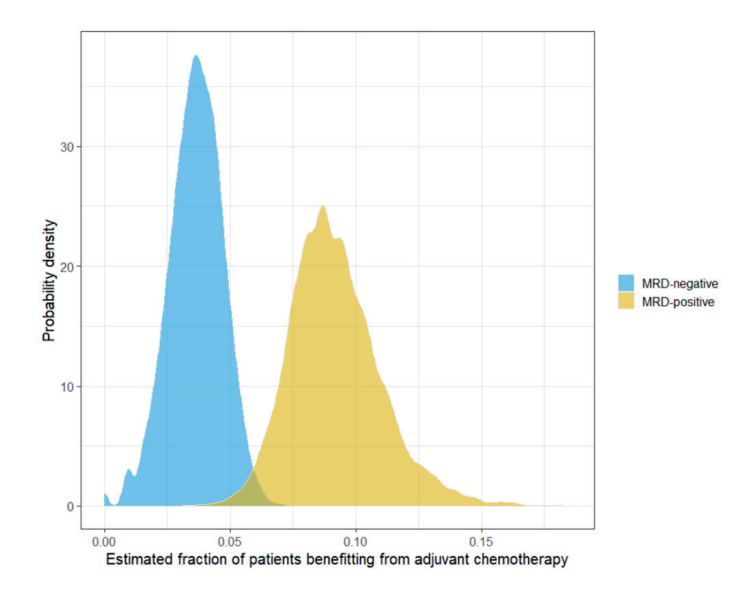
A. Variation in patient-level FS when sampling 1,000 to 1,000,000 reads of non-malignant patients (red, n=15), preoperative (green, n=36) and postoperative patients (blue, n=36). **B.** Violin plot with confidence interval of patient-level FS presented as four times the standard deviation when sampling 1,000 to 1,000,000 reads of non-malignant (red, n=15), preoperative (green, n=36), and postoperative patients (blue, n=36).

			#days	ng/ml plasma						Tw	rent	y tir	nes	10-	fold	CV	iter	atic	n						
		ID	postoperative	postoperative	1	2	3	4	5	6	7	8	9	10	11	12	13	14	15	16	17	18	19	20	Mean
		MRD01	6	33.00	0	0	0	0	0	0	0	0	0	0	0	0	0	0	0	0	0	0	0	0	0
		MRD05	3	43.20	0	0	0	0	0	0	0	0	0	0	0	0	0	0	0	0	0	0	0	0	0
		MRD08	9	14.63	0	0	0	0	0	0	0	0	0	0	0	0	0	0	0	0	0	0	0	0	0
		MRD10	3	54.30	0	0	0	0	0	0	0	0	0	0	0	0	0	0	0	0	0	0	0	0	0
_ ا		MRD11	21	8.52	0	0	0	0	0	0	0	0	0	0	0	0	0	0	0	0	0	0	0	0	0
5		MRD12	3	45.20	0	0	0	0	0	0	0	0	0	0	0	0	0	0	0	0	0	0	0	0	0
Patients without progression		MRD16	35	21.50	0	0	0	0	0	0	0	0	0	0	0	0	0	0	0	0	0	0	0	0	0
ē		MRD17	10	34.10	0	0	0	0	0	0	0	0	0	0	0	0	0	0	0	0	0	0	0	0	0
8		MRD18	28	46.30	0	0	0	0	0	0	0	0	0	0	0	0	0	0	0	0	0	0	0	0	0
∣₫		MRD21	36	10.53	0	0	0	0	0	0	0	0	0	0	0	0	0	0	0	0	0	0	0	0	0
旨	n=22	MRD28	27	11.52	0	0	0	0	0	0	0	0	0	0	0	0	0	0	0	0	0	0	0	0	0
1 2	빝	MRD30	16	9.49	0	0	0	0	0	0	0	0	0	0	0	0	0	0	0	0	0	0	0	0	0
₹	_	MRD33	29	5.99	0	0	0	0	0	0	0	0	0	0	0	0	0	0	0	0	0	0	0	0	0
2		MRD34	10	7.86	0	0	0	0	0	0	0	0	0	0	0	0	0	0	0	0	0	0	0	0	0
ᇉ		MRD39	34	13.05	0	0	0	0	0	0	0	0	0	0	0	0	0	0	0	0	0	0	0	0	0
l è.∣		MRD14	6	34.90	0	0	0	0	0	0	0	0	0	0	0	0	0	0	0	1	0	0	0	0	0.05
Pa		MRD37	21	8.66	0	0	0	0	0	0	0	1	0	0	1	0	0	0	0	0	0	0	0	0	0.1
		MRD02	17	14.20	0	0	0	0	0	0	0	1	0	0	1	0	0	0	0	1	0	0	0	0	0.15
		MRD13	3	73.10	1	1	1	0	1	1	1	0	1	1	1	1	1	1	1	0	1	0	1	1	0.8
		MRD03	5	99.70	1	0	1	1	1	1	1	1	1	1	1	1	1	1	1	1	1	1	0	1	0.9
		MRD23	5	61.50	1	1	1	1	1	1	0	1	1	1	1	1	1	1	1	1	0	1	1	1	0.9
		MRD27	21	9.87	1	1	1	1	1	1	1	1	1	1	1	1	1	1	1	1	1	1	1	1	1
		MRD06	6	50.20	0	0	0	0	0	0	0	0	0	0	0	0	0	0	0	0	0	0	0	0	0
5		MRD09	29	18.50	0	0	0	0	0	0	0	0	0	0	0	0	0	0	0	0	0	0	0	0	0
l is		MRD22	23	7.13	0	0	0	0	0	0	0	0	0	0	0	0	0	0	0	0	0	0	0	0	0
es		MRD29	19	14.00	0	0	0	0	0	0	0	0	0	0	0	0	0	0	0	0	0	0	0	0	0
<u> </u>		MRD35	32	5.90	0	0	0	0	0	0	0	0	0	0	0	0	0	0	0	0	0	0	0	0	0
5	=	MRD25	6	18.97	0	1	1	1	1	1	0	1	1	1	0	1	1	1	1	1	0	1	1	1	0.8
ء ا	÷	MRD15	4	152.00	0	1	1	1	1	1	0	1	1	1	1	1	1	1	1	1	1	1	1	1	0.9
Patients with progression	(n=14)	MRD20	8	30.10	1	1	1	1	1	1	1	1	1	1	1	1	1	0	1	0	1	1	1	1	0.9
2		MRD24	4	71.00	1	1	1	1	1	1	1	1	1	1	1	1	1	1	1	1	0	1	1	1	0.95
Ħ		MRD04	23	261.00	1	1	1	1	1	1	1	1	1	1	1	1	1	1	1	1	1	1	1	1	1
E.		MRD19	8	35.40	1	1	1	1	1	1	1	1	1	1	1	1	1	1	1	1	1	1	1	1	1
Pat		MRD26	6	31.10	1	1	1	1	1	1	1	1	1	1	1	1	1	1	1	1	1	1	1	1	1
_		MRD31	6	13.01	1	1	1	1	1	1	1	1	1	1	1	1	1	1	1	1	1	1	1	1	1
		MRD32	4	27.02	1	1	1	1	1	1	1	1	1	1	1	1	1	1	1	1	1	1	1	1	1

Supplemental figure S5. Results of the twenty times repeated ten-fold cross validation (TTF-CV) Results of the twenty times repeated 10-fold cross validation on patient level, in patients grouped in with or without recurrence of disease, where a score of 0 represents an MRD-negative prediction and 1 an MRD-positive prediction by the MRD model. The majority call amongst the twenty repeats was used as input for the Kaplan-Meier curves. The rightmost column, "Mean", was used as input for estimating the fraction of patients that would benefit from adjuvant chemotherapy.



Kaplan-Meier curves of various MRD prediction models in 20 times repeated 10-fold cross validation. Patients were grouped as MRD-negative or MRD-positive by the majority result of the cross validation. A. MRD model using only variant calling. B. MRD model using only the patient-level fragmentation score (FS). C. MRD model using variant calling and a randomly assigned FS.



Supplemental figure S7. Bootstrap simulation of potential clinical implications

A 10,000 times repeated bootstrap simulation with estimates of the fraction of patients in the MRDpositive (yellow) and MRD-negative group (blue) based on the combined MRD model who would benefit from adjuvant chemotherapy. An absolute disease free survival benefit of adjuvant chemotherapy of 0.058 was used.

Supplemental table S1. Clinical characteristics of the nonmalignant control cases (n = 15).

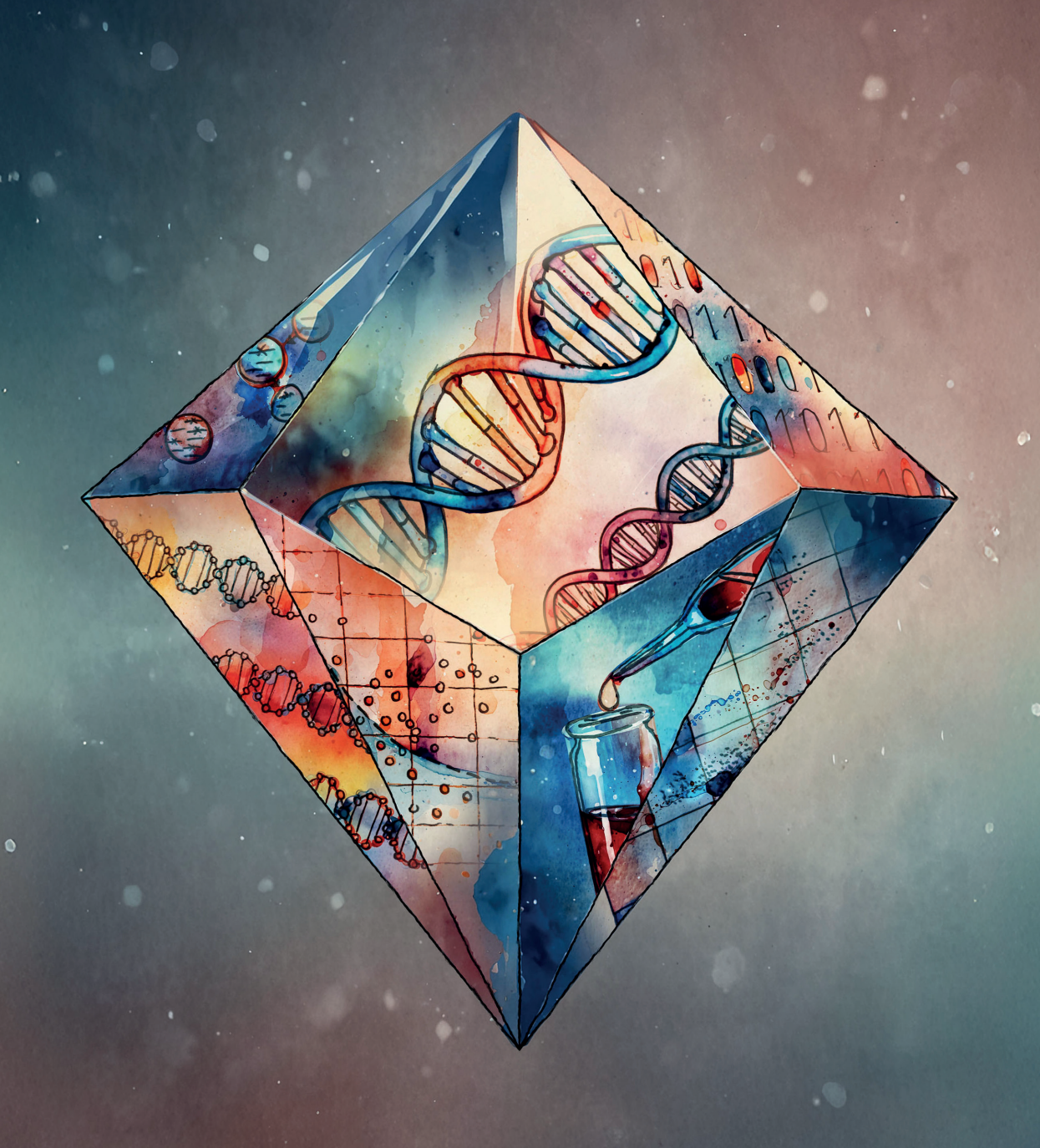
	Age at		Simultaneous Pathologic	Pathologic
MRD-ID S	Sex diagnosis	Diagnosis	malignancy	evidence
MRDHD01	M 61	I Aspergilloma	no	yes
MRDHD02 M	M 67	rounded atelectasis (follow-up PET/CT-scan after 1 year showed mimimal reduction in size and no FDG uptake*)	no	no
MRDHD03 F	F 63	s Necrotic granulomatous inflammation (Mycobacterium kansasii)	no	yes
MRDHD04 M	M 67	Hamartoma	no	yes
MRDHD05 F	F 75	Hamartoma	no	yes
MRDHD06 M	M 51	l Organizing pneumonia	no	yes
MRDHD07 F	F 68	s Granulomatous inflammation	no	yes
MRDHD08 F	F 67	r Inflammation (follow-up CT-scan after three months showed 50% reduction in size)	no	no
MRDHD09 M	72 N	2 Fibrosis	no	yes
MRDHD10 M	M 55	Gastritis	no	yes
MRDHD11 M	M 71	l Nonspecific interstitial pneumonia (NSIP)	no	yes
MRDHD12 M	M 62	Benign pulmonary nodule (follow-up CT scan after three months showed >50% reduction in size)	no	yes
MRDHD13 N	M 64	Fibrosis	no	yes
MRDHD14	M 71	Pulmonary actinomyces	no	yes
MRDHD15 M	M 66	S Rounded atelectasis after fractured rib (follow-up CT scan after 1 year showed minimal reduction in size)	no	no

* FDG= fluorode oxyglucose

Supplemental table 52. Variants derived from plasma and tumour tissue samples. [table too long for print, available from online supplemental materials on https://doi.org/10.1002/1878-0261.13267]

Supplemental table S3. Bivariate Cox proportional hazard ratio of MRD detection, showing hazard ratios (HR) with 95% confidence intervals (CI) for different covariates.

Ha (Hazard ratio of covariate (confidence interval)	C)	Hazard ratio of Hazard ratio of MRD-test ovariate; p-value (confidence interval)	Hazard ratio of MRD-test; p-value
Sample time post surgery (in days)	1.02 (0.96-1.08)	0,596	5.61 (1.48-21.33)	0,011
Simultaneous secondary tumour (no vs. yes)	1.71 (0.53-5.55)	0,370	4.56 (1.50-13.91)	0,008
Adjuvant therapy				
Adjuvant therapy not started vs. started, not completed	1.99 (0.50-7.79)	0,332	[00 /1 61 16 14)	9000
Adjuvant therapy not started vs. completed	0.75 (0.21-2.63)	0,649	3.03 (1.01-10.14)	0,000
Pathological tumour stage (stage II vs. IIIA)	3.06 (1.00-9.31)	0,049	3.86 (1.23-12.08)	0,021



Chapter 6

General discussion and future perspectives

6.1 Summary and general discussion

The conventional approach to diagnostics in solid malignancies is based on tissue biopsies, offering insights into crucial cellular alterations guiding therapeutic decisions. However, the drawbacks associated with tissue biopsies, including invasiveness, susceptibility to sampling errors, and an inability y to capture real-time tumour dynamics, necessitate exploration into alternative methodologies. Liquid biopsies, emerging as a transformative paradigm in oncology, offer a minimally invasive solution to several challenges posed by tissue biopsies. Among the various liquid biopsy modalities, the examination of circulating tumour DNA (ctDNA) has emerged as a focal point of investigation.

The dynamic field of ctDNA, marked by continuous and rapid development, holds potential for significant advancements in cancer diagnostics and monitoring. The clinical uptake of ctDNA testing is among other reasons hampered by the limited sensitivity and specificity of the tests. These challenges arise from a combination of biological and technical factors inherent in the tests. This dissertation aims to address these challenges through improved data utilization and proposing methodological enhancements.

6.1.1 Improvement of standard ddPCR analysis: ALPACA

A method will inherently produce false positive and false negative results. Such erroneous results may pose a serious problem resulting in suboptimal or ineffective treatment. At the same time, standardisation of methods and results are essential in clinical care. In **Chapter 2** we had a close look into the performance of one of the early workhorses of ctDNA analysis: droplet digital PCR. We showed that false positive events (Polymerase induced false positive events: PIFs) are introduced by the Taq polymerase. We observed a skew towards FAM&HEX-positive vs FAM-only-positive droplets that could not be explained by other biological or technical factors. The PIFs appeared in a fan-like pattern and could be recognized *post hoc* as an overabundance of FAM&HEX-positive droplets compared to the FAM-positive and HEX-positive droplets. An *in silico* correction algorithm was developed that classifies excess FAM&HEX-positive droplets as false-positive.

Next, we showed that even after removal of the PIFs, there were still a number of false positive droplets remaining in experiments with wildtype DNA only. The number of false positive droplets correlated with the total amount of input wildtype DNA and was different for different assays used. Based on these observations we developed an assayand input-dependent adaptive threshold to distinguish positive and negative samples.

Together, the PIF correction and adaptive threshold were made publicly available as the 'Adaptive Limit of blank and PIF correction, an Automated Correction Algorithm' (ALPACA). We showed that ALPACA had superior specificity (fewer false positives) with no loss in sensitivity in synthetic reference material, healthy donor cfDNA and a patient cohort of metastatic NSCLC patients (n=203). The total accuracy in the latter cohort was raised from 92% to 98%. Strikingly, the positive predictive value (PPV) was raised from just 56% for the standard procedure to 92% with ALPACA. In other words, with the standard procedure 44% of all ddPCR positive results in this cohort were false positive results and might have led to erroneous treatment administered to patients who would not benefit from it.

The publication of ALPACA was welcomed by the scientific community as an "elegant strategy" to improve ddPCR accuracy (1). Additionally, ALPACA was used as a benchmark method for a more computationally heavy algorithm termed CASTLE (2), Similar to the results in ALPACA, the CASTLE authors conclude that methods with an adaptive limit of blank (LoB) are overall superior to methods with a static LoB. Despite ALPACA's reception and CASTLE's confirmation of the same conclusions, official manufacturer guidelines continue to advocate a static LoB based on a very minimal validation (3,4). In practice, methods with an adaptive LoB like ALPACA and CASTLE are rarely used outside their respective parent institutions' walls. This could lead to the implementation of inferior procedures in routine clinical care, impacting patient treatment and conclusions from studies based on ddPCR (5). Preferably, authorities like the dMIQE-group for reporting standards in digital PCR experiments should start recommending adaptive LoBs, to entice the manufacturer to do the same (6).

6.1.2 Evaluation of ctDNA detection technologies

Not only validation of a single method is important, also knowledge on differences between methods is clinically relevant. Beyond ddPCR, more technologies have become available for the detection of hotspot point mutations in ctDNA. All these methods claim a certain sensitivity and specificity. Comparing these numbers is difficult since a lot of factors influencing sensitivity and specificity are not harmonised over different platforms. As a result, observed differences in sensitivity can result from a multitude of factors, including genuine performance superiority, the utilisation of more input cfDNA, isolation method, analysis procedure, and number of different mutations targeted. Moreover, costs differ significantly between methods, posing additional challenges for hospitals in making informed decisions regarding the most suitable method for their specific clinical applications. With so many variables impacting the final result and performance of a method, a fair and accurate comparison between methods is practically impossible. This prevents us from objectively comparing performance, limiting the incentive for diagnostic laboratories to choose the right method and hampering harmonisation of results.

Against this background we set out in Chapter 3 to compare four commercially available ctDNA detection methods - ddPCR, COBAS z480, Idylla, and BEAMing. While preparing this study it became evident that a straightforward strategy of analysing the same samples on each platform would not allow us to discern whether observed differences were caused by the amount of input cell-free plasma. isolation method, analysis method, or tumour fraction of the sample. To study the impact of these variables we designed the study to systematically remove differences between the methods that could potentially impact the final result. This study demonstrated the complexity of a fair method comparison in ctDNA analyses.

After elimination of confounding factors, we observed that the two digital platforms – ddPCR and BEAMing – were more sensitive than the gPCR-based platforms Idylla and COBAS z480. This fits earlier studies that performed a more straightforward comparison of these and similar methods (7–10). Apart from sensitivity we also investigated the impact of the breadth of target of each method. Not all platforms target the same number of point mutations, yet the number of mutations targeted was found to have a minimal effect on the expected number of mutations detected in a cohort of metastatic CRC patients.

A factor that does not influence the performance of a platform but does play an important role in hospital decisions to use a platform is the cost. By performing an activity-based costing method (11) we found that the overall costs were highest for BEAMing due to high fixed and consumable costs. Up to a throughput of 110 samples per year (2 samples per week), Idylla was the least expensive platform due to low fixed costs. At higher throughput, ddPCR was less expensive due to lower consumable costs. These insights together can help hospitals make an informed choice between various methods.

Understanding of the technology applied, and an extensive validation are both essential criteria to generate trust in the platform's output. Many factors influence the analysis of ctDNA, and this can lead to an impact on clinical practice. Applying the right method for a given clinical situation is a challenge, and failure to do so could for example result in false negative results when a too insensitive technique is applied to a clinical situation that demands high sensitivity.

6.1.3 Clinical impact of NGS analysis of ctDNA

Patients who present with primary metastatic NSCLC (mNSCLC) can be eligible for one of various Tyrosine Kinase Inhibitor (TKI) treatments, provided the tumour is driven by specific activating mutations. For this reason, national and international guidelines dictate that molecular profiling of tumour DNA should cover known NSCLC oncodriver genes such as EGFR, KRAS, BRAF, ERBB2, ALK, ROS1, RET, and MET (12-15).

Detection of these activating mutations typically happens in tumour biopsies, but these are not always feasible and bring risks of complications. In Chapter 4 we explore the added diagnostic value of plasma-based complete molecular profiling (plasma-CMP) next to standard-of-care tissue molecular profiling (SoC-TMP). We employed the Roche AVENIO ctDNA Targeted kit, which targets 17 genes that are highly frequently mutated in cancer (16).

A cohort of patients with mNSCLC (n=209) was selected from the larger Lung cancer Early Molecular Assessment (LEMA) study (17,18). In the LEMA study SoC-TMP was protocolised, leading to a higher standard of mutation detection in tissue compared to similar studies abroad (18–20). In the current cohort, we investigated whether addition of plasma-CMP next to the optimised SoC-TMP would increase the proportion of patients eligible for targeted treatment. Indeed, with the inclusion of plasma-CMP, the fraction of patients for whom a potentially targetable driver mutation was detected increased from 34.4% to 39.7% (p<0.001).

Similar results on the clinical utility of plasma-CMP were obtained in a larger study, covering over 8,000 mNSCLC patients (21). Here, the authors managed to increase the percentage of patients for whom a targetable driver mutation was detected from 25.0% in SoC-TMP alone to 34.7% for SoC-TMP plus plasma-CMP. Moreover, the authors show that targeted therapy response rates were statistically equivalent to those reported from tissue analysis.

These results signify that even with state-of-the-art tissue molecular profiling, the addition of plasma-based molecular profiling will increase the number of patients that are found to be eligible for effective targeted treatments. In part, this increase can be attributed to patients for whom tissue biopsies are not feasible due to the condition of the patient and/or the location of the tumour and its metastases (22–24). Additionally, even in patients for whom the tissue molecular profiling was completed successfully, additional mutations were detected by the inclusion of plasma-CMP. This was the case for a modest 4.4% of patients in our study (8 out of 179 patients with successful SoC-TMP), compared to 6.4% of patients (26 of 409 patients) in the larger study. The additional mutations detected, despite successful SoC-TMP, may indicate intra- and inter- tumour heterogeneity that is not captured by a tissue biopsy of a single lesion or metastatic site (25).

After concluding that plasma-CMP can facilitate a significant increase in the number of actionable mutations detected compared to SoC-TMP alone, a follow-up question remains how to most effectively organise the diagnostic workflow within a hospital. Is it, for example, more effective to perform the plasma-CMP first, then perform reflex SoC-TMP on those patients who were negative on ctDNA, or vice versa? To this end, a follow-up simulation study was conducted based on the data generated in this study. In the follow-up study discrete event simulation (DES) was used to investigate the effects of implementation of plasma-CMP next to SoC-TMP on the turn-around time (TAT), cost of analysis, and fraction of patients with a clinically relevant test result (26).

Two scenarios with plasma-CMP were investigated: One where plasma-CMP was performed first and SoC-TMP was only performed if plasma-CMP did not detect a clinically relevant mutation ("plasma first"). The second scenario employed SoC-TMP first, then reflexed to plasma-CMP if the first tissue biopsy failed ("tissue first"). Compared to the SoC-TMP only baseline, the "plasma first" scenario increased the proportion of patients with a clinically relevant result (93% vs 84%), decreased the TAT (9 days vs 20 days), and increased the mean costs per patient (€3218 vs €2304). The "tissue first" scenario yielded a similarly high proportion of clinically relevant results (also 93%), against comparable TAT (19 days) and costs (€2448) to the baseline scenario. Moreover, compared to the baseline scenario a total of 16% and 9% of tissue biopsies could be prevented in the "plasma first" and "tissue first" scenarios, respectively, signifying a reduced patient burden in the diagnostic workup.

In a recent modelling study, similar results were obtained: Addition of plasma-CMP to SoC-TMP resulted in a slight increase in cost and a slight improvement to patient quality adjusted life years (QALYs) on the care pathway for mNSCLC patients (27). Cost-effectiveness in this study was shown for the subgroup of patients with an activating mutation in *EGFR*, and the authors advocate that the slight increase in cost is justifiable by the significant increase in QALYs for specific subgroups.

These studies support a routine diagnostic procedure for treatment selection in the setting of mNSCLC that includes plasma-CMP. Whether this is done in a tissue-first or plasma-first approach was an open question. Plasma-first decreases the TAT and the

number of tissue biopsies required, while tissue-first is less expensive. Additionally, certain biomarkers, such as the tumour's histopathology or PD-L1 status, can't be deduced from the liquid biopsy. These considerations could suggest a tissue-first approach with reflex plasma-CMP at the time of diagnosis, and plasma-CMP as the primary option at the time of progression on targeted therapies (21). Indeed, recently the Dutch Commission for the Evaluation of Diagnostics (CieBOD) issued a formal evaluation for this diagnostic setting, wherein they advise to perform diagnostics on tissue first, and reflex to plasma when that fails (28,29).

6.1.4 Combining data to improve MRD detection

In chapters 2-4 we focused on patients with metastatic disease, where ctDNA detection is relatively straightforward due to the high tumour burden. In contrast, ctDNA detection in lower-stage NSCLC is more challenging. For stage I-III NSCLC, the primary curative treatment is surgical resection, which achieves five-year recurrence-free survival (RFS) rates of 81%, 50%, and 34% for stage I, II, and III NSCLC, respectively (30). At the time of our study, adjuvant chemotherapy was the standard of care for patients with stage II or III NSCLC, offering a modest absolute disease free survival benefit of 5.8% (31,32).

Predicting which patients will recur remains a subject of considerable research. After surgical removal of the tumour, the amount of ctDNA in the circulation is often diminished to undetectable levels. Post-surgical MRD aims to detect residual ctDNA, distinguishing patients at high recurrence risk from those likely cured. In **Chapter 5** we applied a broad hybrid capture sequencing panel (the Roche AVENIO ctDNA Surveillance kit (33)) targeting 198 cancer-relevant genes to detect MRD in patients with stage II-IIIA NSCLC who underwent curative surgery.

The most straightforward way to detect MRD after surgical removal of the tumour is to detect tumour-related mutations in the post-surgery plasma. Using this panel, we found this approach did not effectively distinguish patients with high or low risk of recurrence. This was due the limited number of mutations we could track per patient (median 3) and false positive mutation calls in recurrence-free patients. In contrast, integrating additional cfDNA fragmentomics analyses significantly improved stratification into high- and low-risk recurrence groups. The test's performance was comparable to state-of-the-art tests in similar patient groups, but lacked sufficient negative predictive value (NPV) to forego adjuvant chemotherapy based on a negative result.

This study demonstrated explicitly that improved integration of data types, even from a single experiment, can drastically increase the performance of the test. Broad sequencing panels generate a lot of data, and when only looking at the detected mutations a lot of that data is left unused. This starts to be recognized by the field of cfDNA research, moving towards integration of various data types to improve the sensitivity of detecting tumour signal.

In clinical practice, an MRD test can serve two scenarios. For patients who would not typically receive adjuvant therapy (i.e. stage I NSCLC), a test with excellent positive predictive value (PPV) could guide escalation of treatment for those with a positive MRD test (34). Conversely, for patients recommended adjuvant therapy, a test with an excellent NPV could support de-escalation, sparing patients unnecessary treatment and associated toxicities. However, no MRD detection approach has yet demonstrated sufficient sensitivity and NPV to reliably inform such decisions in clinical trials or practice (35–37).

The challenges in achieving these clinical thresholds are multifaceted. As highlighted in this thesis, current MRD detection methods face limits in sensitivity, with many patients falling below the limit of detection of existing assays (38). Emerging approaches, such as tracking phased variants or using tumour-informed sequencing of a large number of mutations, have improved detection rates, claiming analytical sensitivity <0.0001% TF, but still depend heavily on the availability of high-quality tumour tissue for assay design (39–41). Meanwhile, plasma WGS-based approaches, which rely on the breadth rather than the depth of sequencing, exploit the statistical improbability of not encountering any tumour-related mutations across thousands of potential sites. This method achieves analytical detection thresholds of 0.001% TF (42,43).

The need for tumour-agnostic MRD tests is becoming increasingly present as new treatment paradigms reshape the landscape of resectable NSCLC. Trials like KEYNOTE-671, IMpower010, and PACIFIC have introduced neoadjuvant immune checkpoint inhibitors (ICIs) and adjuvant chemoimmunotherapy as standards of care (44–47). This reduces the availability of resected tumour tissues in several scenarios. For example, patients achieving pathological complete response (pCR) after neoadjuvant ICI (up to 24%) may avoid surgery altogether (48). This presents a special case of MRD detection, where the goal is to predict which patients achieved pCR and only a biopsy is available. Similarly, in cases where tumour tissue is significantly reduced (but not entirely removed) by neoadjuvant ICI treatment, the reliance on tissue-based assays becomes impractical. Moreover, in stage III patients

treated with definitive chemoradiotherapy followed by ICI, no surgery is performed at all and MRD detection must be entirely plasma-based. For all these cases, resected tissue material is scarce or non-existent, emphasizing the need for tumour tissue-agnostic MRD tests with bespoke analytical and clinical sensitivity (49).

Adding to these challenges is the lack of standardisation across MRD studies. Variability in assay protocols, blood sampling windows, and study designs complicates comparisons between methods and obscures their clinical utility. This lack of standardisation mirrors earlier experiences with PCR-based ctDNA detection technologies. Until robust, reliable, and affordable MRD tests are identified, the potential clinical impact of MRD-quided treatment will remain underutilised.

6.2 Future perspectives

Liquid biopsies, particularly ctDNA analysis, have shown considerable potential in changing clinical practice, and this promise has been recognized for years (50–52). Despite significant progress, there is still a long way to go in fully realizing the clinical value of these technologies, with future research needed to develop them further

In the coming years, two primary research areas will dominate the liquid biopsy field. The first area focuses on novel innovations at the frontiers of research to advance increasingly sensitive assays for detecting ctDNA at extremely low levels, essential for applications like MRD detection and population-wide cancer screening. The second area involves translating existing innovations into clinical practice. We will explore the frontiers of research first, followed by a discussion on implementation.

6.2.1 Frontiers of research

When describing the possible future directions of research in cfDNA, it is often useful to first examine the current trends, to hopefully extrapolate from there. Three trends are reflected in the works in this thesis: First, the field has developed from single hotspot mutation detection assays (chapters 2 and 3) towards broader sequencing assays, allowing the detection of multiple mutations at once from a single sample (chapters 4 and 5). Second, data analysis procedures have grown more complex, moving beyond straightforward thresholds (chapter 3) towards multi-parametric decision boundaries (chapters 2, 4, and 5). Third, benefitting from the improved sensitivity provided by the other two developments, research has moved from ctDNA detection during metastasized disease (chapters 2, 3, and 4) towards analytically more challenging localized disease (chapter 5).

When these developments are extrapolated into the near future, it can be expected that the number of targets will increase further, that data analysis will grow more complex, and that research will focus on earlier detection of cancer (Figure 1). In practice, analysis procedures will likely develop towards whole genome sequencing (WGS), and even procedures that target a mix of multiple omic layers at once; e.g. genomics, methylomics, fragmentomics, transcriptomics, and/or proteomics (53,54). The vast amounts of data points this generates per patient will necessitate advanced data mining procedures, building upon advances in machine learning (ML) and increasingly affordable computational power, Together, these developments will facilitate detection of cancer in liquid biopsies of people who do not have symptoms: i.e. in (at risk) population screening and MRD settings.

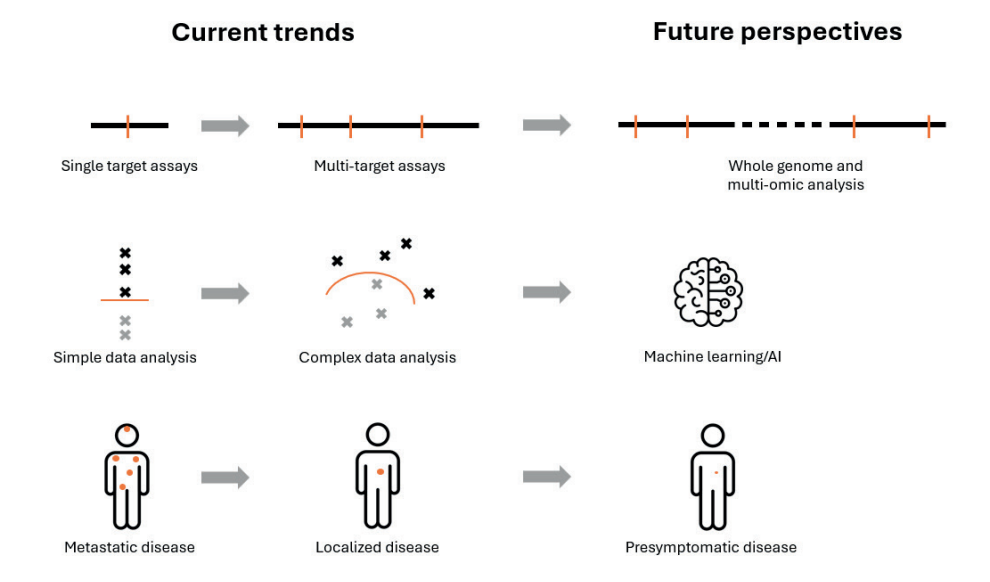


Figure 1. Current trends and future perspectives in cfDNA research. Assays have developed from single targets towards multiple targets, and are projected to expand towards whole genome and multi-omic analysis. Data analysis procedures have moved from straightforward to multi-parametric, and will likely be superseded by machine learning in the near future for many applications. Thirdly, this allows the detection of disease in increasingly early stages.

The costs of sequencing have gone down dramatically over the past two decades. The costs to perform a single WGS experiment have dropped from around \$10,000,000 in 2007 to less than \$1,000 in 2019, and today companies are claiming

technology that drives down the cost to \$100 or \$200 per WGS (55-57). Moreover, even while costs are decreasing, relevant cancer signals are detected from less data, with some single research studies claiming signal from as few as 200,000, 10,000, or even 1,000 reads per patient (58-60). If found to be reproducible, such advances could further drive down the costs per patient drastically. This would be promising especially for population screening programs, where many individuals need to be screened for every positive finding.

In the more distant future, there may come a time when raw sequencing data are fed to an algorithm, and a reproducible, reliable, and interpretable result is returned. Until that time, advances in data analysis will require a combination of advanced data mining techniques, and in-depth domain knowledge from molecular experts (61). ML enables the integration of different kinds of clinical and experimental features, including patient characteristics (e.g. age, pack years, BMI) and clinical care (e.g. protein biomarkers, CT scans, histopathology reports) (62). These could be supplemented with experimental results from various omic layers.

Increasingly, researchers are aiming to unravel multiple omic layers at once (49,54,63,64). Genomics, epigenomics, transcriptomics, and proteomics have all been thoroughly investigated in tumour tissue and have been transitioned to liquid biopsy with varying levels of success (65,66). Another omic layer unique to cfDNA analysis is fragmentomics, which investigates the highly specific DNA fragmentation patterning induced during cell apoptosis or necrosis (67).

When various omic layers are investigated simultaneously, the number of available data points per sample explodes. Conventional statistics fails to adequately resolve this so-called "curse of dimensionality", necessitating ML approaches to reduce the dimensionality of the dataset before an analysis is conducted (61). However, this has the disadvantage of discarding subtle yet potentially valuable effects in the dataset. As an alternative, researchers investigate deep learning models to interpret such high dimensional data, reasoning that if human language can be learned by these models, then why not the language of life. Thankfully, there is some experience with such approaches in tissue-based analysis, making good use of large and wellannotated datasets such as The Cancer Genome Atlas (TCGA) (68,69). These models are trained on vast amounts of paired multi-omics data and learn to represent this data in a way that insights can be unlocked from them.

Application of such models in the space of liquid biopsy is not straightforward, mostly due to compromising factors like exceedingly low tumour fractions. At the same time, there is also hope on the horizon in the form of the fragmentomics layer that is unique to cfDNA (67,70,71). Since the fragmentation of cfDNA is governed by multiple biological processes the fragmentomics layer can be regarded as the confluence of multiple omics layers (54,70,72).

The earliest applications of fragmentomics included investigations into its fragment length, like in chapter 5, and its fragment breakpoints motifs. These have been shown extensively to correlate with disease, both for the canonical short reads (<400 bp) and much longer cfDNA (58,70,73-81). What's intriguing from the viewpoint of developing multi-omic ML approaches is that consistent correlations have been shown between fragmentomics and other omic layers, like methylomics and transcriptomics. For example, fragmentation near methylated cytosines is different compared to unmethylated cytosines, allowing researchers to apply existing methylomics tools to fragmentomics data (70-72,82). Similarly, transcriptomics has been associated with aberrant fragmentomics profiles near gene promoters, transcription start sites, transcription factor binding sites, and on the gene bodies themselves (70,72,79,83-87). With its strong correlations to other omic layers, fragmentomics could in the future be exploited by advanced multiomic ML models to impute missing layers of omics data from liquid biopsies to enhance its predictive capabilities, thereby increasing its sensitivity.

Compared to methylomics and transcriptomics, fragmentomics is a relatively straightforward experimental layer. This is beneficial from a wetlab operations, experimental design, reproducibility, and data harmonisation perspective. However, it remains to be seen whether an indirect read-out of the methylomics and transcriptomics layers through the fragmentomics layer provides as much discriminatory power as the direct measurements.

What is especially promising about multi-omic ML is that recent research has shown that different models detect different cases, even when using the exact same input data (58,72). This suggests that the ability to detect cancer is not just dependent on factors like the sample's tumour fraction and each test's sensitivity. Instead, different cancers may exhibit some cancer-related patterns stronger than other patterns. It is tempting to hypothesize that a single cfDNA WGS experiment analysed through multiple "lenses" can yield higher sensitivity than any individual lens. Potentially, this could overcome barriers that have so far prevented widespread implementation of cfDNA-based cancer screening and MRD-detection programs (88).

As discussed, in many ways the developments in multi-omic ML continue the trends that are already visible in the works in this thesis (figure 1). Like this thesis, they aim to make more of the data that we have, helping to simultaneously improve the performance and decrease the cost of the tests. It is interesting to theorise how multi-omic ML might impact the clinical management of patients in the application domains of cfDNA as outlined in the Introduction (chapter 1). We observe that multiomic ML primarily aims to improve the sensitivity of the test by examining more data points. Second, it is not (yet) predictive but prognostic, as it only detects the presence or absence of cancer. Given this, multi-omic ML will likely first be applied in domains with low tumour fraction such as local disease, particularly MRD and pCR detection, and screening. Domains with higher tumour fraction and where treatment is often palliative rather than curative, such as metastatic disease and recurrence, will benefit less from multi-omic ML and instead rely more on predictive tests where sensitivity is not a key factor, like hotspot mutation detection assays (PCR or NGS).

A key drawback of (multi-omic) ML is that many models are black boxes, offering no insight into how a model reached a conclusion. It seems unlikely that physicians would be willing to administer or withhold therapy on the basis of a prediction from a ML model without further information. Explainable Al is a research field on its own that aims to provide insight from black box models.

For now, multi-omic ML is predominantly demonstrated in single-study results, and have a long way to go before they can be implemented in clinical practice. As previously seen with PCR-based hotspot mutation detection tests, an initial plethora of different methods is expected before a select few emerge that are most commonly applied (Figure 2).

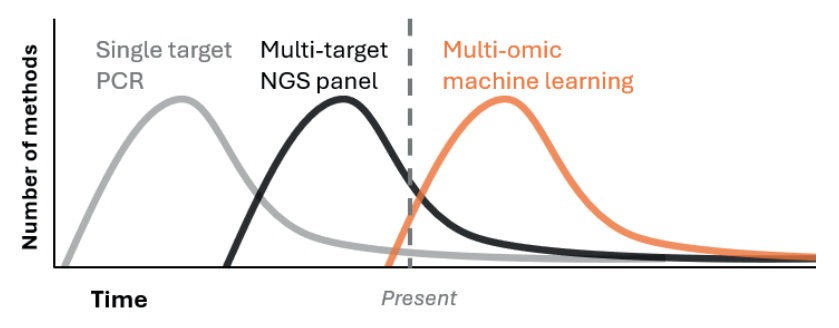


Figure 2. Schematic illustration of the past and expected future developments for the number of available tests in various categories. An initial abundance has been observed in the past for single target PCR tests and multi-target NGS panels, before a minority emerges that stands the test of time. A similar trend is predicted for multi-omic ML-based tests.

6.2.2 The road towards implementation

In a way, research and innovation can be considered forces that lead to a proliferation of new tests ("upward" in terms of the schematic in figure 2). Unrestricted proliferation is unhealthy, and there is a complementary "downward" force that vitally drives progress: Implementation (**Figure 3**). The rigorous process of implementation, when viewed in this way, is like a filter that streamlines the outgrowth of methods to a more sustainable minimum.

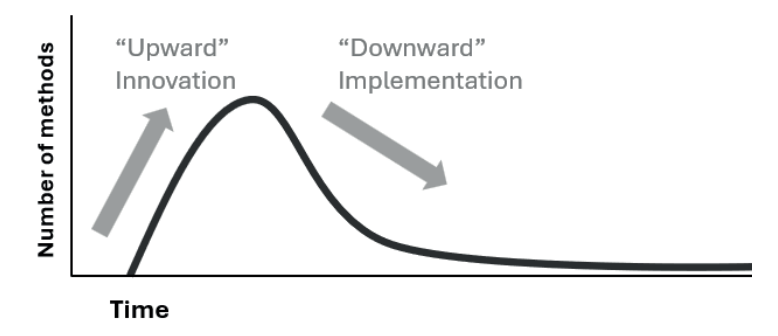


Figure 3. Schematic illustration of the driving forces behind diagnostic progress: Innovation and research lead to an "upward and forward" development, while implementation leads to a "downward and forward" motion.

For example, MRD testing (**chapter 5**) holds promising clinical prospects, but real impact is only made when a test is implemented in the clinic (89). There is a multitude of single study results using a diversity of methods, impeding straightforward comparison of results (36). Before they can be implemented, these methods must demonstrate among others clinical validity, utility, and cost-effectiveness, as well as approvals from relevant authorities and health insurance companies, and each method may fail along each step of the way. In the end, there will be a very limited number of tests remaining that are considered ready to implement.

Implementation, when viewed as the full trajectory from initial test development towards officially approved uptake in clinical care, is a long and arduous process. No diagnostic modality will be the 'holy grail' for cancer diagnostics; every form has advantages and disadvantages, so every test must be carefully selected and applied at the right place in the diagnostic path of a patient to have maximum impact. Additionally, the efforts to implement a test are often significantly greater than the efforts to develop it. To prove a test's clinical utility and validity often requires clinical studies of a significant size, as well as quality certifications, authority compliance and reimbursement programs.

Due to its more rigorous and extensive nature, implementation always lags behind innovation. Not every test can and should be implemented in routine clinical practice. To determine which tests stand a better chance of implementation down the line, there is interest in early health technology assessments (HTA). Such assessments, though inherently prone to uncertainties, offer valuable insights into whether it is worth further developing an expensive diagnostic test when the expected clinical gains are marginal. This is another reason why researchers are increasingly trying to make more of the data we have, in line with this thesis.

In practice even the process of implementation is not well-defined. Significant additional efforts will be required to introduce a standardised route towards implementation, such as defining the steps towards implementation, and the required body of evidence. International consortia like the European Liquid Biopsy Society (ELBS) and the International Liquid Biopsy Standardisation Alliance (ILSA) aim to coordinate and standardise liquid biopsy efforts (90,91). In the Netherlands, a roadmap towards implementation is sketched by the ctDNA on the road to implementation in the Netherlands (COIN) consortium. COIN aims to "bring ctDNA applications from uncoordinated anecdotal observations to evidence-based implementation in the Dutch healthcare system" (92). Such collectives may help ensure that the promising status of ctDNA analysis can be valorised, by providing a framework in which the ctDNA analyses can be implemented in routine clinical care.

Accordingly, in the Netherlands, the Committee for the Evaluation of Diagnostics, abbreviated as cieBOD, was initiated in 2021. The goal of the cieBOD is to "come to a better coordination between diagnosticians and treating physicians on the implementation of diagnostic and predictive tests" (28). In 2024, the cieBOD issued its first official ctDNA-related advice, relating to the use of ctDNA in the context of mNSCLC (29). This marks a significant milestone in the route towards integration of ctDNA-based diagnostics in Dutch healthcare.

6.3 Conclusions

In conclusion, the field of cfDNA testing has been on the move. In this thesis, we have sought to optimise cfDNA analysis methods for solid malignancies, with a focus on making more of the data we have. In chapter 2 we showed that specificity of ddPCR results was improved by a novel algorithm termed ALPACA. ALPACA employs a dynamic limit of blank and an in-silico correction of false positive droplets. In chapter 3 we compared four hotspot mutation detection platforms, and concluded that the choice of platform depends on the clinical application like throughput times, cost, and desired sensitivity. In **chapter 4** we applied a commercial NGS panel for treatment selection in mNSCLC, concluding that inclusion of plasma-CMP next to protocolised SoC-TMP led to a significant increase in the number of patients for whom a targeted treatment would be available. In **chapter 5** we applied a broader NGS panel to detect MRD in patients with limited stage NSCLC. We concluded that combining mutation detection and fragmentomics led to a significant distinction between patients at high or low risk of disease recurrence. Lastly, in **chapter 6**, we summarised our findings and put them in a broader perspective and explored the future perspectives of cfDNA testing. We envision a two-way focus in the near future: First, on new innovations to further improve sensitivity, and second, on rigorous implementation to consolidate the substantial research that has been performed to date. We conclude that innovation and implementation are two partially opposing forces that are both vitally important for progress.

References

- Huggett JF, Devonshire AS, Whale AS, Cowen S, Foy CA. Pushing the Envelope with Clinical Use of Digital PCR. Clin Chem. 2021 Jul 6;67(7):921-3.
- Henriksen TV, Drue SO, Frydendahl A, Demuth C, Rasmussen MH, Reinert T, et al. Error 2. Characterization and Statistical Modeling Improves Circulating Tumor DNA Detection by Droplet Digital PCR. Clin Chem. 2022 May 18;68(5):657-67.
- Bio-Rad Laboratories Inc. Droplet digital PCR applications guide (bulletin 6407 ver B) [Internet]. 2020. Available from: https://www.bio-rad.com/webroot/web/pdf/lsr/literature/Bulletin_6407. pdf
- Bio-Rad Laboratories Inc. Rare mutation detection best practices guidelines (bulletin 6628) [Internet]. 2020. Available from: https://www.bio-rad.com/webroot/web/pdf/lsr/literature/ Bulletin_6628.pdf
- Arnolda R, Howlett K, Chan T, Raleigh J, Hatzimihalis A, Bell A, et al. Clinical validation and implementation of droplet digital PCR for the detection of BRAF mutations from cell-free DNA. Pathology (Phila). 2022 Oct;54(6):772-8.
- The dMIQE Group, Whale AS, De Spiegelaere W, Trypsteen W, Nour AA, Bae YK, et al. The Digital MIQE Guidelines Update: Minimum Information for Publication of Quantitative Digital PCR Experiments for 2020. Clin Chem. 2020 Aug 1;66(8):1012-29.
- 7. Garcia J, Forestier J, Dusserre E, Wozny AS, Geiguer F, Merle P, et al. Cross-platform comparison for the detection of RAS mutations in cfDNA (ddPCR Biorad detection assay, BEAMing assay, and NGS strategy). Oncotarget. 2018 Apr 20;9(30):21122-31.
- Vivancos A, Aranda E, Benavides M, Élez E, Gómez-España MA, Toledano M, et al. Comparison of the Clinical Sensitivity of the Idylla Platform and the OncoBEAM RAS CRC Assay for KRAS Mutation Detection in Liquid Biopsy Samples. Sci Rep. 2019 Jun 20;9(1):8976.
- Thress KS, Brant R, Carr TH, Dearden S, Jenkins S, Brown H, et al. EGFR mutation detection in ctDNA from NSCLC patient plasma: A cross-platform comparison of leading technologies to support the clinical development of AZD9291. Lung Cancer. 2015 Dec;90(3):509-15.
- 10. Wang W, Song Z, Zhang Y. A Comparison of ddPCR and ARMS for detecting EGFR T790M status in ctDNA from advanced NSCLC patients with acquired EGFR-TKI resistance. Cancer Med. 2017 Jan;6(1):154-62.
- 11. Lievens Y, Van Den Bogaert W, Kesteloot K. Activity-based costing: a practical model for cost calculation in radiotherapy. Int J Radiat Oncol. 2003 Oct;57(2):522-35.
- 12. Novello S, Barlesi F, Califano R, Cufer T, Ekman S, Levra MG, et al. Metastatic non-small-cell lung cancer: ESMO Clinical Practice Guidelines for diagnosis, treatment and follow-up. Ann Oncol. 2016 Sep;27:v1-27.
- 13. Planchard D, Popat S, Kerr K, Novello S, Smit EF, Faivre-Finn C, et al. Metastatic non-small cell lung cancer: ESMO Clinical Practice Guidelines for diagnosis, treatment and follow-up. Ann Oncol. 2018 Oct;29:iv192-237.
- 14. Integraal Kankercentrum Nederland I. Landelijke richtlijn niet kleincellig longcarcinoom. [Internet]. Available from: https://iknl.nl/nkr/evaluatie-met-nkr-data/richtlijnen
- 15. NVALT. KNT-lijst NSCLC versie 2 2024-01-08 [Internet]. [cited 2024 Aug 8]. Available from: https:// www.nvalt.nl/vereniging/beleid/belangrijke-documenten/_/Klinische%20Noodzakelijke%20 Targets/KNT-lijst%20NSCLC%20versie%202%202024-01-08.pdf

- Roche Sequencing Solutions. AVENIO ctDNA Targeted Kit. [Internet]. Available from: https://sequencing.roche.com/content/dam/rochesequence/worldwide/resources/brochure-avenio-ctdna-targeted-kit-SEQ100046.pdf
- The Netherlands Cancer Institute. clinicaltrials.gov identifier NCT02894853 [Internet]. U.S. National Library of Medicine, ClinicalTrials.gov; 2016 [cited 2024 Apr 26]. Available from: https://classic.clinicaltrials.gov/ct2/show/NCT02894853
- Schouten RD, Schouten I, Schuurbiers MMF, Van Der Noort V, Damhuis RAM, Van Der Heijden EHFM, et al. Optimising primary molecular profiling in NSCLC [Internet]. 2023 [cited 2024 Apr 26]. Available from: http://medrxiv.org/lookup/doi/10.1101/2023.08.20.23294346
- 19. Aggarwal C, Thompson JC, Black TA, Katz SI, Fan R, Yee SS, et al. Clinical Implications of Plasma-Based Genotyping With the Delivery of Personalized Therapy in Metastatic Non–Small Cell Lung Cancer. JAMA Oncol. 2019 Feb 1;5(2):173.
- Leighl NB, Page RD, Raymond VM, Daniel DB, Divers SG, Reckamp KL, et al. Clinical Utility of Comprehensive Cell-free DNA Analysis to Identify Genomic Biomarkers in Patients with Newly Diagnosed Metastatic Non–small Cell Lung Cancer. Clin Cancer Res. 2019 Aug 1;25(15):4691–700.
- 21. Mack PC, Banks KC, Espenschied CR, Burich RA, Zill OA, Lee CE, et al. Spectrum of driver mutations and clinical impact of circulating tumor DNA analysis in non–small cell lung cancer: Analysis of over 8000 cases. Cancer. 2020 Jul 15;126(14):3219–28.
- 22. Rangachari D, VanderLaan PA, Le X, Folch E, Kent MS, Gangadharan SP, et al. Experience with targeted next generation sequencing for the care of lung cancer: Insights into promises and limitations of genomic oncology in day-to-day practice. Cancer Treat Commun. 2015;4:174–81.
- 23. Lim C, Tsao MS, Le LW, Shepherd FA, Feld R, Burkes RL, et al. Biomarker testing and time to treatment decision in patients with advanced nonsmall-cell lung cancer. Ann Oncol. 2015 Jul;26(7):1415–21.
- 24. Kuijpers C, Heuvel M, Overbeek L, van Slooten HJ, Lindert A, Damhuis R, et al. National variation in molecular diagnostics in metastatic lung cancer. Ned Tijdschr Geneeskd. 2018 Dec;162.
- 25. Gilson P, Merlin JL, Harlé A. Deciphering Tumour Heterogeneity: From Tissue to Liquid Biopsy. Cancers. 2022 Mar 8;14(6):1384.
- Koole SN, Vessies DCL, Schuurbiers MMF, Kramer A, Schouten RD, Degeling K, et al. Cell-Free DNA at Diagnosis for Stage IV Non-Small Cell Lung Cancer: Costs, Time to Diagnosis and Clinical Relevance. Cancers. 2022 Mar 31;14(7):1783.
- 27. Englmeier F, Bleckmann A, Brückl W, Griesinger F, Fleitz A, Nagels K. Clinical benefit and cost-effectiveness analysis of liquid biopsy application in patients with advanced non-small cell lung cancer (NSCLC): a modelling approach. J Cancer Res Clin Oncol. 2023 Apr;149(4):1495–511.
- 28. NVVP. Commissie ter BeOordeling Diagnostiek (cieBOD) [Internet]. [cited 2024 Aug 1]. Available from: https://pathologie.nl/ciebod/
- cieBOD. CieBOD advies ctDNA in bloedplasma voor primaire predictieve analyse bij NSCLC [Internet]. 2024 [cited 2024 Aug 1]. Available from: https://pathologie.nl/wp-content/ uploads/2024/07/CieBOD-advies-ctDNA-bij-NSCLC-versie-1-12062024-voor-publicatie.pdf
- Rajaram R, Huang Q, Li RZ, Chandran U, Zhang Y, Amos TB, et al. Recurrence-Free Survival in Patients With Surgically Resected Non-Small Cell Lung Cancer. CHEST. 2024 May;165(5):1260–70.
- 31. Pignon JP, Tribodet H, Scagliotti GV, Douillard JY, Shepherd FA, Stephens RJ, et al. Lung Adjuvant Cisplatin Evaluation: A Pooled Analysis by the LACE Collaborative Group. J Clin Oncol. 2008 Jul 20;26(21):3552–9.
- 32. Pirker R. Adjuvant chemotherapy in patients with completely resected non-small cell lung cancer. Transl Lung Cancer Res. 2014 Oct;3(5):305–10.

- 33. Roche Seguencing Solutions. AVENIO ctDNA Surveillance Kit [Internet]. Available from: https:// sequencing.roche.com/content/dam/rochesequence/worldwide/resources/brochure-avenioctdna-surveillance-kit-SEQ100046.pdf
- 34. Schuurbiers M, Smith CG, Hartemink K, Rintoul R, Monkhorst K, Van Den Broek D, et al. Validation of recurrence prediction using circulating tumor DNA in patients with curatively treated early stage non-small cell lung cancer. J Clin Oncol. 2023 Jun 1;41(16_suppl):8535-8535.
- 35. Peng Y, Mei W, Ma K, Zeng C. Circulating Tumor DNA and Minimal Residual Disease (MRD) in Solid Tumors: Current Horizons and Future Perspectives. Front Oncol. 2021 Nov 18;11:763790.
- 36. Faulkner LG, Howells LM, Pepper C, Shaw JA, Thomas AL. The utility of ctDNA in detecting minimal residual disease following curative surgery in colorectal cancer: a systematic review and meta-analysis. Br J Cancer. 2023 Jan 19;128(2):297-309.
- 37. Zheng J, Qin C, Wang Q, Tian D, Chen Z. Circulating tumour DNA-Based molecular residual disease detection in resectable cancers: a systematic review and meta-analysis. eBioMedicine. 2024 May;103:105109.
- 38. Kurtz DM, Soo J, Co Ting Keh L, Alig S, Chabon JJ, Sworder BJ, et al. Enhanced detection of minimal residual disease by targeted sequencing of phased variants in circulating tumor DNA. Nat Biotechnol. 2021 Dec;39(12):1537-47.
- 39. Parsons HA, Blewett T, Chu X, Sridhar S, Santos K, Xiong K, et al. Circulating tumor DNA association with residual cancer burden after neoadjuvant chemotherapy in triple-negative breast cancer in TBCRC 030. Ann Oncol. 2023 Oct;34(10):899-906.
- 40. Haystack Oncology. Haystack Oncology website [Internet]. [cited 2024 Apr 26]. Available from: https://haystackmrd.com/biopharma/
- 41. Flach S, Howarth K, Hackinger S, Pipinikas C, Ellis P, McLay K, et al. Liquid BlOpsy for MiNimal RESidual DiSease Detection in Head and Neck Squamous Cell Carcinoma (LIONESS)—a personalised circulating tumour DNA analysis in head and neck squamous cell carcinoma. Br J Cancer. 2022 May 3;126(8):1186-95.
- 42. Zviran A, Schulman RC, Shah M, Hill STK, Deochand S, Khamnei CC, et al. Genome-wide cellfree DNA mutational integration enables ultra-sensitive cancer monitoring. Nat Med. 2020 Jul;26(7):1114-24.
- 43. Widman AJ, Shah M, Øgaard N, Khamnei CC, Frydendahl A, Deshpande A, et al. Machine learning quided signal enrichment for ultrasensitive plasma tumor burden monitoring [Internet]. 2022 [cited 2024 Apr 26]. Available from: http://biorxiv.org/lookup/doi/10.1101/2022.01.17.476508
- 44. Spicer JD, Garassino MC, Wakelee H, Liberman M, Kato T, Tsuboi M, et al. Neoadjuvant pembrolizumab plus chemotherapy followed by adjuvant pembrolizumab compared with neoadjuvant chemotherapy alone in patients with early-stage non-small-cell lung cancer (KEYNOTE-671): a randomised, double-blind, placebo-controlled, phase 3 trial. The Lancet. 2024 Sep;404(10459):1240-52.
- 45. Wakelee HA, Altorki NK, Zhou C, Csőszi T, Vynnychenko IO, Goloborodko O, et al. IMpower010: Primary results of a phase III global study of atezolizumab versus best supportive care after adjuvant chemotherapy in resected stage IB-IIIA non-small cell lung cancer (NSCLC). J Clin Oncol. 2021 May 20;39(15_suppl):8500-8500.
- 46. Spigel DR, Faivre-Finn C, Gray JE, Vicente D, Planchard D, Paz-Ares L, et al. Five-Year Survival Outcomes From the PACIFIC Trial: Durvalumab After Chemoradiotherapy in Stage III Non-Small-Cell Lung Cancer. J Clin Oncol. 2022 Apr 20;40(12):1301–11.
- 47. Banna GL, Hassan MA, Signori A, Giunta EF, Maniam A, Anpalakhan S, et al. Neoadjuvant Chemo-Immunotherapy for Early-Stage Non-Small Cell Lung Cancer: A Systematic Review and Meta-Analysis. JAMA Netw Open. 2024 Apr 16;7(4):e246837.

- 48. Forde PM, Spicer J, Lu S, Provencio M, Mitsudomi T, Awad MM, et al. Neoadjuvant Nivolumab plus Chemotherapy in Resectable Lung Cancer. N Engl J Med. 2022 May 26;386(21):1973–85.
- 49. Li Y, Jiang G, Wu W, Yang H, Jin Y, Wu M, et al. Multi-omics integrated circulating cell-free DNA genomic signatures enhanced the diagnostic performance of early-stage lung cancer and postoperative minimal residual disease. eBioMedicine. 2023 May;91:104553.
- 50. Pappas L, Adalsteinsson VA, Parikh AR. The emerging promise of liquid biopsies in solid tumors. Nat Cancer. 2022 Dec 20;3(12):1420–2.
- 51. Reina C, Šabanović B, Lazzari C, Gregorc V, Heeschen C. Unlocking the future of cancer diagnosis promises and challenges of ctDNA-based liquid biopsies in non-small cell lung cancer. Transl Res. 2024 Oct;272:41–53.
- 52. Pando-Caciano A, Trivedi R, Pauwels J, Nowakowska J, Cavina B, Falkman L, et al. Unlocking the promise of liquid biopsies in precision oncology. J Liq Biopsy. 2024 Mar;3:100151.
- 53. Rolfo C, Russo A, Malapelle U. The next frontier of early lung cancer and minimal residual disease detection: is multiomics the solution? eBioMedicine. 2023 Jun;92:104605.
- 54. Tivey A, Lee RJ, Clipson A, Hill SM, Lorigan P, Rothwell DG, et al. Mining nucleic acid "omics" to boost liquid biopsy in cancer. Cell Rep Med. 2024 Sep;5(9):101736.
- 55. Illumina. NovaSeq 6000 Sequencing System [Internet]. [cited 2024 Jun 6]. Available from: https://www.illumina.com/systems/sequencing-platforms/novaseq.html
- Ultima Genomics. Ultima Genomics website [Internet]. [cited 2024 Jun 6]. Available from: https:// www.ultimagenomics.com/
- 57. National Human Genome Research Institute, Wetterstrand KA. The Cost of Sequencing a Human Genome [Internet]. [cited 2024 Jun 6]. Available from: https://www.genome.gov/about-genomics/fact-sheets/Sequencing-Human-Genome-cost
- 58. Vessies D, Bucho T, Post E, Roohollahi K, Van Den Berg J, Foster A, et al. 1174P FLAMINGO: Accurate cancer detection from ultra-low-pass whole genome sequencing of cell-free DNA. Ann Oncol. 2024 Sep;35:S763.
- 59. Shen H, Liu J, Chen K, Li X. Language model enables end-to-end accurate detection of cancer from cell-free DNA. Brief Bioinform. 2024 Jan 22;25(2):bbae053.
- Liu J, Shen H, Hu J, Shen X, Zhang C, Yang Y, et al. A deep learning approach for cancer diagnosis exclusively from raw sequencing fragments of bisulfite-treated plasma cellfree DNA [Internet]. 2023 [cited 2024 Jul 25]. Available from: http://medrxiv.org/lookup/ doi/10.1101/2023.08.08.23293813
- 61. Moser T, Kühberger S, Lazzeri I, Vlachos G, Heitzer E. Bridging biological cfDNA features and machine learning approaches. Trends Genet. 2023 Apr;39(4):285–307.
- 62. Spratt DE, Liu VYT, Jia AY, Royce TJ, Sandler HM, Pugh SL, et al. Meta-analysis of Individual Patient-level Data for a Multimodal Artificial Intelligence Biomarker in High-risk Prostate Cancer: Results from Six NRG/RTOG Phase 3 Randomized Trials. Eur Urol. 2024 Oct;86(4):369–71.
- 63. Nguyen TCVV, Nguyen AN, Nguyen TPH, Nguyen HTH, Tran TH, Nguyen TA, et al. A novel cell-free multi-omics approach for enhancing multi-cancer early detection. J Clin Oncol. 2024 Aug 10;42(23_suppl):103–103.
- 64. Campos-Carrillo A, Weitzel JN, Sahoo P, Rockne R, Mokhnatkin JV, Murtaza M, et al. Circulating tumor DNA as an early cancer detection tool. Pharmacol Ther. 2020 Mar;207:107458.
- 65. Ding Z, Wang N, Ji N, Chen ZS. Proteomics technologies for cancer liquid biopsies. Mol Cancer. 2022 Feb 15;21(1):53.

- 66. In 't Veld SGJG, Arkani M, Post E, Antunes-Ferreira M, D'Ambrosi S, Vessies DCL, et al. Detection and localization of early- and late-stage cancers using platelet RNA. Cancer Cell. 2022 Sep;40(9):999-1009.e6.
- 67. Chiu RWK, Heitzer E, Lo YMD, Mouliere F, Tsui DWY. Cell-Free DNA Fragmentomics: The New "Omics" on the Block. Clin Chem. 2020 Dec 1;66(12):1480-4.
- 68. Wang F ao, Zhuang Z, Gao F, He R, Zhang S, Wang L, et al. TMO-Net: an explainable pretrained multi-omics model for multi-task learning in oncology. Genome Biol. 2024 Jun 6;25(1):149.
- 69. Sokač M, Kjær A, Dyrskjøt L, Haibe-Kains B, Jwl Aerts H, Birkbak NJ. Spatial transformation of multi-omics data unlocks novel insights into cancer biology, eLife, 2023 Sep 5;12:RP87133.
- 70. Che H, Jiang P, Choy LYL, Cheng SH, Peng W, Chan RWY, et al. Genomic origin, fragmentomics, and transcriptional properties of long cell-free DNA molecules in human plasma. Genome Res. 2024 Feb;34(2):189-200.
- 71. Zhou Q, Kang G, Jiang P, Qiao R, Lam WKJ, Yu SCY, et al. Epigenetic analysis of cell-free DNA by fragmentomic profiling. Proc Natl Acad Sci. 2022 Nov;119(44):e2209852119.
- 72. Noë M, Mathios D, Annapragada AV, Koul S, Foda ZH, Medina JE, et al. DNA methylation and gene expression as determinants of genome-wide cell-free DNA fragmentation. Nat Commun. 2024 Aug 6;15(1):6690.
- 73. Berman BP, Erdman SA, Turatsinze JV, Cayford J, Kelly TK. Long-read seguencing reveals aberrant fragmentation patterns and origins of circulating DNA in cancer [Internet], 2024 [cited 2024 Sep 5]. Available from: http://biorxiv.org/lookup/doi/10.1101/2024.05.02.592182
- 74. Choy LYL, Peng W, Jiang P, Cheng SH, Yu SCY, Shang H, et al. Single-Molecule Seguencing Enables Long Cell-Free DNA Detection and Direct Methylation Analysis for Cancer Patients. Clin Chem. 2022 Sep 1;68(9):1151-63.
- 75. Cristiano S, Leal A, Phallen J, Fiksel J, Adleff V, Bruhm DC, et al. Genome-wide cell-free DNA fragmentation in patients with cancer. Nature. 2019 Jun;570(7761):385-9.
- 76. Mathios D, Johansen JS, Cristiano S, Medina JE, Phallen J, Larsen KR, et al. Detection and characterization of lung cancer using cell-free DNA fragmentomes. Nat Commun. 2021 Aug 20;12(1):5060.
- 77. Mazzone PJ, Bach PB, Carey J, Schonewolf CA, Bognar K, Ahluwalia MS, et al. Clinical validation of a cell-free DNA fragmentome assay for augmentation of lung cancer early detection. Cancer Discov [Internet]. 2024 Jun 3 [cited 2024 Jun 6]; Available from: https://aacrjournals.org/ cancerdiscovery/article/doi/10.1158/2159-8290.CD-24-0519/745696/Clinical-validation-of-acell-free-DNA-fragmentome
- 78. Peneder P, Stütz AM, Surdez D, Krumbholz M, Semper S, Chicard M, et al. Multimodal analysis of cell-free DNA whole-genome sequencing for pediatric cancers with low mutational burden. Nat Commun. 2021 May 28;12(1):3230.
- 79. Maansson CT, Thomsen LS, Meldgaard P, Nielsen AL, Sorensen BS. Integration of Cell-Free DNA End Motifs and Fragment Lengths Can Identify Active Genes in Liquid Biopsies. Int J Mol Sci. 2024 Jan 19;25(2):1243.
- 80. Markus H, Chandrananda D, Moore E, Mouliere F, Morris J, Brenton JD, et al. Refined characterization of circulating tumor DNA through biological feature integration. Sci Rep. 2022 Feb 4:12(1):1928.
- 81. Linthorst J, Nivard M, Sistermans EA. GWAS shows the genetics behind cell-free DNA and highlights the importance of p.Arg206Cys in DNASE1L3 for non-invasive testing. Cell Rep. 2024 Oct;43(10):114799.

- 82. Liu Y, Reed SC, Lo C, Choudhury AD, Parsons HA, Stover DG, et al. FinaleMe: Predicting DNA methylation by the fragmentation patterns of plasma cell-free DNA. Nat Commun. 2024 Mar 30:15(1):2790.
- 83. Esfahani MS, Hamilton EG, Mehrmohamadi M, Nabet BY, Alig SK, King DA, et al. Inferring gene expression from cell-free DNA fragmentation profiles. Nat Biotechnol. 2022 Apr;40(4):585–97.
- 84. Wan N, Weinberg D, Liu TY, Niehaus K, Ariazi EA, Delubac D, et al. Machine learning enables detection of early-stage colorectal cancer by whole-genome sequencing of plasma cell-free DNA. BMC Cancer. 2019 Dec;19(1):832.
- 85. Snyder MW, Kircher M, Hill AJ, Daza RM, Shendure J. Cell-free DNA Comprises an In Vivo Nucleosome Footprint that Informs Its Tissues-Of-Origin. Cell. 2016 Jan;164(1–2):57–68.
- 86. Sun K, Jiang P, Cheng SH, Cheng THT, Wong J, Wong VWS, et al. Orientation-aware plasma cell-free DNA fragmentation analysis in open chromatin regions informs tissue of origin. Genome Res. 2019 Mar;29(3):418–27.
- 87. Stanley KE, Jatsenko T, Tuveri S, Sudhakaran D, Lannoo L, Van Calsteren K, et al. Cell type signatures in cell-free DNA fragmentation profiles reveal disease biology. Nat Commun. 2024 Mar 12;15(1):2220.
- 88. Turning the tide of early cancer detection. Nat Med. 2024 May;30(5):1217–1217.
- 89. Chae YK, Oh MS. Detection of Minimal Residual Disease Using ctDNA in Lung Cancer: Current Evidence and Future Directions. J Thorac Oncol. 2019 Jan;14(1):16–24.
- ELBS. European Liquid Biopsy Society (ELBS) website [Internet]. [cited 2024 Jun 13]. Available from: https://www.uke.de/english/departments-institutes/institutes/tumor-biology/european-liquid-biopsy-society-elbs/index.html
- 91. ILSA. International Liquid Biopsy Standardization Alliance (ILSA) website [Internet]. [cited 2024 Jun 13]. Available from: https://fnih.org/our-programs/international-liquid-biopsy-standardization-alliance-ilsa/
- 92. COIN consortium. ctDNA on the road to implementation in The Netherlands COIN website [Internet]. [cited 2024 Jun 13]. Available from: https://cfdna.nl/coin-home-english/



Chapter 7

Appendices

- Nederlandse samenvatting
- research data management
- list of publications
- PhD portfolio
- curriculum vitae
- dankwoord

Nederlandse samenvatting

De gangbare aanpak voor diagnostiek bij solide tumoren is gebaseerd op weefselbiopten, die inzicht bieden in cruciale cellulaire veranderingen die therapeutische beslissingen sturen. Echter, de nadelen van weefselbiopten, zoals de invasiviteit, gevoeligheid voor bemonsteringsfouten en het onvermogen om realtime tumorontwikkeling vast te leggen, maken het noodzakelijk om alternatieve methodologieën te onderzoeken. Liquid biopsies, een opkomend paradigma in de oncologie, bieden een minimaal invasieve oplossing voor verschillende uitdagingen die gepaard gaan met weefselbiopten. Onder de verschillende vormen van liquid biopsies is het onderzoek naar circulerend tumor-DNA (ctDNA) een belangrijk speerpunt geworden.

Het dynamische veld van ctDNA wordt gekenmerkt door voortdurende en snelle ontwikkelingen, en biedt mogelijkheden voor significante vooruitgang in kankerdiagnostiek en monitoring. De klinische implementatie van ctDNA-testen wordt echter onder andere belemmerd door de beperkte sensitiviteit en specificiteit van deze testen. Deze uitdagingen vloeien voort uit een combinatie van biologische en technische factoren die inherent zijn aan de testen. Dit proefschrift heeft als doel deze uitdagingen aan te pakken door verbeterd datagebruik en het voorstellen van methodologische verbeteringen.

Hoofdstuk 2 - Verbetering van standaard ddPCR-analyse: ALPACA

Elke methode produceert inherent vals positieve en vals negatieve resultaten. Dergelijke foutieve resultaten kunnen een ernstig probleem vormen en resulteren in suboptimale of ineffectieve behandelingen. Tegelijkertijd is standaardisatie van methoden en resultaten essentieel in de klinische zorg. In Hoofdstuk 2 hebben we de prestaties van een van de eerste werkpaarden van ctDNA-analyse, droplet digital PCR (ddPCR), onder de loep genomen. We toonden aan dat valspositieve signalen (Polymerase-Induced False positives, PIFs) worden veroorzaakt door de Taq-polymerase. We observeerden een scheve verdeling van FAM&HEX-positieve versus alleen FAM-positieve druppels, die niet verklaard kon worden door andere biologische of technische factoren. De PIFs verschenen in een waaiervormig patroon en konden achteraf worden herkend als een overmaat aan FAM&HEX-positieve druppels ten opzichte van de FAM- en HEX-positieve druppels afzonderlijk. Hiervoor ontwikkelden we een in silico correctie-algoritme dat overtollige FAM&HEX-positieve druppels classificeert als vals-positief.

Vervolgens toonden we aan dat, zelfs na het verwijderen van de PIFs, er nog steeds vals-positieve druppels aanwezig waren in experimenten met uitsluitend wildtype DNA. Het aantal vals-positieve druppels correleerde met de totale hoeveelheid ingebracht wildtype DNA en verschilde per gebruikte assay. Op basis van deze observaties ontwikkelden we een assay- en inputafhankelijke adaptieve drempelwaarde om positieve en negatieve monsters te onderscheiden.

Samen zijn de PIF-correctie en adaptieve drempelwaarde openbaar beschikbaar gemaakt als de 'Adaptive Limit of blank and PIF Correction, an Automated Correction Algorithm' (ALPACA). We toonden aan dat ALPACA een superieure specificiteit (minder vals-positieven) had zonder verlies van sensitiviteit, getest met synthetisch referentiemateriaal, cfDNA van gezonde donoren en een patiëntencohort met gemetastaseerd NSCLC (n=203). De totale nauwkeurigheid in dit cohort steeg van 92% naar 98%. Opvallend was dat de positief voorspellende waarde (PPV) steeg van slechts 56% met de standaardprocedure naar 92% met ALPACA. Met andere woorden: bij de standaardprocedure was 44% van alle ddPCR-positieve resultaten in dit cohort vals-positief en hadden deze kunnen leiden tot foutieve behandeling van patiënten die hier geen baat bij zouden hebben.

Hoofdstuk 3 - Evaluatie van ctDNA-detectietechnologieën

Niet alleen de validatie van een enkele methode is belangrijk, maar ook kennis over verschillen tussen methoden is klinisch relevant. Naast ddPCR zijn er meer technologieën beschikbaar gekomen voor de detectie van hotspotpuntmutaties in ctDNA. Al deze methoden claimen een bepaalde sensitiviteit en specificiteit. Het vergelijken van deze cijfers is echter lastig omdat veel factoren die van invloed zijn op sensitiviteit en specificiteit niet geharmoniseerd zijn over verschillende platforms. Hierdoor kunnen waargenomen verschillen in sensitiviteit voortkomen uit meerdere factoren, waaronder daadwerkelijke prestatievoordelen, het gebruik van meer input-cfDNA, de isolatiemethode, analysemethoden en het aantal mutaties dat bepaald kan worden. Bovendien verschillen de kosten aanzienlijk tussen methoden, wat extra uitdagingen met zich meebrengt voor ziekenhuizen om een geschikte methode te kiezen voor specifieke klinische toepassingen. Met zoveel variabelen die de uiteindelijke resultaten en prestaties van een methode beïnvloeden, is een eerlijke en nauwkeurige vergelijking tussen methoden praktisch onmogelijk. Dit belemmert een objectieve vergelijking van prestaties, beperkt de stimulans voor diagnostische laboratoria om de juiste methode te kiezen en remt harmonisatie van resultaten.

In dit kader hebben we in Hoofdstuk 3 vier commercieel beschikbare ctDNA-detectiemethoden vergeleken: ddPCR, COBAS z480, Idylla en BEAMing. Tijdens de voorbereidingen van deze studie werd duidelijk dat een eenvoudige strategie waarbij dezelfde monsters op elk platform worden geanalyseerd, ons niet in staat zou stellen om vast te stellen of waargenomen verschillen werden veroorzaakt door de hoeveelheid input-plasma, de isolatiemethode, analysemethode of tumorfractie van het monster. Om de impact van deze variabelen te onderzoeken, hebben we het onderzoek zodanig ontworpen dat verschillen tussen de methoden die het eindresultaat zouden kunnen beïnvloeden, systematisch werden geëlimineerd. Deze studie toonde de complexiteit aan van een eerlijke methodevergelijking in ctDNA-analyses.

Na eliminatie van storende factoren observeerden we dat de twee digitale platforms – ddPCR en BEAMing – gevoeliger waren dan de op qPCR gebaseerde platforms Idylla en COBAS z480. Dit sluit aan bij eerdere studies die een meer eenvoudige vergelijking van deze en soortgelijke methoden hebben uitgevoerd. Naast sensitiviteit onderzochten we ook de impact van het aantal bepaalde mutaties van elke methode. Niet alle platforms richten zich op hetzelfde aantal puntmutaties, maar we vonden dat het aantal bepaalde mutaties een minimale invloed had op het verwachte aantal gedetecteerde mutaties in een cohort van gemetastaseerde CRC-patiënten.

Een factor die de prestatie van een platform niet beïnvloedt, maar wel een belangrijke rol speelt bij ziekenhuisbeslissingen om een platform te gebruiken, zijn de kosten. Met behulp van een activiteit-gebaseerde kostenberekeningsmethode ontdekten we dat de totale kosten het hoogst waren voor BEAMing vanwege hoge vaste en verbruiksafhankelijke kosten. Daarentegen was tot een doorvoer van 110 monsters per jaar (2 monsters per week) ldylla het minst dure platform vanwege lage vaste kosten. Bij een hogere doorvoer was ddPCR goedkoper vanwege lagere verbruiksafhankelijke kosten. Deze inzichten kunnen ziekenhuizen helpen bij het maken van een geïnformeerde keuze tussen verschillende methoden.

Inzicht in de toegepaste technologie en een uitgebreide validatie zijn beide essentiële criteria om vertrouwen te genereren in de output van het platform. Veel factoren beïnvloeden de analyse van ctDNA, wat kan leiden tot een impact op de klinische praktijk. Het toepassen van de juiste methode voor een specifieke klinische situatie is een uitdaging, en het falen hierin kan bijvoorbeeld resulteren in vals-negatieve resultaten wanneer een te ongevoelige techniek wordt toegepast in een klinische situatie die een hoge gevoeligheid vereist.

Hoofdstuk 4 - Klinische impact van NGS-analyse van ctDNA

Patiënten met primair gemetastaseerd niet-kleincellig longcarcinoom (mNSCLC) kunnen in aanmerking komen voor verschillende Tyrosine Kinase Inhibitor (TKI)behandelingen, mits de tumor wordt aangedreven door specifieke activerende mutaties. Om deze reden schrijven nationale en internationale richtlijnen voor dat moleculaire profilering van tumor-DNA zich moet richten op bekende NSCLConcogenen zoals EGFR, KRAS, BRAF, ERBB2, ALK, ROS1, RET en MET.

Detectie van deze activerende mutaties gebeurt doorgaans in tumorbjopten, maar het verkrijgen hiervan is niet altijd haalbaar en brengt risico's op complicaties met zich mee. In Hoofdstuk 4 onderzoeken we de aanvullende diagnostische waarde van plasma-gebaseerde volledige moleculaire profilering (plasma-CMP) naast de standaard moleculaire profilering van weefsel (SoC-TMP). We maakten gebruik van de Roche AVENIO ctDNA Targeted kit, die zich richt op 17 genen die zeer frequent gemuteerd zijn in kanker.

Een cohort van patiënten met mNSCLC (n=209) werd geselecteerd uit de bredere Lung cancer Early Molecular Assessment (LEMA)-studie. In de LEMA-studie was SoC-TMP geprotocolleerd, wat leidde tot een hogere standaard van mutatiedetectie in weefsel vergeleken met vergelijkbare studies in het buitenland. In het huidige cohort onderzochten we of toevoeging van plasma-CMP aan de geoptimaliseerde SoC-TMP het aandeel patiënten zou verhogen dat in aanmerking komt voor gerichte behandeling. Dit bleek inderdaad het geval: met de toevoeging van plasma-CMP steeg het aandeel patiënten bij wie een potentieel targetbare drivermutatie werd gedetecteerd van 34,4% naar 39,7% (p<0,001).

Hoofdstuk 5 - Het combineren van data om MRD-detectie te verbeteren

In hoofdstukken 2-4 richtten we ons op patiënten met gemetastaseerde ziekte, waar ctDNA-detectie relatief eenvoudig is vanwege de hoge tumorlast. Daarentegen is ctDNA-detectie bij NSCLC in een vroeger ziektestadium aanzienlijk uitdagender. Bij stadium I-III NSCLC is chirurgische resectie de primaire curatieve behandeling, met een vijfjaar recidiefvrije overleving van respectievelijk 81%, 50% en 34% voor stadium I, II en III NSCLC. Ten tijde van onze studie was adjuvante chemotherapie de standaardbehandeling voor patiënten met stadium II of III NSCLC, met een bescheiden absolute ziektvrije overlevingswinst van 5,8%.

Het voorspellen welke patiënten een recidief zullen krijgen, blijft een belangrijk onderzoeksgebied. Na chirurgische verwijdering van de tumor daalt de hoeveelheid ctDNA in de circulatie vaak tot niet-detecteerbare niveaus. Postoperatieve MRD-detectie richt zich op het opsporen van residueel ctDNA om patiënten met een hoog recidiefrisico te onderscheiden van patiënten die waarschijnlijk genezen zijn. In hoofdstuk 5 gebruikten we een breed hybrid capture-sequencing panel (de Roche AVENIO ctDNA Surveillance kit), gericht op 198 kankergenen, om MRD te detecteren bij patiënten met stadium II-IIIA NSCLC die curatieve chirurgie hadden ondergaan.

De meest eenvoudige manier om MRD te detecteren na chirurgische verwijdering van de tumor is door tumorgerelateerde mutaties in het postoperatieve plasma op te sporen. Met dit panel konden we echter geen effectief onderscheid maken tussen patiënten met een hoog of laag recidiefrisico. Dit kwam door het beperkte aantal mutaties dat we per patiënt konden volgen (mediaan 3) en fout-positieve mutatiebevindingen bij patiënten zonder recidief. Daarentegen verbeterde de integratie van aanvullende fragmentomics-analyses van ctDNA de stratificatie aanzienlijk, waarbij patiënten beter konden worden ingedeeld in hoog- en laagrisicogroepen voor recidief. De testprestaties waren vergelijkbaar met state-of-theart tests in soortgelijke patiëntengroepen, maar hadden onvoldoende negatieve voorspellende waarde (NPV) om af te zien van adjuvante chemotherapie op basis van een negatieve testuitslag.

Deze studie toont expliciet aan dat een betere integratie van datatypes, zelfs uit een enkel experiment, de prestaties van de test drastisch kan verbeteren. Brede sequencing panels genereren veel data, waarvan een groot deel onbenut blijft als alleen wordt gekeken naar de gedetecteerde mutaties. Dit wordt steeds meer erkend in het onderzoeksveld van ctDNA, dat zich steeds meer richt op de integratie van verschillende datatypes om de gevoeligheid voor het detecteren van tumorsignalen te verbeteren.

Research data management

All human studies included in this thesis were conducted in accordance with the principles of the Declaration of Helsinki. The studies meet the criteria for proper use of human samples of the Netherlands. Studies were approved by the medical ethics committee of the University Medical Center Utrecht (Utrecht, the Netherlands) (**chapter 3**), or the medical ethics committee of the Netherlands Cancer Institute (NKI; Amsterdam, the Netherlands) (**chapters 2, 4, 5**). The research data obtained during this PhD trajectory is archived according to the Findable, Accessible, Interoperable and Reusable (FAIR) principles where possible.

Clinical information was collected from electronical medical records in the participating hospitals using an electronic case record form in CastorEDC. All CastorEDC databases are accessible for members of the research team only. The privacy of the participants in this study is ensured by using pseudonymized study codes, with a key file stored in a separate location to which only selected members of the research team have access.

At the time of publication, the author was fully affiliated with the NKI, and all data are owned and managed by the NKI. The NKI maintains responsibility for publishing and sharing the data. Most data collected during this PhD trajectory are included in the chapters of this thesis and are part of published articles. Additional data access requests can be directed to dr. Daan van den Broek, head of the department of Laboratory Medicine at the NKI.

For **chapter 2**, plasma samples from the LEMA biobank at the NKI were collected and analysed. Digital source files and files relating to the analyses are stored on a server of the NKI, to which members of the research team have access. The ALPACA method developed is shared at https://github.com/DCLVessies/ALPACA.

For **chapter 3**, plasma samples from the PLCRC biobank at the UMC Utrecht were collected and analysed at the NKI. All files are stored on a server at the NKI.

For **chapter 4**, the same samples as those for chapter 2 were used, and additional genotyping was performed at the NKI. Genotyping result files relating to the analyses are stored at a server at the NKI and raw, interoperable genotyping files are stored at a separate server at the NKI, which is accessible only to select members of the research team.

For **chapter 5**, plasma and tissue samples from the LEMA biobank were analysed at the NKI. All genotyping raw, interoperable data are stored at a server of the NKI to which only select members of the research team have access, while processed results and files relating to the analyses are stored in another server of the NKI. The fragmentomic methods described in the paper are shared publicly: https://github. com/DCLVessies/Fragmentomics.

PhD portfolio of Daan Christiaan Laurens Vessies

Department: Department of Pulmonary Disease

PhD period: 12/02/2024 - 17/02/2025
PhD Supervisor(s): **Prof. M.M. van den Heuvel**

PhD Co-supervisor(s): Dr. D. van den Broek (Netherlands Cancer Institute; NKI)

Training activities	Hours
Courses	
NKI - Introduction to R (2019)	32.00
NKI - Scientific Integrity in Science (2021)	56.00
Genomic Data Science online course (2022)	40.00
Machine Learning online course (2023)	90.00
VRIJSTELLING - Radboudumc - In the lead - Radboudumc	0.00
introduction for PhD candidates (2024)	
Conferences	
 Poster presentation: 10th CNAPS International Symposium- 	32.00
Recent advances in circulating DNA and RNA (2017)	
 Poster presentation: Annual OOA PhD day (2018) 	8.00
Poster presentation: AACR annual meeting 2019 (2019)	56.00
• 2x Poster presentation: EACR-ESMO Joint Conference on Liquid Biopsies (2019)	32.00
Other	
VRIJSTELLING - Radboudumc - General Radboudumc	0.00
introduction for research personnel (2024)	
Teaching activities	
Supervision of internships / other	
HLO student supervision - Mustafa Turgut (2017)	50.00
BSc student supervision - Patrick Pik (2017)	25.00
 HLO student supervision - Bastiaan Boerrigter (2018) 	100.00
HLO student supervision - Mehek Mian (2018)	100.00
HLO student supervision - Patricia Ceven (2018)	50.00
HLO student supervision - Widad Ait Iddouch (2019)	50.00
Total	721.00

Curriculum vitae

Daan Christiaan Laurens Vessies was born on the 2nd of November 1988 in Oude Wetering, Alkemade. After enjoying a carefree and loving youth, he graduated from the gymnasium of the Visser 't Hooft Lyceum in Leiden in 2007. He studied Life Science & Technology at the Delft University of Technology and Leiden University (joint degree). He performed an internship at the Genomics Core Facility of the Netherlands Cancer Institute (NKI) under the supervision of dr. Ron Kerkhoven in 2012/2013, focusing on the optimal sequencing library loading on Illumina HiSeq and MiSeq machines. He was subsequently hired at the same department to work in the 'NGS into clinic' program, which sought to clinically validate the use of hybrid capture sequencing of 178 cancer-related genes in a clinical setting.

In 2015 he moved to the department of laboratory medicine at the NKI to work on the 'Liquid biopsies' project under the joint supervision of dr. Daan van den Broek and dr. Michiel van der Heijden. He continued his work in liquid biopsies at the same department in his PhD, resulting in the publications in this thesis. Having tasted the intricacies of advanced data analyses, he is employed as a Bio Data Scientist at RenovaroCube (Amsterdam) since 2024, where he is involved in developing multiomic machine learning models for early detection of cancer and cancer recurrence using liquid biopsies.

List of publications

Publications included in this thesis are in **bold**. Oldest first.

- Vessies DCL, Greuter MJE, Van Rooijen KL, Linders TC, Lanfermeijer M, Ramkisoensing KL, et al. Performance of four platforms for KRAS mutation detection in plasma cell-free DNA: ddPCR, Idylla, COBAS z480 and BEAMing. Sci Rep. 2020 May 15;10(1):8122.
- Van 'T Erve I, Greuter MJE, Bolhuis K, Vessies DCL, Leal A, Vink GR, et al. Diagnostic Strategies toward Clinical Implementation of Liquid Biopsy RAS/ BRAF Circulating Tumor DNA Analyses in Patients with Metastatic Colorectal Cancer. J Mol Diagn. 2020 Dec;22(12):1430–7.
- 3. Verheijen RB, Van Duijl TT, Van Den Heuvel MM, Vessies D, Muller M, Beijnen JH, et al. Monitoring of EGFR mutations in circulating tumor DNA of non-small cell lung cancer patients treated with EGFR inhibitors. Cancer Chemother Pharmacol. 2021 Feb;87(2):269–76.
- Vessies DCL, Linders TC, Lanfermeijer M, Ramkisoensing KL, Van Der Noort V, Schouten RD, et al. An Automated Correction Algorithm (ALPACA) for ddPCR Data Using Adaptive Limit of Blank and Correction of False Positive Events Improves Specificity of Mutation Detection. Clin Chem. 2021 Jul 6:67(7):959–67.
- Schouten RD, Vessies DCL, Bosch LJW, Barlo NP, Van Lindert ASR, Cillessen SAGM, et al. Clinical Utility of Plasma-Based Comprehensive Molecular Profiling in Advanced Non-Small-Cell Lung Cancer. JCO Precis Oncol. 2021 Nov;(5):1112–21.
- 6. Koole SN, Vessies DCL, Schuurbiers MMF, Kramer A, Schouten RD, Degeling K, et al. Cell-Free DNA at Diagnosis for Stage IV Non-Small Cell Lung Cancer: Costs, Time to Diagnosis and Clinical Relevance. Cancers. 2022 Mar 31;14(7):1783.
- 7. In 't Veld SGJG, Arkani M, Post E, Antunes-Ferreira M, D'Ambrosi S, Vessies DCL, et al. Detection and localization of early- and late-stage cancers using platelet RNA. Cancer Cell. 2022 Sep;40(9):999-1009.e6.

- 8. Vessies DCL, Schuurbiers MMF, Van Der Noort V, Schouten I, Linders TC, Lanfermeijer M, et al. Combining variant detection and fragment length analysis improves detection of minimal residual disease in postsurgery circulating tumour DNA of stage II-IIIA NSCLC patients. Mol Oncol. 2022 Jul:16(14):2719-32.
- 9. Kramer A, Schuuring E, Vessies DCL, Van Der Leest P, Geerlings MJ, Rozendal P, et al. A Micro-Costing Framework for Circulating Tumor DNA Testing in Dutch Clinical Practice. J Mol Diagn. 2023 Jan;25(1):36-45.
- 10. Kramer A, Rubio-Alarcón C, Van Den Broek D, Vessies DCL, Van'T Erve I, Meijer GA, et al. A scenario-drafting study to explore potential future implementation pathways of circulating tumor DNA testing in oncology. Mol Oncol. 2024 Nov:18(11):2730-42.
- 11. Rubio-Alarcón C, Stelloo E, Vessies DCL, Van 'T Erve I, Mekkes NJ, Swennenhuis J, et al. High Prevalence of Chromosomal Rearrangements and LINE Retrotranspositions Detected in Formalin-Fixed, Paraffin-Embedded Colorectal Cancer Tissue. J Mol Diagn. 2024 Dec;26(12):1065-80.

Dankwoord

Zo aan het eind van dit traject is het een mooi moment om eens stil te staan en te reflecteren op wat er allemaal gedaan en gebeurd is. Er is veel om dankbaar voor te zijn. In het algemeen, en wat betreft mijn promotietraject in het bijzonder. De kuil is altijd minder diep dan hij leek toen je er nog in stond, en dat is toch wel de grootste les van allemaal.

Sommige paden zijn recht en geplaveid. Andere zijn wat hobbeliger. Michel, zoals je zei bewandelt ieder zijn eigen pad op zijn eigen manier. Ik ben dankbaar dat jij je hard hebt gemaakt voor de menselijke maat in een ongewone situatie. Bedankt dat je er was op het moment dat ik dat het hardst nodig had.

Daan, OpperDaan, het is lastig op papier te zetten hoeveel ik aan je te danken heb. Vanaf het eerste begin heb je mij op een positieve manier gestimuleerd. Ruimte gegeven om in de data te duiken, te exploreren, maar ook sturing wanneer dat nodig was. En op zijn tijd een stok achter de deur wanneer het schrijven niet opschoot. Jouw steun in moeilijke tijden waren voor mij een belangrijke motivatie om het geheel tot een mooi einde te brengen.

Mijn vrienden van A&O: Dorothé, Mirthe, Kalpana, Lennart, Ruben, en alle stagiairs. Dat ik kan terugkijken op een geweldige tijd bij het NKI is voor een groot deel aan jullie te danken. Wat hebben we veel lol gehad met zijn allen, zowel op werk als in de vele uitjes daarnaast. Dat je in je vrije tijd met veel plezier met je collega's op stap gaat is niet vanzelfsprekend, en ik ben blij dat ik het met jullie heb mogen ervaren.

Het gaat te ver om alle collega's met wie ik met veel plezier heb samengewerkt hier te benoemen. Jullie mogen ervan uitgaan dat ik jullie dankbaar ben, of je hier nu wel of niet genoemd staat. De leden van de TGO-, TRC-, en de LEMA-groep, en de vele, vele fijne samenwerkingen die in een wat minder vast verband zaten, binnen en buiten het NKI: Het was altijd leuk om het over ctDNA te hebben, plannen te smeden, en analyses uit te voeren.

Natuurlijk gaan mijn dank en bewondering ook uit naar alle patiënten en gezonde vrijwilligers die met hun bloed en medische gegevens hebben bijgedragen aan de onderzoeken. Het was nooit makkelijk om vanuit mijn werkplek uit te kijken op de centrale hal, in de wetenschap dat iedereen voor dezelfde ziekte komt. Ik hoop dat ik op mijn manier, met deze publicaties, een heel klein steentje bij heb mogen dragen aan een sprankje hoop voor de toekomst.

Naast de hulp van alle collega's, zou dit boekje toch ook niet tot stand zijn gekomen zonder de mensen die mij dierbaar zijn. Vrienden en familie vormen een onzichtbaar vangnet, waarvan je pas weet dat het er is als je valt. Ik prijs mij gelukkig met veel goede vrienden om mij heen. Sommigen gaan terug tot de basisschool, anderen de middelbare school, en anderen heb ik later pas ontmoet. Bedankt dat jullie er zijn en mij helpen met humor, liefde, en begrip.

In het bijzonder wil ik noemen mijn schoonfamilie, die na al die jaren (en een huwelijk) gewoon-familie zijn geworden. Marcel, Ellen, Esmee, Dennis, Minte, Silmen en Mandy, dank voor alle mooie momenten, weekendies en uities. Vanaf het allereerste begin heb ik me bij jullie welkom gevoeld, en daarmee prijs ik mij heel gelukkig.

Lieve Koen, Sanne, Kate en Nina. We zien elkaar misschien minder dan ik zou wensen, maar als we elkaar zien is het goed en fijn. Ik bewonder jullie avontuurlijkheid en tomeloze energie. Ik hoop dat jullie volgende avontuur weer een mooie verrijking zal zijn, en dat de onzekerheid die nu op jullie pad ligt jullie niet zal belemmeren.

Lieve mama en papa, bedankt voor het warme en veilige nest waarin wij opgegroeid zijn. De stabiliteit en geborgenheid die ik bij jullie heb mogen ontvangen zijn een bouwsteen voor hoe ik vandaag in het leven sta. Jullie liefde en saamhorigheid zijn een voorbeeld voor hoe ik mijn huwelijk verder voor me zie. En dat is het grootste cadeau dat ik me wensen kan.

Tot slot, mijn eigen gezin is mij het allermeeste waard. Als je eigen basis goed en stabiel is, dan kan geen aardschok die aan het wankelen krijgen. Lieve Lex en Pim, voordat ik vader werd had ik niet gedacht dat ik het zo leuk zou vinden. Ik ben elke dag trots op jullie.

Lieve Tinke, ik hoop dat je dit dankwoord niet nodig hebt om te weten hoeveel je voor me betekent. Jouw onvoorwaardelijke steun is mijn grootste geluk. Dit boekje zou er zonder jou zeker niet gelegen hebben. Ik hoop en wens dat wij samen oud en gerimpeld mogen worden, de kinderen in liefde mogen zien opgroeien, en elkaar tot steun mogen zijn in goede en kwade dagen.

